



HHS Public Access

Author manuscript

Chem Rev. Author manuscript; available in PMC 2024 May 22.

Published in final edited form as:

Chem Rev. 2022 July 13; 122(13): 11247–11286. doi:10.1021/acs.chemrev.1c00677.

Recent Advances in Microscale Electroporation

Sung-Eun Choi¹,

Department of Mechanical Engineering, Johns Hopkins University, Baltimore, Maryland 21218, United States

Harrison Khoo¹,

Department of Mechanical Engineering, Johns Hopkins University, Baltimore, Maryland 21218, United States

Soojung Claire Hur

Department of Mechanical Engineering, Institute for NanoBioTechnology, and Department of Oncology, Johns Hopkins University, Baltimore, Maryland 21218, United States; Sidney Kimmel Comprehensive Cancer Center, Johns Hopkins University, Baltimore, Maryland 21231, United States

Abstract

Electroporation (EP) is a commonly used strategy to increase cell permeability for intracellular cargo delivery or irreversible cell membrane disruption using electric fields. In recent years, EP performance has been improved by shrinking electrodes and device structures to the microscale. Integration with microfluidics has led to the design of devices performing static EP, where cells are fixed in a defined region, or continuous EP, where cells constantly pass through the device. Each device type performs superior to conventional, macroscale EP devices while providing additional advantages in precision manipulation (static EP) and increased throughput (continuous EP). Microscale EP is gentle on cells and has enabled more sensitive assaying of cells with novel applications. In this Review, we present the physical principles of microscale EP devices and examine design trends in recent years. In addition, we discuss the use of reversible and irreversible EP in the development of therapeutics and analysis of intracellular contents, among other noteworthy applications. This Review aims to inform and encourage scientists and engineers to expand the use of efficient and versatile microscale EP technologies.

Graphical Abstract

Corresponding Author: Soojung Claire Hur – Department of Mechanical Engineering, Institute for NanoBioTechnology, and Department of Oncology, Johns Hopkins University, Baltimore, Maryland 21218, United States; Sidney Kimmel Comprehensive Cancer Center, Johns Hopkins University, Baltimore, Maryland 21231, United States; schur@jhu.edu.

¹Author Contributions

S.-E.C. and H.K. contributed equally to this manuscript.

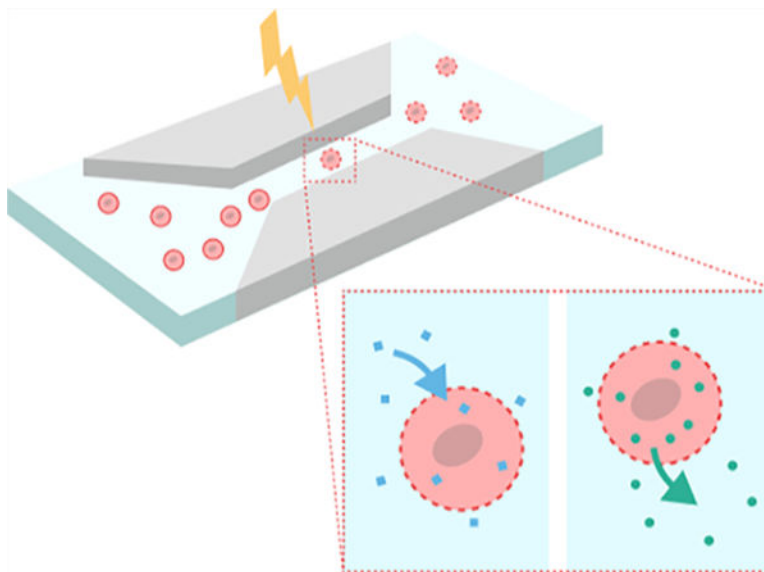
ASSOCIATED CONTENT

Special Issue Paper

This paper is an additional review for *Chem. Rev.* 2022, volume 122, issue 7, “Microfluidics”.

Complete contact information is available at: <https://pubs.acs.org/10.1021/acs.chemrev.1c00677>

The authors declare the following competing financial interest(s): S.C.H. benefits financially from royalty payments from the Vortex Biosciences, Inc.



1. INTRODUCTION

Electroporation (EP), or electroporation, is a powerful technique to increase cell membrane permeability via the application of electric fields. EP temporarily or permanently impairs cell membrane integrity depending on electric field conditions and is applicable to both prokaryotic and eukaryotic cells. The phenomenon of biomembrane poration with an electric field was first observed in 1972¹ and was applied toward the delivery of plasmid DNA into mouse lymphoma cells in 1982.² Since then, EP has been used for intracellular delivery of genetic materials and drugs, disinfection and extraction of biomolecules,³ and cell–cell/vesicle fusion.^{4–6}

Intracellular delivery enables modifications of cellular function for cell-based therapy such as adoptive immunotherapies, cell reprogramming,^{6–9} biomanufacturing,³ biomass and food processing,^{10–12} and biofuel production.¹³ A plethora of intracellular delivery methods exist and are categorized as carrier-mediated and membrane-disruption-mediated methods.^{14,15} Carriers include viral vectors,¹⁶ liposomes, and dendrimers,¹⁷ whereas membrane disruption methods are considered to be chemical (detergents¹⁸), mechanical (particle bombardment,¹⁹ scrape loading,²⁰ bead loading,²¹ and syringe loading²²), or field-assisted (sonoporation,²³ optoporation,²⁴ and magnetoporation²⁵). While various strategies exist to achieve these purposes, there are associated challenges with cargo size capacity, cargo preparation complexity, and toxicity associated with high doses or viral genome integration.^{26–28} In comparison, EP is a physical cell membrane disruption method that is not limited to specific cell–cargo interactions or cell cycle stage^{29,30} and can be readily repurposed for different cell types or molecules in a scalable manner. EP is widely used to transport DNA, RNA, proteins, and other biomolecules into individual cells. EP is also a key tool for biomedical research to introduce different stimuli and observe cell response.

Conventional batch EP systems commonly require a millimeter-sized cuvette lined with two parallel electrodes.³¹ Cell suspensions are mixed with cargo molecules in an EP buffer

for intracellular delivery, and high electric fields are applied for permeabilization. The working principle is simple and robust, and several systems are commercially available from companies such as Biorad and Eppendorf. However, bulk EP requires high voltages (> 1 kV) to achieve sufficiently strong conditions for cell permeabilization.³² Such high voltages are required because the electric field intensity, E , is related to the gradient of the electric potential, V .

$$E = -\nabla V \quad (1)$$

There are challenges associated with cuvette EP. Since the parallel plate electrodes in macroscale cuvettes are spaced millimeters apart, high operational voltages are inevitable. These high voltages not only are associated with safety hazards but also trigger and exacerbate electrolysis, which decreases cell viability. Electrolysis generates gas bubbles and hydroxyl and hydrogen ions near the electrodes, all of which are toxic to cells. Additionally, high current increases Joule heating, caused by the passage of an electrical current through the solution, which harmfully increases cell suspension temperature and reduces cell viability.³³ Aluminum electrodes, commonly used in commercial cuvette EP, degrade and release toxic metal ions into the buffer at higher voltages, further decreasing cell viability.³⁴ Furthermore, interactions between randomly distributed cells in the cuvette generate nonuniform electric fields, which diminishes EP performance.³⁵ Overall, cuvette EP has shown inconsistent EP efficiency and is ineffective in transfecting hard-to-transfect primary cells,³⁶ such as T cells.^{14,37}

EP technology development has shifted toward the microscale and integration with microfluidic devices. Microscale EP devices consist of a microfluidic channel that enables small volumes of fluid to be exposed to precisely controlled electric fields that are generated by embedded external wires or micro-/nanopatterned electrodes. External wires simplify the fabrication process while leveraging the benefits provided by microscale fluidic device features. Alternatively, fully integrated microelectrodes provide better localization and precise control of electric fields while operating at lower voltages. This shift away from cuvettes offers several benefits, including improved EP uniformity, safety, and control. Microfluidic cell EP was first demonstrated in 1999 by Huang and Rubinsky, where mammalian cells were electroporated with different pulse conditions and amplitudes.³⁸ Since then, many examples of microscale reversible^{32,36,39–45} and irreversible^{46–49} cell EP have emerged and enabled cellular investigations with better resolution than conventional methods.

Microscale EP devices, with electrode gaps or features on the order of micrometers apart, require lower voltages to achieve electric field strengths identical to those in cuvette EP. Low voltages mean reduced power consumption and minimal electrolysis, so cells are less likely to be nonspecifically harmed. Additionally, as devices are on the same length scale as cells targeted for manipulation, cells are more controllably positioned within the device with the possibility for single-cell EP, which is particularly useful in studying individual cell behaviors. Small sample volumes (micro- to attoliter) can be processed with high precision,

so microscale EP is suitable to handle rare and fragile samples with minimal reagent use. Moreover, large quantities of cells can be electroporated with less batch-to-batch variation, and reduced human error using a continuous and automated system. There are excellent reviews about microfluidic devices for EP^{32,36,39,40,42–44,50–52} and their clinical applications.^{8,41}

In this comprehensive Review, we discuss advances in different microscale EP systems to electrically permeabilize the plasma membrane. We explain not only reversible EP to deliver external cargo into cells but also cell lysis and electrofusion, as the underlying physical mechanism and technological concepts are related for these EP purposes. We begin with an overview of governing principles that enable EP on a cellular level. We then classify and explain trends in recent microscale EP systems based on whether they operate in static or continuous modalities. Static systems maintain cell position during electric field treatment, whereas continuous systems involve a constant flow-through of cell suspensions. This discussion is followed by a summary of how microfluidic EP technologies have been applied in clinical and research settings to develop and deliver therapeutics, analyze cellular contents, and inactivate and fuse cells (Figure 1). We conclude with an outline of future directions for this multidisciplinary field.

2. MECHANISM OF ELECTROPORATION

Cell EP is the controlled application of an external electric field to a cell membrane to increase its permeability. In this section, we discuss the mechanism by which applied electric fields generate pores in cell membranes and mention critical equations and parameters that influence EP performance.

2.1. Electroporation at the Cellular Level

The cell membrane separates intracellular contents from the external microenvironment and mediates selective material exchange.⁵³ The barrier is formed by a lipid bilayer with membrane proteins with a range of functions, including highly defined transport of peptides, amino acids, and sugars across the barrier, even actively against concentration gradients.⁵⁴ The entry of hydrophilic, membrane impermeable cargos—including dyes, DNA, and proteins that do not have a dedicated transporter—is restricted. External stimuli are needed to reprogram cells or extract cytosolic contents for additional analysis.

EP techniques apply an electric field to override natural cell behavior and allow for the indiscriminate passage of molecules. Without external disturbance, thermal fluctuations cause lateral movement of amphiphilic lipids in the membrane and randomly generate transient hydrophobic pores that are insufficient for hydrophilic molecule transit.^{55–57} Electric fields elicit the generation of larger hydrophilic pores, which permits free travel of biomolecules across the membrane.^{39,55,57,58} The mathematical representation of the transmembrane potential (TMP) relates to changes in free energy of the cell membrane caused by pore formation. The free energy change is affected by the hydrophilic and hydrophobic surface tension, pore edge tension, hydrophobic interactions, and applied electric fields.⁵⁸ In particular, the hydrophilicity of a pore is determined by its size, as a radius larger than ~ 0.5 nm signifies the transition from a hydrophobic to hydrophilic pore.

Pores with radii or at least ~ 0.8 nm reach an energy minimum, in which pores are stable even after the removal of the electric field. At a wider radius, the membrane is irreversibly porated past a second energy maximum. The threshold energy maxima are adjusted based on the TMP⁵⁸ (Figure 2).

The electrically induced TMP ($\Delta \Phi$) under a uniform electric field is calculated with the Laplace equation and expressed as the Schwan equation (eq 2; Figure 3).^{56,59–61}

$$\Delta \Phi (E, M, t) = -f_s g r E \cos(\theta(M)) (1 - e^{-t/\tau}) \quad (2)$$

Here, f_s is a factor determined by cell shape, g is controlled by the electric permeability of the membrane, r is the target cell radius, $\theta(M)$ is the polar angle of the point M on the cell membrane, measured from the center of a cell with respect to the electric field direction, t is the time since initial electric field application, and τ is a time constant.⁶² The TMP is highest at $\theta(M) = 0^\circ$ and 180° , or directly facing the electrode, and lowest at the point of $\theta(M) = 90^\circ$ and 270° . Thus, poration most likely starts at the poles of the cell facing electrodes (Figure 3). Several assumptions are commonly made to simplify this relationship. The cell is typically modeled as a sphere, so $f_s = 1.5$. Additionally, the cell membrane acts as a dielectric material because its conductivity is much lower than both the extracellular medium⁵⁸ and cytoplasm.^{63–65} Thus, the membrane is assumed to be a pure dielectric, and $g = 1$. Finally, in most scenarios, the charging time is much shorter than the pulse duration, so the Euler's number term is often disregarded. Thus, the Schwan equation can be simplified (eq 3).

$$\Delta \Phi (E, M) = -1.5rE \cos(\theta(M)) \quad (3)$$

Some EP devices operate using alternating current (AC), which switches polarity at a given frequency. To account for such differences, the Schwan equation is adapted (eq 4) to reflect the frequency term, f .^{66,67}

$$\Delta \Phi (E, M) = -\frac{1.5rE \cos(\theta(M))}{(1 + (2\pi f\tau)^2)^{1/2}} \quad (4)$$

In this instance, $\tau = rC_m(\rho_{env} + \rho_{ct}/2)$, where C_m is the membrane capacitance, and ρ is the resistivity of the cellular environment and cytoplasm.

The external electric field increases the TMP and decreases the requisite energy for stochastic membrane poration. A cell normally maintains a resting TMP between -20 and -200 mV,⁶⁹ which is insufficient for hydrophilic pore formation. The probability of pore formation increases under a higher external electric field intensity, as the first free

energy maximum decreases (Figure 2).^{58,70} Sufficient cell permeabilization is achieved at a TMP between 0.2 and 1 V.^{70,71} The threshold value does not represent a binary change between the intact and porated status but rather the point at which EP is experimentally detectable, often gauged by visualizing dye molecule uptake or measuring impedance change.⁵⁸ Fluorescence detection of EP events is more accessible to research facilities with basic fluorescence microscopes, but impedance recordings provide more information and context about the status of cell EP. The permeabilized surface membrane area is dictated by the applied voltage amplitude.⁷²

Cell permeability decreases within milliseconds after completion of the electric pulse.^{73,74} Membrane impermeable biomolecules continue to traverse the barrier while the cell begins to heal, and pores are sealed over the course of seconds to minutes.^{14,58} The cell membrane will eventually fully seal, but it takes several more hours to regain homeostatic cytoplasmic composition. The exception to cellular recovery occurs in high TMP conditions or excessively long electric field durations, which form bigger pores. While widening pores improves cargo permeability, at a certain size, the pores are overly large, and the cell is unable to recover, leading to irreversible EP.⁵⁷

It is notoriously difficult to experimentally determine on the molecular level how nanopores are generated on the cell membrane because they are too small for optical detection and too fragile for electron microscopy.⁵⁸ Molecular dynamics (MD) simulations can provide insights about the molecular mechanism of pore formation and membrane resealing. EP has been simulated with a lipid bilayer model with hundreds to thousands of lipid molecules, as permitted with existing computational capabilities. Pore formation begins when a high TMP is applied to a lipid bilayer (Figure 4).⁷⁵ Water molecules move through defects in the lipid bilayer, and phospholipid head groups reorganize until a mature hydrophilic pore is generated. As soon as the electric field is removed, the pore annihilation sequence occurs as water molecules and phospholipid head groups move to the outer layer of lipid membrane, and the pore shrinks. Pore annihilation is complete when lipid head groups are separated into two separate layers, and water molecules have been pushed out of the bilayer. Pore creation time decreases exponentially with respect to TMP, but the pore annihilation time is tens to hundreds of nanoseconds and is independent of the applied voltage.⁷⁵ Pore creation and annihilation time are also dependent on the composition of lipids and ions.⁷⁶ Incorporation of anionic phospholipids or Ca^{2+} ions to the zwitterionic bilayer increases and decreases the pore creation and annihilation times, respectively, because they change the area per lipid and surface tension of the lipid bilayer. MD simulations of membrane resealing time are 9 orders of magnitude shorter than experimental observations. Kotnik et al. explained this discrepancy with other mechanisms not represented in simulations, such as lipid peroxidation and the interaction of electric field to membrane proteins and cytoskeletons during EP.⁵⁸

2.2. Performance Affecting Factors

Beyond device design, EP systems must apply optimized experimental variables to achieve the best performance. Understanding the biological characteristics of the experiment, such as cell and cargo types, provides insight for a general range of desirable electric field

conditions. Additional tuning of electrical pulse parameters around this target is requisite to improve EP effectiveness.

2.2.1. Experimental Components.—An important first step in designing an EP device is understanding the general experimental protocols. EP parameters have to be experimentally optimized for each cell, cargo, and EP system. As a starting point, the target cell type influences the required electrical pulse because different cell types have intrinsic membrane characteristics that affect the electrical conditions necessary to achieve EP. The Schwan equation (eq 3) shows how cell size and electric field intensity are inversely related to reach a target TMP. Larger cells require lower electric field strengths than small cells to achieve EP. Thus, $>10\ \mu\text{m}$ mammalian cells require approximately $10\times$ lower electric field strengths than $\sim 1\ \mu\text{m}$ bacteria to achieve EP. Experiments show that this correlation holds true, although not on a linear scale.⁷⁷ The induced TMP is also affected by cell shape and interactions with adjacent cells.⁷¹ Immortalized cell lines are typically used when establishing and gauging its performance of an EP system because they are easy to handle and electroporate efficiently. Primary and stem cells are more difficult to electroporate, a tendency that has also been observed with other permeabilization techniques.¹⁴ Nevertheless, EP has demonstrated improved transfection efficiency for lymphocytes,⁷⁸ dendritic cells,⁷⁹ and hematopoietic cells⁸⁰ compared to other transfection methods.¹⁴

Conversely, delivered cargo characteristics, including size, shape, and charge, affect intracellular delivery efficiency.⁸¹ Small, neutral molecules enter the cell via diffusion when membrane pores are open.^{30,82} Charged molecules, such as propidium iodide (PI) and nucleic acid, are transported with additional electrophoretic forces into the cell.^{30,83,84} During nucleic acid delivery, cellular uptake is biased toward the cathode-facing side of the cell because negatively charged molecules move from the cathode to anode (Figure 3).⁸⁵ Electrophoresis is more dominant than diffusion in driving nucleic acid movement. Smaller nucleic acid strands readily enter cell pores, whereas large DNA plasmids require a multistep mechanism to enter the cell.^{61,86} The electric field also causes large charged DNA to aggregate outside the cathode-facing membrane. Later, plasmids are transferred into the cytoplasm using endocytosis and are trafficked by endosomes within several hours.⁸⁷ Nucleic acid delivery into the nucleus is more challenging because it relies on additional biological processes such as endosomal escape, intracellular migration, and passage through the nuclear membrane. The mechanism for plasmid trafficking through the nuclear membrane for transfection is still under study.^{14,61} Large molecules, such as antibodies or dextran, rely on diffusion because they are neutral or weakly charged.⁷² The size distribution for larger nanoparticles ($>10\ \text{nm}$) affects the delivery efficiency and dispersion within each cell during EP.⁸⁸

The choice of EP buffers affects EP efficiency and cell viability during electrical treatment. A range of commercial and custom buffers vary in conductivity and osmolarity.^{89,90} Buffer composition is designed to mitigate pH changes during EP. Some additives, such as Mg^{2+} , ATP, glucose, and antioxidants, are included to mimic native cellular microenvironments and have led to improved EP efficiency.¹⁴ Usage of hypoosmolar buffers that swell the cell has also demonstrated better EP performance.⁹¹ Buffers with low conductivity increased

cell viability without altering reversible EP efficiency because the low current reduced the harmful Joule heating.^{92–94} High conductivity buffer performance is limited by pulse generator hardware, which may not be able to handle high currents to matched the desired energy input.⁹⁵

2.2.2. Electric Pulse Parameters.—Adjusting the applied electric pulse alongside experimental components greatly improves device effectiveness. EP performance is directly affected by electric pulse parameters, such as waveform shape.^{14,58} Exponential decay waves were used widely in early conventional EP systems, where an initial peak voltage is applied, and the electric field decays based on electrical component properties.⁹⁶ DC square waves are commonly used for cell EP, and Jordan et al. reported better transfection rates for hard-to-transfect cells using square compared to exponential decay waveforms.⁹⁷ Nevertheless, there is no consensus regarding the best universal electrical conditions for EP. Selected studies have opted for a more gentle bilevel signal with a short, strong pulse followed by a longer, weaker pulse.^{98,99} The high initial pulse forms pores rapidly at a sufficiently high TMP. Later, the lower, sustained pulse prevents premature pore closure and facilitates electrophoretic movement of biomolecules without the toxicities relevant in more extreme conditions.

Electric field polarity has significant implications for reducing cellular toxicity because the membrane permeabilization and delivery depend on the polarity of electrodes. In addition, the polarity affects the direction of electrophoretic movement of charged molecules. EP typically requires voltages that are sufficiently high and/or pulses that are adequately long to induce harmful electrolysis.⁴⁰ Brief DC voltages reduce the formation of toxic electrolysis byproducts that compromise cell viability. Alternatively, bipolar square pulses with time-averaged current of zero have been shown to be more effective for EP because both cell poles are permeabilized, and electrolysis is minimized.^{40,81} Switching the polarity causes the byproducts of redox reactions to neutralize one another and to limit pH changes. More commonly, EP systems use an AC voltage source to mitigate these effects.¹⁰⁰ AC voltage pulses are effective in the delivery of charged DNA into both ends of the cell membrane facing electrodes for more efficient transport.¹⁰¹

Pulse length may also induce different cell membrane and organelle behaviors after exposure to electric fields. Most EP implementations use microsecond pulses, which are sufficiently long to charge the membrane.^{58,73} The membrane acts as a capacitor that causes plateaus and decay of electric fields exponentially at the completion of the pulse. Pulse durations must be limited to prevent excessive pore expansion for reversible EP. In contrast, if the pulse is only nanoseconds long, then the cell membrane does not adequately charge and will not experience maximum TMP.¹⁰² Under such conditions, organelles, with their own cell membranes, may experience sufficiently high TMPs for EP if their contents are more conductive than the cellular cytoplasm.^{102,103} Nanosecond pulses have been used for proof-of-concept gene delivery into the nucleus.¹⁰⁴ The mitochondrion also has a higher resting TMP than the cell membrane, which may cause an additive effect and can reach the threshold more easily for organelle poration. Organelle membranes have been selectively permeabilized using high electric fields (MV/m).^{105–107}

3. TECHNOLOGICAL IMPROVEMENTS

Microfluidic EP systems that exploit physics at the microscale have been developed to improve device performance, reduce variation in conditions exerted between cells, and improve ease-of-use. The transition from macro- to microscale separation of parallel planar electrodes decreases the requisite voltage to achieve the target electric field strength and TMP for permeabilization (eq 1). Interdigitated electrodes further decrease the separation distance with a higher electric field strength closer to the patterned features. Alternatively, wire electrodes may be placed on the fluidic inlet and outlet, and the solution in the microchannel acts as a conductor because biological solutions are inherently conductive. According to Ohm's law, the electric field is defined as

$$E = \frac{J}{\sigma} = \frac{I}{\sigma A} \quad (5)$$

where J represents current density, σ represents conductivity, I represents current, and A represents cross-sectional area. Compared to a macroscale channel, microchannels have smaller cross-sectional areas, so the electric field within the microchannel is higher. Novel designs in electrode or microchannel geometry may further reduce required voltages, improve the uniformity of applied conditions, or limit cellular damage during EP.

EP system performance is commonly evaluated by the delivery/lysis efficiency, cell viability, and throughput. EP efficiency is defined as the fraction of cells with successful molecular delivery or lysis relative to the number of cells introduced into the system. For reversible EP, cell viability is widely represented by how many cells are alive post-EP. Like other delivery methods, there is a trade-off, as a higher electric field contributes to improved EP efficiency at the cost of decreased cell viability.^{41,108} In this section, we classify recent technological innovations based on whether the devices operate as static or continuous systems and broadly discuss trends in device features. Finally, we discuss additional advances that are universally applicable to EP systems or improve the experimental workflow.

3.1. Static Electroporation

Static EP systems confine target cells in a defined region during the application of electric fields. Innovative static EP devices integrate small micro-/nanoscale electrodes or structures in the channel to locally enhance the electric field. These design choices are integrated with on-chip cell positioning strategies to form tight interfaces between cells and micro-/nanoscale features to best leverage their effects. Compared to batch EP in which cells experience uneven conditions and must be processed and analyzed in bulk, static EP systems enable individual cell monitoring during and after EP, which is especially useful in biomedical research settings. The earliest microfluidic EP devices were static systems capable of real-time observation of cells.^{38,109–112} Static systems uniquely provide deterministic cell positioning to localized electric fields. Thus, devices generally exert even electric field conditions across several cells for better consistency. Static systems are relatively throughput-limited because the maximum number of cells processed is restricted by the size of the device. Nevertheless, up to 10^5 cells have been electroporated in a

single experiment by scaling up unique features.^{113,114} Below, we discuss how static EP devices incorporate geometrical changes and integrate other microfluidic elements to improve overall EP performance.

3.1.1. Localization of Enhanced Electric Field.—Recent innovations in static microscale EP design leverage highly replicable control of cell positioning to generate localized electric fields. Static EP devices generally exert consistent electric field conditions across all cells within the system. Electric fields are highly concentrated in a defined region for more selective EP of a portion of the cell. Since cell permeabilization focuses on small regions of the membrane, the cell generally experiences fewer stresses, and viability is improved. Localized EP demonstrates an ideal balance between minimizing cellular stressors and maximizing throughput relative to chemical, viral, and bulk EP cargo delivery.¹¹⁵ Adhering to eq 1, localized EP has been achieved by reducing the counter electrode gap to as narrow as 70–500 nm.^{116–120} The electric field is highly concentrated at the cell membrane regions directly above the electrode nanogap. A range of additional modifications to electrode or device geometries have been implemented to achieve localized electric field amplification.

3.1.1.1. Subcellular Channels.: Recent improvements in micro-/nanofabrication methods have enabled the creation of small features with high precision. Subcellular channels, with constrictions that are smaller than the diameter of target cells, have been fabricated for localized and scalable EP (Figure 5A,B). Each subcellular channel is flanked by larger microchannels reserved for cell suspensions and biomolecules. Electrodes positioned in both microchannels are activated to trigger localized, static EP. In accordance with eq 5, the highest electric field strength is generated at the subcellular channel, and the intensity rapidly wanes further from the ends of the channel. Thus, cells must be positioned close to the subcellular channel to experience the enhanced electric field, surpass the threshold TMP, and permeabilize. For intracellular delivery, biomolecules loaded in the opposing microchannel are swept up through the subcellular channel into the cell. Conversely, intracellular biomolecules may diffuse out of the cell through the same passage. Different iterations of subcellular channels have been devised for efficient static EP.

The earliest demonstration of a subcellular channel for EP was reported by Rubinsky and colleagues, who immobilized a cell on a micropore on a silicon nitride membrane.^{38,109,121,122} Single-cell EP was observed by electrical and optical methods in real time with 100% EP efficiency after parameter optimization. Later, Kapton films with a UV-patterned micro-orifice array¹²³ and lateral trapping channels^{111,124,125} were used to trap and electroporate multiple cells in a single experiment. Khine et al. used polydimethylsiloxane (PDMS) channels with a height only a fraction of the diameter of HeLa cells for trapping for parallelized activity.^{111,124} These channels were easy to fabricate, and an array of trapped cells could be monitored simultaneously during EP to optimize conditions. With this strategy, not only did localized EP occur at a low voltage through the trapping channel, but also, anionic molecules were delivered through the channel more efficiently via electrophoresis.¹²⁶

After these fundamental works, there was a desire for device fabrication that was less specialized and amenable to higher-throughput processing, as conventional complicated nanofabrication steps were prohibitive to broader adoption of subcellular channel devices. For example, Lu and colleagues filled straight microchannels with nonconductive silica microbeads to trap *Escherichia coli* and hard-to-lyse mycobacteria for cell lysis.^{127,128} The narrow gaps between the beads achieved the same effect in locally increasing the electric field intensity 3× compared to open channels. Commercially available poly(ethylene terephthalate) (PET), alumina porous, or polycarbonate (PC) membranes with randomly distributed micro-/nanopores have been modified to achieve similar localized EP effects. Works by Fei et al.^{129–131} and Ishibashi et al.¹³² demonstrated the integration of porous membranes into EP devices to enhance the electric field applied on immobilized cells on the membrane surface. A second negatively charged porous membrane was placed above the cell layer to confine DNA to areas close to the cells.^{129–132} The charged membrane restricted gene diffusion away from the cells during EP, causing increased local DNA concentration and transfection efficiency. Kang et al. developed a localized EP device (LEPD) using a PC porous membrane coated with poly-D-lysine for adherent cell EP.¹³³ The process was gentle enough to culture and transfect fragile differentiated neuronal stem cells on the integrated microfluidic platform. Mukherjee et al. found that cells in hypoosmolar buffers in the LEPD had higher membrane tension, which caused wider, more stable cell membrane pore formation and more uniform transport of large cargos.¹³⁴ Cao et al. designed an affordable nanopore EP device using a water filter PC membrane with 100 nm pores to deliver macromolecules into both adherent and centrifuged suspended cells.¹³⁵ Only 0.05% of the cell membrane was in contact with the nanopores, so most the cell membrane maintained its integrity with an applied voltage. Islam et al. used a multilayered device divided by a PC membrane to collect *E. coli* for lysis.¹³⁶ The bacterial suspension was loaded above the membrane, and 0.5 μm cells were electrophoretically driven to plug 0.4 μm pores prior to EP at elevated electrical conditions. Additional photolithographic membrane patterning helps to spatially organize cells and apply more uniform conditions. Microwells have been patterned on top of the membrane to organize a subset of adherent cells for efficient optical observation.^{131,132,137,138} Small, 20 μm microwells have been fabricated to compartmentalize single cells for characterization of thousands of cells per experiment.¹³⁷ Even smaller, subcellular channels have been lithographically patterned on top of porous membranes to control the number of nanopores in contact with each cell.^{130,139} These wells helped better control the uniformity of delivered macromolecule dosages than bare membranes because pore density per cell was consistent.

Incorporating nanofabrication protocols has enabled static EP with more control of cargo delivery. For example, nanochannel EP (NEP) was proposed for single-cell, dose-controlled static EP. In the initial study, Boukany et al. bridged two microchannels with a 90 nm nanochannel fabricated using DNA combing (Figure 5A,C).¹⁴⁰ Individual cells were aligned close to the nanochannel using optical tweezers for the delivery of a range of charged cargos. Active cargo injection through the nanochannel with electrophoresis permitted controllable biomolecule dosage based on the applied pulse length. Electrolysis effects on cell viability were minimal because cells were placed far from the electrodes; thus, electrolysis byproducts were unlikely to diffuse from the electrodes to the cells.¹⁴¹

Nonendocytic uptake of larger cargos, such as plasmids, into the cell improved dosage control and enabled more rapid transcription compared to delivery with bulk EP. Early studies used 2D NEP devices for precise and uniform delivery of macromolecules.^{141–145} Higher-throughput 3D NEP systems have since been developed using microchannel^{114,146} and nanochannel arrays (Figure 5A).^{35,139,147–150} The configuration of these devices is similar to previously described membrane devices, except that the subcellular channels here are more orderly. Subcellular channels are accessible from a single microchamber for parallelized cell to subcellular channel pairing. Delivery cargos are loaded in a separate microchamber beneath the subcellular channel array, and the channel fabrication density is controlled to regulate the number of channels per cell to maintain dosage control. 3D NEP devices have demonstrated biomolecule delivery into hard-to-electroporate cell types, including natural killer (NK) cells,¹⁴⁷ cardiomyoblasts,¹⁴⁸ and primary cardiomyocytes.³⁵ This principle has also been applied for the delivery of cargos and the formation of exosomes from adherent cells.¹⁵¹

Nanostraws achieve the same localized EP effect with hollow needle nanostructures protruding from planar membranes (Figure 5A). Xie et al. first developed the nanostraw EP system (NES), in which 1.5 μm tall, 250 nm wide aluminum oxide nanostructures separated cells and biomolecule suspensions (Figure 5D).¹⁵² Adherent cells cultured on the patterned surface maintained high cell viability while engulfing 10–50 nanostraws. The permeabilized cell membrane region was small enough to recover within 10 s after the last electrical pulse, which improved cell viability.¹⁵² Cao et al. optimized the NES and demonstrated tight dosage control for a plethora of cell types and cargos.¹¹³ The platform was robust enough to culture several hard-to-transfect primary cell types, including human-induced pluripotent stem cell (iPSC)-derived cardiomyocytes, human embryonic stem cells, human fibroblasts, mouse glia cells, and mouse primary neuron cells with 60–80% transfection efficiency. Importantly, the protocol for electroporating these cell types was identical to that for the immortalized HEK 293 cell line, proving the universality of this approach without additional process optimization. Fang et al. optimized EP conditions using a custom image processing software that determined cell viability and EP efficiency via fluorescence images of cells on the NES membrane.¹⁵³ The surface of nanostraws may be modified to specifically capture cancer cells^{154–156} and/or be repurposed to study intracellular contents.^{154,157–159} Tay and Melosh determined that localized EP with nanostructures was more efficient and less damaging to cells compared to viral, chemical, and bulk EP methods.¹¹⁵ Pretreating the surface can reduce the potential cytotoxicity of nanostructures to certain sensitive primary cell types. Pop and Almquist found that the nanostructures were harmful specifically when culturing primary basal keratinocytes on-chip without additional treatments.¹⁶⁰ Cell viability significantly increased by adding a fetal bovine serum coating, which reduced membrane perturbations caused by the nanoscale protrusions.

Nanofountain probes (NFP) have also been fabricated for more spatially controlled single-cell EP (Figure 5E).^{161–165} NFP chips are designed with a 750 nm tip opening, a ~ 3 pL microreservoir, and a connection to a conductive wire. Low-voltage, bilevel pulses are sufficient to permeabilize individual cells with good cell–probe contact. NFPs can be positioned with a nanomanipulator for lower-throughput, but spatially precise, EP of single cells. NFPs enable selection of specific cells for processing, which could be especially

useful to target specific cells in heterogeneous populations. Recently, an image processing algorithm was created to identify cells in a field of view and deliver cargos using the NFP for faster automated processing.¹⁶⁵

3.1.1.2. Nonplanar Micro-/Nanoelectrodes: Alongside innovations in channel design, novel electrode geometry helps to locally amplify the electric field. Specifically, electrodes with sharp or pointed features are subject to enhanced electric fields at their tips. Relevant electrode geometries include 1D nanofibers or thicker 3D electrodes that still maintain high aspect ratios and conductive microparticles. With an applied voltage, charges spread out on the conductive surface and gather at the electrode tip, as it is furthest from other surfaces. The accumulated charge generates a large surface charge density and electric field intensity. Importantly, this phenomenon only enhances the electric field close to sharp electrode tips, so electric fields that are sufficiently high for pore formation are generated only close to these features. Static EP devices position cells close to the features for localized, efficient membrane poration.

3D hollow nanoelectrodes harness the field enhancement at needle tips for efficient local EP at low voltages. Unlike NES, the nanostructures themselves are fabricated from conductive materials to serve as the electrodes for electric field enhancement (Figure 6A). Hollow nanoelectrodes are used to electroporate nearby cells and act as the path for intracellular delivery. Caprettini et al. developed hollow, 700 nm wide nanoelectrodes arrays that achieved highly efficient EP of adherent cells with applied voltage pulses at 2 V.¹⁶⁶ The nanoelectrode sharpness aided tight cell adhesion, EP, and diffusion of biomolecules through the nanoneedle into the cell. The 3D hollow nanoelectrode system was gentle enough for EP of human iPSC-derived cardiomyocytes.¹⁶⁷ Caprettini et al. used the hollow nanoelectrodes for surface-enhanced Raman scattering (SERS) to study intracellular contents.¹⁶⁸ The nanoelectrode served multiple roles of providing biomolecule passage for electrophoretic delivery and amplifying SERS signals for cargo monitoring. The SERS system detected changes in membrane configuration, amino acid vibrations, and nuclear poration. Huang et al. used hollow nanoelectrodes for on-demand delivery and monitoring of $25 \times 90 \text{ nm}^2$ gold nanorods into cells.¹⁶⁹ Wire electrodes on the cell and biomolecule channels, separate from the nanoelectrodes, generated electrophoretic biomolecule movement, allowing for on-demand, single nanorod delivery, detectable using SERS.

Solid 3D nanoneedles achieve the same electric field enhancement at their tips as hollow nanoneedles (Figure 6B). Riaz et al. designed scalable, $1 \mu\text{m}$ tall nanospikes (NSPs) that demonstrated improved cell viability compared to a parallel plate equivalent.¹⁷⁰ The NSP aspect ratio was controlled by changing anodization parameters, and higher aspect ratios enabled up to $\sim 9\times$ higher maximum generated electric fields than planar electrodes. The primary limitation of further enhancement is fabrication complications at higher aspect ratios. Liu et al. powered solid nanoneedles with a triboelectric nanogenerator (TENG) for highly localized cell EP.¹⁷¹ Electrical pulses applied with the nanostructures increased the EP efficiency of adherent cells $>4\times$ compared to mechanical perturbations from the nanoneedles alone. The system enabled gentle EP of hard-to-transfect primary rat bone mesenchymal stem cells. Madiyar et al. used randomly dispersed, vertically aligned carbon nanofiber nanoelectrode arrays to reversibly electroporate vaccinia virus samples.¹⁷² The 1D

electrodes first used dielectrophoresis (DEP) to attract viral particles before generating an electric field upward of 10^5 V/cm for the delivery of small molecules. Liu et al. similarly added carbon nanotubes on the surface of micropillar electrodes,¹⁷³ which provided many locally amplified regions and improved EP over previous device iterations without the nanostructures.^{174,175}

Localized EP is also achievable using suspended microparticles that act as mobile point electrodes. Half metal, half dielectric Janus particles were fabricated to trap and electroporate bacterial¹⁷⁶ and mammalian cells.¹⁷⁷ When magnetically drawn to an indium tin oxide (ITO) electrode, Janus particles generated an enhanced electric field between the electrodes on the bottom substrate and hemisphere of the metal and dielectric surfaces, respectively. At different voltages and AC frequencies, cells were collected at these regions via DEP and electroporated for cargo delivery. The application of positive DEP (pDEP) forces aided the aggregation of plasmids on the Janus particle alongside single-cell capture, which improved transfection efficiency due to the increased local concentration of DNA.¹⁷⁷ Moreover, these mobile electrodes can be controlled to transport smaller cells or locally EP a larger cell with spatial precision on its membrane.

3.1.2. Microscale Cell Positioning.—In tandem with recent innovations in electric field enhancement based on micro-/nanostructures, cells must be placed at predefined positions to monitor single-cell activity or maximize EP efficiency because the electric field strength rapidly wanes away from electrode or device features, as outlined in section 3.1.1. Static EP devices have integrated a range of microfluidic techniques to encourage precise cell alignment with device features with increased throughput.

3.1.2.1. Passive Methods.: Passive techniques rely on biochemical processes, gravity, or hydrodynamic forces generated by microstructures to arrange cells rather than secondary forces generated by external equipment. Generally, these strategies are effective in positioning cells without significantly increasing device complexity. The easiest method to implement simple and scalable cell positioning is to incubate cells in the microfluidic system and allow cells to adhere to the substrate.^{120,133–135,139,152,171} Cell adhesion may be aided by pretreating the device with a protein coating,¹³⁵ a common practice for cell culture, or nanofibers.¹³¹ Adherent cells may be cultured for prolonged time periods and periodically transfected.¹³⁸ Alternatively, the earliest microscale EP chips used a gentle vacuum to trap cells to micropores^{38,109,111,121–124,126} and remain a viable option for cell positioning on micropores.^{114,129,130,148} Cells are hydrodynamically trapped by the negative pressure applied across micropores. Hydrodynamic forces generated at high flow rates have been used for the trapping of cells in rectangular chambers for EP.^{178–181} Cells were trapped at higher flow rates using inertial microfluidics, where inertial lift forces cause larger cells to stay trapped in microvortices within chambers patterned with interdigitated electrodes (Figure 7A). This configuration offers the benefit of continuous flow to flush out electrolysis byproducts generated during EP while keeping the cells circulating within the chambers for further analysis. Additionally, rare cells in biologically relevant mediums, such as blood, may be separated based on physical cell properties for EP.¹⁸¹

Structural elements have been designed to assist with cell loading. A simple dip trapping technique has been optimized for high-throughput cell alignment with U-shaped caps to capture individual cells above individual nanopores (Figure 7B).³⁵ When the membrane was dipped in a cell suspension solution, cells naturally settled on each cap and remained lodged during withdraw. An opposing U-shaped structure has been implemented to trap cell pairs in an orderly array for observation of EP and fusion.¹⁸² The combination of an applied vacuum and a pyramidal pore shape allowed for better cell alignment compared to planar pores, so EP could be achieved at lower voltages.¹¹⁴ Particular device geometries are designed for device centrifugation load cells and promote tight adhesion.^{115,135,142,143} Microwells are designed to guide single cells toward nanochannels during centrifugation.¹⁴³ Centrifugation is highly scalable, fast, cheap, and suitable for suspended cells, though a direct comparison revealed that centrifuged cells require stronger EP conditions for permeabilization than cells that naturally adhere to membranes due to worse cell–pore contact.¹³⁵

Microstructures may be covered with additional surface modifications to improve cell capture efficiency. Zhou et al. constructed a degradable, porous nanoflower structure for cell capture and EP (Figure 7C).¹⁵⁶ Submerging ZnO nanostraws in a magnesium buffer solution altered the structure into a nanoflower with cracks large enough for large biomolecule passage. The structure was functionalized with anti-epithelial cell adhesion molecule (anti-EpCAM) antibodies to promote adhesion with cancer cells overexpressing EpCAM. The nanoflower could later be degraded for processed cell release. He et al. added branched networks on nanostraw surfaces to mimic the extracellular matrix and improve cell–post interactions.¹⁵⁴ The nanostructures were further coated with anti-EpCAM antibodies for cell targeting and assaying without cellular release. Together, these strategies vastly improved rare cancer cell isolation from blood on the nanostraws for subsequent EP. Antibody-labeling is not always effective when sample cells heterogeneously express target markers. Thus, Feng et al. incubated cancer cells spiked in blood on a branched nanostraw device for several hours to achieve stronger cell adhesion to the nanostructures.¹⁵⁵ The adhered cancer cells remained on the chip during a subsequent wash step to flush other blood cells out of the system. Cancer cells were later released from the device by further increasing the flow rate and hydrodynamic shear forces to strip the cells away from the nanostructures.

3.1.2.2. Active Methods.: Active cell organization methods using secondary forces are versatile and effective in providing more spatial control of cells. These on-chip techniques incorporate optical, electrical, and magnetic forces to reversibly bring cells closer to electrodes or microscale features. For single-cell applications, optical tweezers have demonstrated high precision in cell manipulation.^{140,141,143–145,183,184} Optical tweezers trap cells using a focused, movable laser beam to align cells near desired features.¹⁸⁵ Although optical tweezers are useful for precise manipulation, their low throughput is a significant limitation. It takes 3–5 min to align a single cell, parallelization is challenging, and optical forces may not be sufficiently strong to easily move particularly sticky cells.¹⁴³ Instead, DEP forces have been used frequently to position cells in microscale EP devices.^{139,147,149,172,176,186–193} Unlike optical tweezers, DEP forces are effective for large numbers of cells in parallel. DEP forces are exerted on polarizable particles

using a nonuniform electric field to manipulate cells at the microscale and have been widely used for microfluidic cell sorting.^{194,195} The earliest example of DEP to assist microscale EP used triangular electrode arrays to draw cells toward sharp-edged electrodes in a microfluidic channel for yeast, bacteria, plant, and mammalian cell lysis at low voltages.^{186,196} Kim et al. used DEP forces to guide bacteria into a microwell array with single-cell trapping.^{197–199} The DEP forces were stronger than bacteria motility to restrict cells from swimming out of the microwells. DEP forces were also used to attract and center cells in lateral microchambers for homogeneous EP.¹⁸⁷ Madiyar et al. used DEP forces to attract viral particles toward nanofibers prior to EP.¹⁷² Punjiya et al. manipulated cell position by changing the flow rate and drag forces applied to cells in relation to DEP forces generated using half-ring and flat electrodes.¹⁸⁹ In subcellular channel devices, DEP is a label-free positioning technique that can be applied by changing voltage pulses.^{139,147,149} In other systems, dedicated DEP electrodes have been fabricated on-chip for single-cell loading over separate EP electrodes.^{188,200} Jayasooriya et al. used DEP forces to align large numbers of primary T cells along the gap between interdigitated electrodes to apply more uniform conditions across all samples.²⁰¹ Magnetic forces can also be applied to reposition cells conjugated with magnetic beads.^{146,202} Using patterned, on-chip magnetic features, magnetic tweezers may be formed for parallelized loading of cells onto static cell arrays (Figure 7D).¹⁴⁶ In contrast, Wu et al. actively steered Janus particles using a movable magnet under ITO electrodes.^{176,177} The magnet brought the particles close to the electrodes to help generate localized electric field amplification for cell aggregation and EP. Uniquely, this platform was advantageous in developing an integrated cell selection, navigation, and EP workflow by moving the magnet and applying different electric pulse conditions.

3.1.3. Rapid Parameter Optimization.—A recurrent step in EP operation is a trial-and-error-based-optimization of electric field parameters to balance cell viability and EP efficiency. Microscale EP offers better control of electric field strength and allows for testing of different conditions simultaneously with lower reagent use. Pioneering works from Huang and Rubinsky incorporated optical and electrical monitoring of single cells during EP, but this required sequential experiments to optimize experimental conditions.³⁸ The incorporation of transparent PDMS elements improved the ease of optical detection of EP.¹¹⁰ Recently, single-cell tracking capabilities with static EP have facilitated parallelization of experimental conditions to more rapidly assess optimal EP parameters.^{109–111}

A range of electric field strengths can be tested within a single experiment to compare the extent of cell permeabilization. Early on, Kim et al. demonstrated this benefit by bridging inlet and outlet electrodes with five microchannels of varying lengths.²⁰³ Since electric field strength is dependent on the distance between electrodes (eq 1), different electric field conditions are simultaneously generated between the different microchannels for parallelized trials. A continuous electric field gradient was generated across bilaterally converging devices, as decreasing cross-sectional areas from the wall curvature increase the electric field (eq 5).^{204,205} Tuning the degree of channel curvature affected the steepness of the gradient. Confluent cell suspensions were loaded into the channel and electroporated to deliver dye molecules. The physical boundary of fluorescent and nonfluorescent cells

represented the threshold electric field strength for reversible EP. Bilaterally converging electrodes were also used to generate a gradient of electric field conditions based on the decreasing distance between the electrodes.²⁰⁶ Different pulse conditions could be tested alongside different electric field strengths to determine the most energy efficient conditions for cell inactivation.

Array-based techniques are also informative in testing multiple experimental conditions or different cargo delivery without the need for repetitive and labor-intensive experiments. The NFP system is unique in its control of electrode positioning on cells.^{161–165} Yang et al. cultured cells on a protein patterned substrate to generate separate cell wells within the same field of view.¹⁶⁴ Monoclonal cell lines were generated by stably transfecting individual cells in each well and allowing them to proliferate. The patterned colonies could be used to compare different cargos or EP conditions in parallel on the same plate. Since electrodes interfacing with each cell well/drop are independently controlled, multiple EP parameters could be tested in parallel in a single experiment. Bian et al. loaded cells into an open-faced microwell array patterned with electrodes for parallelized cargo delivery.²⁰⁷ The sealing glass slide was spotted with droplets containing different biomolecules and carefully aligned for to seal each well with no cross contamination. Zhang et al. electroporated cells in separate open wells to test different EP conditions.²⁰⁸ By adding dyes at different time points, the membrane resealing time was determined to be ~10 min.²⁰⁸

3.2. Continuous Electroporation

Continuous EP systems permeabilize a constant stream of randomly dispersed cells in flow while exerting more uniform electric field conditions than bulk EP. Unlike in static EP, electric fields in continuous EP are often not as spatially localized, so electric fields are enhanced across larger areas of the fluidic chamber. Harsher conditions generate more toxic electrolysis byproducts, but continuous systems maintain constant flow to minimize the buildup of contaminants. Additional measures have been used to further reduce the cellular damage for reversible EP. Continuous EP devices are intrinsically high throughput due to the constant cell suspension flow. In practice, continuous microscale EP devices have demonstrated processing rates up to 10^9 cells/min while maintaining high EP efficiency.²⁰⁹ In this section, we examine current research to improve continuous EP device performance.

3.2.1. Electric Field Enhancement.—Continuous EP devices have incorporated design choices reminiscent of static EP systems to increase electric field strength. However, cells are not immobilized at the optimal location with the maximum electric field strength. Innovations are geared toward localizing electric field strength to defined regions of the microchannel where cells pass. Below, we discuss different measures used in continuous EP devices to achieve sufficient electric field strength at lower voltages.

3.2.1.1. Channel Constrictions.: Channel constrictions have been designed to permeabilize cell membranes for reversible EP^{100,210–212} and lysis^{213–219} of cells in defined flow-through regions without necessitating high voltages. Constrictions are capped by wider microchannels that facilitate the continuous flow of cell suspensions and serve as entry points for electrode placement. The operating principle of channel constrictions is

guided by eq 5, where narrow microchannels exhibit the highest electric field intensity, so cells are electroporated when traveling through this region.^{220,221} These microchannels are just wide enough for the passage of single or small numbers of cells at a time, which allows easier single-cell observation.²²² By remaining comparable in size to the diameter of target cells, the microchannel provides the maximal electric field enhancement and minimizes undesirable cell–cell interactions during electropermeabilization. EP conditions are affected by device geometries (i.e., constriction cross-sectional area, length, and count) and operational parameters (i.e., flow rate and applied voltage).

Simple channel constrictions are easy to fabricate and have demonstrated considerable success for continuous EP. Ye et al. developed a single narrow constriction for EP where the channel was 60% the diameter of an average A549 cell (Figure 8A).²²³ Thus, each cell formed a tight seal while passing through the constriction, and applied voltages were as low as 3 V. The leading and lagging ends of each cell surpassed the threshold TMP for permeabilization and intracellular delivery was achieved with up to 96% efficiency. Other works have implemented repeated constrictions in series to mimic a series of pulses with a DC voltage source (Figure 8B).^{210–212,224–227} Simple DC voltage source can be used to electroporate Chinese hamster ovary (CHO) cells with 75% efficiency under flow rate of 1.87 mL/min.²²⁵ Pudasaini et al. fabricated an array of insulated cylindrical micropillars to act as a yeast lysis region amid continuous flow.²²⁸ The narrowest region between two pillars generated a locally enhanced electric field to electroporate passing yeast cells irreversibly. At fixed conditions, the pillars enabled 56% cell inactivation versus 24% in an equivalent device without the constricted regions. Later, Pudasaini et al. found that rhombus micropillars caused higher electric field enhancement relative to straight channels (29×) and cylindrical micropillars (13×) due to their sharp corners.²²⁹ Packed microbeads achieved a similar feat while avoiding the need for micropillar fabrication.²³⁰

Within a channel constriction, the electric field distribution can be further altered by changing the cross-sectional dimensions. Garcia et al. found that channels with nonuniform cross-sectional areas have a higher maximum electric field (15–17 kV/cm) compared to that of a uniform constriction channel (9 kV/cm) with the same minimum feature width (Figure 8C).²³¹ Bilaterally converging constrictions were the most consistent in electroporating different strains of *E. coli* with >1000× better throughput than that of cuvette EP. Gomaa et al. reported the first demonstrated transfection of *Priapulius caudatus*, a marine protist, and compared the effectiveness of using the bilaterally converging microfluidic device and a cuvette.²³² The microfluidic device had the highest transfection efficiency with 100× better throughput than bulk EP.

3.2.1.2. Novel Electrode Design.: Electric fields at the edges of micro-/nanostructures in EP systems are sufficiently enhanced to efficiently permeabilize cells at lower voltages. However, field enhancement is restricted to regions close to the electrodes, as with static EP devices. The same issue occurs with 2D planar electrodes, where the electric field exponentially decays from the plane of the features. Maintaining cell position close to the electrodes is possible in static EP systems, as discussed in section 3.1.2, but is an added challenge in continuous methods. Pressure-driven flow in a channel causes buoyant spherical particles to migrate away from channel walls with a lower flow rate,²³³ so most cells

flow distant from channel walls and patterned electrodes on the wall surfaces. Continuous microscale EP devices address this issue by adjusting electrode placement or manipulating cell flow paths to force cells to move closer to electrodes without obstructing flow. This effort significantly improves device performance while maintaining high throughput.

One strategy for more thorough EP is the addition of multiple 1D electrodes within a microchannel. 1D electrodes are effective in locally enhancing the electric field at their tips so long as cells can reliably come in close contact. Shahini and Yeow used a commercial substrate with randomly aligned carbon nanotubes as an electrode to lyse bacteria²³⁴ and mammalian cells.²³⁵ The localized field enhancement at the nanoelectrodes' tips enabled more efficient cell lysis using half of the voltage needed without nanostructures. Poudineh et al. used similar ideas when patterning bands of 1D metal electrodes and applying alternating polarities on each strip (Figure 9A).²³⁶ High-throughput bacterial cell lysis (1600 cells/s) was achieved with 2.5× stronger electric fields than a planar electrode equivalent. A different guiding strategy involved flowing cells through meshes or sponges decorated with high-aspect-ratio nanoelectrodes. The porous structures enable flow-through of cell suspensions for high-throughput EP, and the decorated nanostructures provide a surplus of locations with an amplified electric field. Liu et al. modified flexible polypyrrole microfoam with silver 1D nanowires for hand-powered EP with a TENG (Figure 9B).²³⁷ The nanowires generated a 90 000× higher electric field intensity at their tips compared to nondecorated microfoam at 20 V. In this system, microfoam pores were ~300 μm wide so that throughputs of 10⁵ cells/min were achievable without cell clogging. Microfoam has also been decorated with carbon nanotubes,²³⁸ Cu₃P nanowires,²³⁹ or CuO nanowires^{229,240–243} with applications in cell inactivation for water disinfection. Nanostructures were densely packed throughout the microfoam for ample contact surface areas, which improved disinfection efficiency during device operation.

Alternatively, cells may be forced to interact with electrodes by changing the electrode or channel geometry. Lu et al. used 3D carbon electrode pillars so that cells flowed closer to the electrodes.²⁴⁴ This caused a leukocyte lysis efficiency (>30%) higher than that of 2D electrodes at low voltages (10 V). Mernier et al. employed 3D carbon electrode pillars to achieve a similar effect.²⁴⁵ These carbon electrodes were not only easier and cheaper to fabricate but also more electrochemically stable than metals. Up to 600 μL/min of samples at 10⁸ cells/mL were processed with 90% lysis efficiency. Experton et al. electroporated *E. coli* by forcing cells through hollow 3D gold microtubes (Figure 9C).²⁴⁶ While the microtubes generated the highest electric field gradient rings at their edges, most cells did not interact with the electrode edge, so the bulk electric field within the microtubes was only considered when optimizing device geometries. Device performance was 20× more efficient and had 500× higher throughput relative to commercial systems. Chen et al. electroporated cells passing across one side of a metal-coated, porous membrane.²⁴⁷ Deformable cells were squeezed through a short microchannel to ensure consistent contact between the cells and electrode. The electric fields at the electrode edges were 3.2× larger than the bulk electric field strength, so cells could be electroporated at low voltage conditions (1–4 V). Lo and Lei found that a long rectangular channel with an array of interdigitated electrodes caused Joule heating and electrothermally induced flow, which brought red blood cells (RBCs) close to the electrodes and improved cell lysis.²⁴⁸

3.2.2. Minimizing Cellular Damage.—Continuous EP prevents the accumulation of electrolysis-derived heat, bubbles, and ions while fluid flows throughout the device. Additionally, electroporated cells and generated byproducts are diluted with cell culture media immediately after EP to create more favorable conditions for recovery. In some devices, the simple addition of flow is sufficient to improve cell viability. Lin et al. first reported in 2001 that cell viability after continuous EP was increased with higher flow rates because of greater heat dissipation.²⁴⁹ del Rosal et al. observed a negligible temperature difference within a channel constriction at flow rates of 21 $\mu\text{L}/\text{min}$, compared to a 16 °C temperature increase at low flow rates ($\sim 2 \mu\text{L}/\text{min}$) (Figure 10).²⁵⁰ Zu et al. previously designed a dense array of micropillar electrodes such that cells were exposed to a different number of pillars based on their size.¹⁷⁴ The addition of flow to this electrode geometry increased cell viability by 10–15% due to the constant flushing.¹⁷⁵

The concentration of toxic EP byproducts is the highest near electrode surfaces, so cell viability can be improved if cells are separated from the electrodes. Kim et al. placed highly conductive, polyelectrolyte salt bridges between flowing cell suspensions and Ag/AgCl wire electrodes.²⁵¹ Electrolysis did not decrease cell viability because generated bubbles were not in contact with cells and easily vented. Similar objectives were achieved using highly conductive sheath flow for hydrodynamic cell positioning to separate cells and electrodes. It is compatible with continuous EP because it only relies on the constant fluidic force, so no strong external controllers are needed. Wei et al. first introduced a sheath buffer layer in laminar flow to isolate cells from electrodes and showed enhanced EP efficiency and cell viability.²⁵² Lissandrello et al. used a similar strategy but with a high-conductivity buffer as sheath flow, separating the electrodes from cell media to concentrate the electric field at the cell suspension and minimize the voltage drop at the sheath layer.²⁵³ Flow rates were controlled to remain in the laminar regime to limit sheath flow mixing with cell media. Kang et al. shielded hard-to-transfect microalgae from parallel plate electrodes by introducing 3D sheath flow, created by stacking patterned layers of polyimide film (Figure 11A).²⁵⁴ Experiments comparing microalgae EP with and without the sheath layers revealed 30% higher cell viability when cells were hydrodynamically focused away from electrodes. The sheath layer additionally aligned cells at the center of the channel in both lateral and vertical axes for more uniform electric field application. Luo and Yobas added a series of microcapillaries between outer buffer channels and a center cell suspension channel (Figure 11B).²⁵⁵ Flow rates were controlled so that the buffer/cell suspension interface was located within the microchannels to minimize the crossover of buffer to cell suspension and fluidic perturbations. Cell media and sheath layers did not mix within the microcapillaries, so generated toxins did not affect passing cells or affect viability. Huang et al. devised a curved channel that uses a sheath layer and Dean flow to separate toxins from cells (Figure 11C).²⁰⁹ The relative cell and sheath flow positions controllably changed within the channel due to the Dean flow. Thus, ions generated at the electrodes were kept separate from the flowing cells and rapidly neutralized. This device could process 10^7 primary cells/min due to the high flow rates needed for Dean flow.

Long-term exposure to EP buffers can be harmful to cells, so the dwelling time in the buffer should be minimized.^{92,256–259} Microfluidic technologies help to perform solution

exchange on-chip to minimize buffer exposure and increase cell viability. Lee et al. used micropost array railing (μ PAR) structures to exchange cell culture media with EP buffer on-chip for EP with optically induced electrodes (Figure 12A).²⁵⁹ μ PAR structures consisted of tightly packed pillars that gradually confine cells into central streamlines with 80% transfer efficiency. Active methods have also been designed for cell manipulation with higher precision. Hsi et al. devised a straight channel with central EP buffer flow and sheath cell suspension streams controlled by acoustophoresis (Figure 12B).²⁵⁸ Cells continuously migrated from the outer streams into the EP buffer, away from the electrodes, using ultrasonic waves without solution mixing. Immediately after EP, cells in the buffer were diluted in cell culture media, lowering the residence time in the hypotonic environment to under 3 s. This device demonstrated 87% transfer efficiency into and out of the EP buffer with throughputs as high as 1.2×10^5 cells/min. Microfluidic manipulation techniques are also applicable to sort live cells from dead cells after EP. Wei et al. used DEP forces to manipulate the cell viability of the collected sample after EP.²⁶⁰ After passing EP electrodes, cells were focused in more uniform streamlines with a sheath buffer layer, similar to their previous device.²⁵² Focused cells experienced DEP forces generated from angled electrodes (Figure 12C). Intact, viable cells were polarizable and deflected toward a collection outlet, whereas dead cells flowed out of the waste outlet. DEP sorting improved the overall EP performance of several hard-to-transfect cell types.

3.3. General Advances

Recent engineering progress in microscale EP systems includes improvements relevant to both static and continuous modalities. These developments include efforts toward improving accessibility in designing and fabricating devices in non-specialized laboratories. In addition, more broadly applicable innovative techniques are developed to reduce cellular toxicity and improve EP performance. Such strategies are outlined in this section.

3.3.1. Electrode Passivation.—Electrodes in microfluidic systems are usually fabricated out of gold, aluminum, platinum, or ITO, which do not inhibit electrolysis byproduct formation. Passivation layers have been added on top of electrodes to shield cells from damaging EP byproducts. In several studies, nanogap planar ITO electrodes were passivated with a SiO_2 layer for localized single-cell EP.^{117–120} Pulses of 2–10 V caused ITO electrode degradation in a nonpassivated device, which was evident in an electrode color change, significant bubble formation, and cell death.¹¹⁹ A SiO_2 -passivated device did not display such effects under the same conditions and had increased cell viability after EP. TiO_2 has also been proposed as a suitable dielectric material for titanium electrodes.^{77,261,262} This layer limits the passage of off-target currents through the electrolyte solution. Wimberger et al. found that passivated electrodes led to more consistent cell inactivation at different electric field strengths than exposed electrodes because stochastic electrolysis effects were minimized (Figure 13A).²⁶² 18 μm thin layers of PDMS have also been used as a passivating layer for interdigitated electrodes.²⁶³ The PDMS layer protected electrodes under conditions as extreme as an applied DC voltage of 800 V for several hours (Figure 13B). Higher voltages were necessary for EP because the PDMS layer dampened the electric field experienced by the cells. Talebpour et al. used surface-enhanced blocking (SEB) electrodes with a dielectric layer to improve microbial

lysis efficiency.²⁶⁴ Importantly, the dielectric layer was patterned with micro-structures to increase its surface area and capacitance, which lengthened the surface charging time and period of enhanced electric field.

3.3.2. Improving Permeabilization Uniformity.—The permeabilized area of the cell membrane is dependent on the angle between the electric field axis and the cell membrane in a uniform electric field (eq 3).^{68,72,184} Cells treated with parallel plate electrodes are primarily permeabilized on its electrode-facing poles. Other configurations, such as interdigitated electrodes, have a similar imbalance in poration locations across the cell membrane.²⁶⁵ A suboptimal number of generated pores leads to fewer points of entry for biomolecules into the cell. Longer poration durations, creating a higher density of pores, are required to achieve a desired intracellular concentration, but they reduce cell viability. Spreading the pore distribution across the entire cell membrane helps to create a higher number of entry points across the entire cell membrane, enabling EP with milder conditions. Microscale EP devices are designed to enable this gentle EP with more efficient experimental workflows.

An imbalance of permeabilized regions on the membrane is common in continuous systems because cells undergo laminar flow, which minimizes cell perturbances. Electrodes patterned on the bottom of the channel exert a nonhomogeneous electric field on cells, so only a portion of the cell is porated. Continuous EP accommodates hydrodynamic cell manipulation to produce cell rotation and generate more evenly distributed pores in flow. Wang et al. first utilized the rotation of cells using Dean flow generated in a spiral-shaped channel for efficient DNA delivery.²⁶⁶ The combination of rotation and transverse advection from the curved channel caused plasmids to be delivered more uniformly across the cell surface compared to microscale EP in a straight channel. This vortex-assisted EP method almost doubled the transfection efficiency of CHO cells. Bhattacharjee et al. designed a serpentine microfluidic channel with repeated expansions and constrictions to change the polarity of the electric field to the cells while traveling along the channel.²²⁶ Hyperpolarized and depolarized halves of cells flipped at every turn to maximize the permeabilized area of the cell membrane for improved delivery homogeneity. Zheng et al. used pinched flow with a sheath layer to control cell rotation in flow (Figure 14A).²⁶⁷ Particles experienced shear forces and rotated near the wall in laminar flow due to nonslip boundary conditions. By increasing the ratio of shear flow rate to cell suspension flow rate, the cell-containing stream was narrowed, and cells experienced greater rotation. This increased the homogeneity of PI delivery compared to laminar conditions with minimal cell rotation.

EP-induced pores can also be more evenly distributed by applying permeabilizing forces in multiple directions. Long-sine-Parker et al. combined EP with sonoporation for more evenly distributed pore formation around the cell.²⁶⁸ In a straight channel, cells were exposed to a horizontal electric field and a vertical ultrasonic wave. The combined orthogonal electric fields and acoustic waves generated pores on different axes of each cell and yielded a higher EP efficiency (95%) compared to that of EP (77%) or sonoporation (84%) alone while maintaining high viability. Zhu et al. constructed an EP system for 3D cell cultures with multidirectional electric field application.²⁶⁹ Electrodes were positioned on four sides of a 25-cell spheroid, and the electric field was programmed in a different direction for each

pulse (Figure 14B). EP efficiency was higher when fields were applied in four different directions (~80%) compared to maintaining the same polarity (~40%).

3.3.3. Droplet Encapsulation.—Droplet microfluidics involves the encapsulation of cells in fluid droplets with diameters ranging from tens to hundreds of micrometers.^{270,271} Integration of EP with droplet microfluidics offers benefits from both techniques. Individual droplets containing cells and reagents are isolated from other empty droplets, so entire EP and screening workflows are performed continuously without cross contamination. The ratio between cells and biomolecules is more controlled within small discrete droplets compared to that in continuous, bulk fluid volumes.²⁷² Cells and cargo molecules within a droplet are quickly mixed during droplet formation and EP, so there is an increased likelihood of cargo molecules interacting with permeabilized areas of the cell membrane. Finally, the high surface area to volume ratio of each droplet can improve cell viability by rapidly dissipating excess heat.²⁷³ Different forms of droplet microfluidics that mirror continuous and static EP have been effective in cell EP.

Continuous droplet microfluidic devices have been adapted for microscale EP. In this modality, cell-containing droplets are continuously formed in an immiscible fluid. Thus, high-throughput encapsulation for cell EP and screening is achieved solely by increasing operation time rather than device size. Ji et al. first reported the EP of cells encapsulated in droplets.²⁷² Yeast cells were suspended in aqueous phase and formed picoliter droplets in a T-junction channel. Droplets experienced an electric field high enough to electroporate cells only when they are simultaneously in contact with two micro-patterned electrodes while migrating across the channel. This design was versatile to electroporate plant²⁷³ and mammalian²⁷⁴ cells. Pulse generators were not required because each droplet experienced a short, flow-rate-dependent electric pulse when in brief contact with electrodes. A serpentine channel upstream of the electrodes induced chaotic mixing of cells and cargo within the droplet, which improved transformation efficiency 3× relative to a straight channel.²⁷⁵ Transformation efficiencies of plant cells encapsulated in droplets were reported to be ~200× higher than that in the bulk EP system without cell wall removal treatment.²⁷³

Digital microfluidics systems differ by handling individual droplets simultaneously on an electrode array.²⁷⁶ Such systems resemble static EP systems that isolate individual cells in microwells, but with additional sample maneuverability. Programmable droplet movement, splitting, and merging are controlled with high precision by tuning the applied electric field on the array, which affects droplet surface tension and hydrophilicity. Digital microfluidics is advantageous for controlling many heterogeneous droplets in parallel and to generate and manipulate droplets on demand. Experimental workflows can be performed autonomously by programming sequences of active electric fields on the electrode array, decreasing the cost of parallelized experiments. Minute reagent volumes are required for plasmid construction with interchangeable fragments²⁷⁷ or genome engineering that require sequential washing and transferring steps.^{278,279} Droplets containing cells and biomolecules migrated across the electrode array to a dedicated EP electrode for intracellular delivery.

3.3.4. Impedance Measurements.—Changes in fluorescence intensity are a common indicator of EP because delivery of biomolecules and expression of transfected DNA

can be monitored easily in real-time with fluorescence labeling using broadly available fluorescence microscopes. However, fluorescent indicators require sufficient time to accumulate adequate quantities for optical detection, which limits the sensitivity of dynamic EP monitoring, and these molecules may interfere with downstream assay or cell metabolism study.²⁸⁰ Other methods of verifying EP are desirable for applications beyond novel device validation. Physical measurements, such as impedance change, taken of electroporated membranes can be used for label-free, dynamic EP monitoring.²⁸⁰ Microfluidic impedance cytometry has been developed for cell counting, size measurements, and label-free subcellular characterization at the single-cell level.^{281,282} Electrical current between dedicated electrodes changes in the presence of a cell, based on cell size and conductivity. When a cell is electroporated, there is a sharp drop in cellular impedance because cell permeabilization increases the conductivity of the cell membrane.¹⁸⁸ As the cell membrane recovers, membrane pores reseal, and the impedance returns to pre-EP levels (Figure 15A). If the cell is irreversibly electroporated, the cell membrane remains permeabilized, and the impedance will not revert.

Impedance measurements can reveal sample characteristics prior to EP. Madiyar et al. used DEP forces to collect virus particles on the tip of carbon nanofibers.¹⁷² Electrical measurements showed an increase in impedance as more particles collected on the nanofiber array. A limit of detection of $\sim 3 \times 10^3$ particles/mL was determined after viral collection. Sukas et al. designed a continuous microfluidic device with dedicated impedance electrodes upstream of irreversible EP.²⁸³ Upstream cell count was validated with both fluorescence- and impedance-based methods on the device. Impedance measurements can determine cell size, which is relevant in single-cell applications where heterogeneous cell size distribution may demand changes in EP conditions. Ghadami et al. developed a theoretical model, based on cell diameter, that proposed a 20% increase in EP efficiency and 9% increase in cell viability.²⁸⁴ Impedance could be used to estimate cell size prior to EP and adjust cell pulse conditions using a feedback control system.

Impedance measurements have been used in the earliest microfluidic EP systems to monitor electropermeabilization events and efficiency at the single-cell level.^{38,109,111,122,124} Early work from Khine et al. revealed how impedance measurements were rapidly collected to permit real-time, feedback-controlled EP of single-cell arrays.¹²⁴ Square waves with increasing magnitudes were applied until there was a 150% change in current. Mernier showed how the combination of low- and high-frequency impedance measurements on a single device revealed cell size and membrane conductance, respectively.²⁸⁵ The latter measurement provided evidence of cell lysis and was a robust technique irrespective of cell size. Guo and Zhu used DEP to align cells along central electrodes and applied an electric field to perform EP.¹⁸⁸ Immediately after alignment, the same electrodes were used to continuously measure cell impedance. The impedance of reversibly electro-porated cells reverted after 200–300 s, whereas the impedance of lysed cells never recovered. Zhang et al. used the same device to track changes in impedance across a wide range of EP conditions, including voltage, pulse length, number of pulses, and pulse frequency.²⁰⁰ Optimal EP conditions were determined by monitoring an impedance curve over time with a sharp descent, indicating maximum poration, followed by signal recovery, indicating high cell viability. Ye et al. compared the impedance drop with fluorescent signals measured

during single-cell continuous EP.²²³ The authors noted a ~186 ms delay from the initial impedance drop until the earliest fluorescence detection. This lag is attributed to the time between initial cell poration and the time it takes for enough transported dye molecules to accumulate inside the cell to exceed the microscope limit of detection. Bürgel et al. reached similar conclusions after repeated electrical measurements of single cells before and after EP.²⁸⁶ Impedance changes due to EP were almost instantaneously recognized, whereas fluorescence images revealed a gradual uptake of dye over time. The most significant change in impedance and phase signals occurred within 200 ms of cell EP (Figure 15B). Stolwijk and Wegener delivered bioactive proteins into cells and used impedance measurements to determine the effect of the biomolecules of cells.²⁸⁷ As expected, the delivery of an apoptosis trigger caused a permanent drop in normalized impedance, but its codelivery with a protein inhibitor caused impedance recovery and improved cell viability.

3.3.5. Reducing Device Complexity.—Many recent developments in microfluidic EP stem from highly specialized research laboratories that have access to sophisticated fabrication facilities and significant engineering expertise. Additionally, coupling EP devices with conventional biological assays requires protocol modification and optimization. Reducing the costs and complexity of device fabrication and operation would increase the use of microscale EP devices for end users and those interested in furthering these technologies with novel applications. From a manufacturing standpoint, selecting cheaper material alternatives or integrating commercial products helps to make the design process more economical. After fabrication, automation of experimental protocols simplifies user input and enables consistent treatment of both rare and large-scale samples.

Selection of cheaper or more readily accessible materials helps reduce fabrication costs while maintaining operational precision. For example, nanofeatures produced with cutting-edge technologies have been implemented to improve EP performance, but they require complicated fabrication protocols and equipment.¹³⁵ Efforts have been made to develop devices that achieve the core benefits of microscale EP with cheap, commercially available porous membranes or beads, as shown in section 3.1.1.1.^{127–139,246} Gold and other noble metals are common electrode materials that are stable and demonstrate consistent EP performance. However, precious metals can be expensive to deposit and pattern using conventional lithography. Riaz et al. used an inexpensive nanoimprinting and anodization step to fabricate NSPs on aluminum foil.¹⁷⁰ The entire workflow did not rely on costly microfabrication steps and was highly scalable for cheap device fabrication. Alternatively, carbon electrodes have been cheaply produced using a pyrolysis process and have demonstrated comparable EP performance.¹⁷⁵ Carbon electrodes were easier to fabricate and more resilient against electrode degradation than metal electrodes. Additive manufacturing is an emerging technique for microfluidic device fabrication because it is automated and economical and may be employed to generate more unique 3D features.^{288,289}

Other works have taken steps to avoid micropatterned electrode deposition, which is time-consuming and costly. One alternative is inserting electrical wires at defined locations within the channel to generate appropriate electric fields.²⁹⁰ Such a design is suitable for devices where cells are not required to be processed in direct contact with the electrodes,

as the further electrode gap requires higher voltages and increases electrolysis. In an early demonstration, Kim et al. replaced a conventional cuvette with a microscale capillary with wire electrodes.²⁹⁰ Cell suspensions were loaded into the capillary with a pipet. pH changes from electrolysis were reduced, and viability was improved relative to bulk EP because the wire electrodes were smaller than those used in a conventional cuvette. Alternatively, to fabricate microelectrodes without sputter deposition, a PDMS channel has acted as a template for flowing conductive materials that solidify as electrodes, such as a silver-PDMS mixture,²⁹¹ silver-plating solution,²⁹² and liquid alloy.²⁹³ The device proposed by Han et al. used passive capillary pressure to fill side channels with the liquid alloy solution (Figure 16).²⁹³ Altogether, the system was powered with 1.5 V batteries and controlled with a programmable printed circuit board (PCB) using a smartphone, for a total system cost of \$150.

EP devices commonly require a flow controller, a voltage source, and a pulse generator. Device costs may be reduced by replacing expensive external hardware to simple microfluidic elements. For *in situ* EP of cells cultured on-chip, pulse generators are needed because application of a continuous electric field will damage the sample. Wang et al. used PDMS valves to generate an electric pulse with a DC power supply instead of a pulse generator.²⁹⁴ Pneumatically controlled elastomeric valves²⁹⁵ were used to selectively block the channel and prevent current flows. The valves were computer controlled to generate electrical pulses as short as 30 ms without a dedicated pulse generator. As an alternative to an external flow source, electroosmotic flow has been generated using a pair of platinum wire electrodes at the inlet and outlet.²¹⁵ RBCs traversed the channel via electroosmotic flow and were lysed upon reaching a narrow gap. EP devices have been powered using TENG, a portable, cheap voltage source that is powered using mechanical hand slapping or cranking.^{171,237}

4. APPLICATIONS

Microscale EP encompasses a wide variety of functions with both basic research and translational applications. Microscale EP is capable of more efficient and gentler permeabilization of cell membranes for delivery of biomolecules or cell inactivation than traditional cuvette EP, as examined in section 3. Microscale EP offers single-cell functionality because integration with existing microfluidic technologies allows for control of cell position and targeted processing of individual cells. The devices are designed to handle nano- to picoliters of fluid, so the systems are inherently capable of handling samples with sensitive or low cell counts. Moreover, such capabilities are also scalable when needed for more expansive operations. Finally, unique applications are realized because EP can be monitored in real time, and cell response can be tracked over time. Collectively, these devices are unique tools that offer functionalities useful for biomedical research.

4.1. Development of Therapeutics

A primary objective of EP is the delivery of cargos to modify cell function and behavior. Recent progress in sequencing technologies has yielded unprecedented insight into the physiological and pathological roles of genes,^{296,297} linking gene sequences to biological

function and creating the opportunity to synthesize sequences to program cells and alter gene expression for novel therapeutic development. Microscale EP technologies are well-equipped for cargo transfer because delivery into cells is highly controlled. Most commonly, nucleic acids, such as oligonucleotides, RNA, or plasmids, are delivered into cells to modify gene expression. The emergence of various gene editing technologies has created emergent opportunities to apply microscale EP devices. Alongside nucleic acid deliverables, different biomolecules may be screened with microscale EP for efficient testing of multiple dosing regimens. Cargos may also be delivered into other membrane-based vessels that may aid with *in vivo* trafficking of therapeutics to desired disease targets. Novel, proof-of-concept microfluidic technologies for reversible EP are often validated with the delivery of reporter cargos, such as dyes, green fluorescent protein (GFP)-encoding plasmids, and fluorescently tagged dextran, to demonstrate the potential of such capabilities.^{32,36,39–45} As such, references in this section primarily include studies that have used microscale EP to deliver biologically functional cargos that modify cell behavior. Microscale EP serves as an experimental validation of therapeutic efficacy before translation to *in vivo* cargo delivery. In this section, we discuss the demonstrated potential of both static and continuous microscale EP in the therapeutic workflow.

4.1.1. Genetic Engineering.—A common application of intracellular delivery is the delivery of nucleic acids and proteins to genetically engineer cells and shape cell behavior. EP is excellent in delivering a range of cargos at these different length scales. Microscale EP devices have proven versatile in different contexts to transiently silence or upregulate specific genes or in permanent gene editing.

Microscale EP enables controlled post-transcriptional gene silencing and modulates protein production to inhibit cell function and induce cell death. RNA interference (RNAi) is achieved through the delivery of 20–25 bp small interfering RNA (siRNA) and microRNA (miRNA) mimics into cells.²⁹⁸ Within the cell, the sequence-specific RNA strands bind to mRNA (mRNA) and induce nucleic acid cleavage, transiently inhibiting gene-specific protein production. miRNA and siRNA are commonly delivered into cells using liposomes, but results have been inconsistent due to the reliance on endosomal escape and inconsistent miRNA loading.^{299,300} Microscale EP enables consistent, dose-specific delivery of siRNA and miRNA into target cells to affect cell function. Several proof-of-concept studies have delivered siRNA or miRNA targeting previously transfected GFP genes^{174,180} or calcium channel proteins¹⁷¹ in cell lines with improved delivery efficiency compared to bulk EP. Several studies have demonstrated the therapeutic efficacy of microscale EP in the delivery of miR-29b^{35,141,180} or siRNA^{140,142,145} silencing Mcl-1, a protein that regulates apoptosis, at toggleable doses. Experiments with different dosages revealed that the delivery of frequent, low-concentration doses is preferable to a single large dose, as the continuous approach maintained a comparable response while requiring 22% less siRNA.¹⁴² RNAi has also been used with microscale EP to deliver miR-181a into cells to promote fibroblast proliferation.¹⁶⁰ Additionally, microscale EP was effective in the delivery of cell penetrating peptides conjugated to peptide nucleic acids (CPP-PNAs) into macrophages infected with bacteria.³⁰¹ A PNA sequence was selected to selectively inhibit bacteria growth within

the cell. EP avoided challenges with endosomal escape to improve the overall therapeutic efficacy compared to cell incubation with CPP-PNAs.

Microscale EP devices are capable of efficient delivery of large, several kilobase pair plasmids into cells to modulate cell function. Aside from delivery of GFP-encoding plasmids, some studies transfected bacteria with reporter antibiotic resistance genes.^{164,254,277,302} Microscale EP allows plasmids to be delivered directly into the cytoplasm. This mechanism increases transfection efficiency and consistency relative to traditional methods that rely on endosomal escape. Recent microscale EP devices have delivered biologically relevant plasmids for cellular reprogramming. The 3D NEP device has been used to transfect mouse embryonic fibroblast cells with a plasmid cocktail collectively known to reprogram fibroblasts into induced neurons (iNs).^{139,150} The 3D NEP platform has enabled plasmid dosage control and revealed optimal iN formation at nonuniform plasmid ratios.¹³⁹ Genes from plasmids transfected with NEP were expressed more rapidly than genes delivered via bulk EP methods. This *in vitro* study was a precursor to *in vivo* tissue repair and stroma cell alterations.¹⁵⁰ Zhao et al. used the NEP system to discern the relative strengths of competing intracellular pathways in the production of miR-181a, which is also a known tumor suppressor.¹⁴¹ Indirect upregulation of miR-181a with a plasmid encoding a mutated CEBPA gene, which is present in a fraction of acute myeloid leukemia (AML) patients, upregulated miR-181a synthesis more efficiently than direct upregulation with an miR-181a-encoding plasmid. Despite the success of existing technologies for plasmid delivery, a noted challenge is traversing the second barrier and transporting plasmids from the cytoplasm into the nucleus, which could further improve transfection efficiency. Recent studies have used the combination of nano- and millisecond electrical pulses³⁰³ or mechanical squeezing and EP³⁰⁴ to achieve this feat.

Conversely, the clustered regularly interspaced short palindromic repeats (CRISPR)/Cas9 genome editing system has emerged as a powerful tool in biomedical research to edit genomes with high specificity.^{305,306} This technology enables permanent changes to the genome, in contrast to the transient behavior of siRNA, miRNA, or plasmid delivery. A broad range of emerging applications use genome editing, from engineering new abilities into existing cell lines to removing undesired mutations to treat diseases.^{307,308} Microscale EP enables precise dosage control when delivering large Cas9 ribonucleoproteins (RNPs) or CRISPR/Cas9-encoding plasmids. The process is sufficiently gentle to preserve cargo functionality for efficient gene editing. Proof-of-concept studies have used the CRISPR/Cas9 platform to edit GFP expression in^{207,269} or out.^{164,165} Cas9 RNPs have also been transported into mammalian cells to target the housekeeping *PP1B* gene.^{113,135} The moderate editing efficiency (25–31%) was possibly due to the added challenges of protein navigation from the cytosol into the nucleus for effective activity. In another study, >9 kbp CRISPR/Cas9 plasmids were delivered into cells to knock out *p62* and *CXCR7*, two tumor proliferation genes.¹¹⁴ Alongside slower proliferation, genomic sequencing and Western blot assays revealed successful genome editing and decreased production of target proteins.

High-throughput microscale EP systems are also applicable to program immune cells, potentially for reintroduction into patients to target diseased cells.^{147,193,253,258} Select studies have delivered GFP-encoding mRNA into primary human T cells at up to 2 cells/min

to mimic potential cell engineering for adoptive cell transfer.^{253,258} An emergent cancer therapeutic strategy is the engineering of synthetic chimeric antigen receptors (CARs) to program immune cells to target cells expressing specific antigens.³⁰⁹ Chang et al. transfected NK cells with CAR-encoding plasmids as an early demonstration of immune cell engineering using microfluidics.¹⁴⁷ Jayasooriya et al. characterized the cellular response to CAR-encoding mRNA into primary T cells using interdigitated electrodes.¹⁹³ GFP and CAR levels peaked 24 and 48 h after mRNA delivery, respectively, underscoring the differences in gene expression based on mRNA sequences. CAR T cells formed with microscale EP were effective in killing target cells without off-target cytotoxicity.

4.1.2. Drug Screening and Delivery.—Alongside genetic manipulation of cell behavior, microscale EP is also suited for screening of different cargos and generation of therapies. Operation at the microscale reduces the quantities of therapeutics necessary for screening. Similarly, efficient delivery enables high-throughput generation of therapies that demonstrate *in vivo* localization.

In vitro drug screening is a useful first step in determining the drug efficacy in a biological system. EP is an effective strategy to increase drug uptake of cells to assess therapeutic efficacy. Operating on the microscale reduces the quantities of cells and drug required for experiments and enables more rapid dosage testing. Dong et al. used the 3D EP platform to deliver small chemodrugs into melanoma cells.¹¹⁴ EP-based delivery of dacarbazine caused a greater decrease in cell viability compared to chemical agent-based delivery of the drug. Liu et al. used a porous foam lined with 1D silver nanowires to continuously electroporate the MCF-7 breast cancer cells and a known drug-resistant counterpart (MCF-7/ADR) with doxorubicin hydrochloride (DOX).²³⁷ The MCF-7 cells had a 20% lower cell viability compared to the MCF-7/ADR cells, whereas the EP-free, 24 h DOX treatment of MCF-7/ADR cells had a marginal effect on altering cell viability. Interestingly, Yan et al. found that decreased EP efficiency of different nonsmall cell lung cancer cell lines was linked with higher resistance to erlotinib, a commonly used anticancer drug.³¹⁰ This behavior may be related to changes in membrane tension, which followed the same trend as EP efficiency. Vickers et al. reported an inertial microfluidic device that trapped cells in EP chambers using microvortices for drug cocktail testing.¹⁷⁹ Rapid solution switching kept cells hydrodynamically while allowing the passage of different drugs or wash buffers. This feature enabled rapid sequential delivery of different drugs to identify compounds at different intracellular concentrations with synergistic effects. Sung et al. demonstrated a workflow to simultaneously isolate rare cells spiked in blood samples and test the effects of combinatorial drug delivery on attenuating drug resistance.¹⁸¹

In addition to the validation of therapeutics, microscale EP is also effective in encapsulating molecules in delivery vessels and engineering immune cells. Instead of delivering cargos directly, therapeutics are loaded within an enclosed cell membrane, and the resulting structure is delivered *in vivo*. Cell-membrane-based carriers shield the therapeutic cargo from premature degradation and limit off-target toxicities.³¹¹ Liu et al. delivered fluorescent mRNA probes into blood cells using a micropillar array coated with carbon nanotubes.¹⁷³ Yang et al. used the cellular nanoporation (CNP) device to deliver a plasmid encoding *PTEN*, tumor-suppressor gene, into cells and to generate large quantities of exosomes.¹⁵¹

The CNP device resembled NEP devices with subcellular nanochannels close to adherent cells. Here, the EP process generated localized stresses that increased the release of exosomes containing *P TEN* mRNA in higher, more consistent quantities compared to gold standard exosome delivery methods. CNP-formed exosomes demonstrated significant accumulation at a tumor site and improved clinical outcomes in a mouse model. Zhao et al. developed a workflow to extract and continuously deliver fluorescent RNA to mouse RBCs, which were then reintroduced into a mouse within 1 h.³¹² Several hours after reintroduction, there was significant particle accumulation in the kidney and spleen, two common organ targets for RBC-based nucleic acid therapies. Rao et al. generated a similar construct by stably delivered magnetic nanoparticles into RBC-vessels to form RBC membrane-capped magnetic nanoparticles (RBC-MNs).³¹³ After particle synthesis, RBC-MNs were delivered into mice and accumulated in tumors via the enhanced permeability and retention effect, with applications in both MRI imaging and photothermal therapy.

4.2. Intracellular Sample Preparation

The detection and measurement of intracellular molecules such as nucleic acids, proteins, and metabolites are a fundamental tool in biomedical research. Understanding the internal cell composition, especially after stimuli, helps in the understanding of cellular mechanisms and the efficacy of administered therapeutics. These biomolecules must be harvested from cells before they can be processed with established bioassays, such as gel electrophoresis, polymerase chain reaction (PCR), enzyme-linked immunosorbent assay (ELISA), and mass spectroscopy. Microscale EP addresses the key need of extracting intracellular biomolecules. Extracted analytes remain concentrated after EP because the total working volume is small. The small amounts of fluid are also well-suited for rare samples, which may be extracted from patients for *in vitro* testing. Furthermore, gentle microscale EP maintains cell viability after processing. This section discusses unique functions of microscale EP to isolate and enrich intracellular material.

4.2.1. Longitudinal Intracellular Content Sampling.—Longitudinal intracellular analysis is essential to immunology, stem cell differentiation, and other cell biology applications where cellular response changes over time.³¹⁴ However, sampling intracellular molecules, including mRNA, proteins, and metabolites, from the same cells at repeated intervals with high sensitivity is challenging. Most technologies are limited to studying molecules at a single time point by analyzing the cell lysate, so extended studies characterizing the same cells are not possible. Early work from Zhan et al. demonstrated that microscale EP was sensitive enough to study proteins that diffused out of the cell after reversible membrane permeabilization.³¹⁵ From there, collected contents can be analyzed with diverse, sensitive assays to collect a snapshot of intracellular contents at a given time point. Repeating this process on the same set of cells over the course of hours permits longitudinal studies to examine changes in intracellular contents. Microscale EP is unique for its selective, gentle, and efficient sample processing, along with integrated optical and electrical monitoring systems.

The nanostraw-based EP platform has proven to be appropriately gentle for intracellular sampling. Localized EP at lower voltages reduces cell damage and limits uncontrolled

Microscale EP controls electric field conditions across processed cells to limit these adverse effects. This improves collected analyte yield for more accurate downstream analysis. This section discusses engineering developments that reduced degradation of intracellular molecules.

Electrode materials have been selected to reduce electrolysis and improve the quality of collected cell lysates. Electrode passivation is one approach to protect lysate from electrodes, as discussed in section 3.3.1. The first microfluidic lysis device used sawtooth-shaped gold electrodes coated with Teflon.¹⁸⁶ The sawtooth design attracted cells to the electrode tips with local electric field amplification, and the coating reduces electrode breakdown. This validation was compatible with various cell types, such as yeast, bacteria, and Chinese cabbage and radish protoplasts after cell wall removal by enzymes. Electrodes covered with PDMS dielectric layers facilitated cell lysis for extraction of gDNA.²⁶³ >100 ng/ μ L DNA was collected from multiple mammalian cell populations after an intermediate filtration step. Talebpour et al. found that RNA collected from cells treated with passivated electrodes yielded 16 \times more PCR product compared to cells electroporated with nonpassivated electrodes.²⁶⁴ Ameri et al. opted to use graphene as an electrode material to lyse RBCs.³¹⁷ The combination of the electrochemically inert properties of graphene and low operational voltages at the microscale reduced harmful electrolysis-generated toxins.

Another strategy to reduce sample degradation is to optimize electric field conditions for more gentle lysing conditions. Lu et al. demonstrated continuous on-chip cell lysis on a PDMS chip with sawtooth microelectrodes.³¹⁸ By tuning the operational frequency, the plasma membrane could be porated to release intracellular contents, while the organelle membranes were preserved and could be harvested downstream for organelle analysis. Moreover, the nonhomogeneous electric field generated DEP forces that focused cells to the center of the channel to concentrate low-abundance molecules for downstream assays. Poudineh et al. used 3DSTEs, with local electric field enhancement at the electrode tips, for efficient lysis of bacteria while limiting RNA degradation by avoiding electrochemical lysis.²³⁶ At frequencies of >500 kHz, electrolysis was avoided, and 95% of cells were lysed. >32 \times more RNA was collected from electrically lysed *E. coli* relative to electrochemically lysed samples. Morshed et al. tuned both applied voltage and pulse length to determine optimal conditions for cell lysis and gDNA extraction.³¹⁹ At 20 V, cells were lysed using interdigitated electrodes, but it required a pulse width of 5 s to break up the nucleus and extract the nucleic acids. Similar analyses confirmed nucleus breakup by staining the whole cell, cytoplasm, and nucleus and visualizing the loss of fluorescence after irreversible EP.³²⁰

The implementation of subcellular channels also improved the collection yield of cell lysates. A packed bed of silica beads concentrated bacteria and locally amplified electric fields without severely damaging intracellular molecules.^{127,128,321} Hard-to-lyse mycobacteria were inactivated and intracellular mRNA was extracted with 10–20 \times better efficiency compared to performance with the bead beating method.¹²⁸ The packed bed of beads was also used to capture gDNA of lysed eukaryotic and bacterial cells.³²¹ After electrical lysis, the beads captured gDNA and were washed by pressure-driven oscillatory flow in the channel, with a final yield higher than that from chemical lysis. Similarly, gDNA was preserved after a nanopore membrane was used to concentrate and lyse *E. coli*.¹³⁶ Kim

et al. combined mechanical shearing and electrical cell lysis to inactivate bacteria with low electric field strengths (~ 100 V/cm), reducing harm on intracellular materials and energy requirements.³²² Electroconvective vortices were generated by flowing solutions alongside ion-selective membranes, which served dual roles of mechanically agitating flowing cells and directing cells toward ion-depleted, amplified electric field regions (Figure 17C). Both proteins and RNA were collected downstream with equal or better efficiency than bead beating-induced lysis. Won et al. used microscale EP to lyse cells infected with the varicella-zoster virus.²²⁷ The virus causes shingles and chickenpox, and there are clinical limitations in developing vaccines based on cell-associated virions in infected cells.³²³ Microfluidic cell lysis and off-chip purification extracted viable, cell-free virions for further analyses.

4.2.3. Target Purification.—Microscale EP devices may integrate other microfluidic modules or rely on selective lysis to improve the purity of the processed output. Typical off-chip purification steps increase sample loss due to imperfect solution transfers and filtration elements. Removing cell debris and other undesirable components on-chip reduces user intervention and eliminates intermediate steps, causing improved collection yield. This is especially useful for processing rare or fragile samples, where expected collected biomolecules are already limited. Overall, microscale EP is effective in streamlining experimental workflows to improve sample purity while minimizing user intervention.

Integration of microfluidics into EP enables on-chip, electrophoretic preprocessing of cell lysates for improved purity during final collection. Established capillary electrophoresis technologies were first to demonstrate the combination of cell lysis and electrophoretic movement of lysates. These devices used perpendicular channels to lyse cells and separate lysates from ghost cells continuously^{214,324,325} or semicontinuously.³²⁶ Cells were pumped through one channel, and an electric field was applied across the perpendicular channel. At the junction, cells were lysed, and charged lysate electrophoretically traversed the perpendicular channel for optical detection. McClain first demonstrated the detection of a small fraction of cells that showed an anomaly of dye hydrolyzation with processing speeds $100\times$ faster than the gold standard, benchtop capillary electrophoresis devices.³²⁴ The throughput was increased to 80 cells/min by Wang et al. using a similar channel design.²¹⁴ This capability would be useful to identify anomalous cells for early disease detection. This system³²⁵ has been coupled with electrospray ionization–mass spectroscopy to detect hemoglobin from RBCs.³²⁷ Other works combined cell lysis and electrophoretic purification of short RNA in an integrated device to reduce the processing time, protecting RNA from degradation and increasing the extraction efficiency from rare samples.^{328,329} Recent studies have adopted this idea to separate RNA from DNA to better understand transient cell behaviors. Several microscale EP studies have used isotachopheresis (ITP), which uses similar perpendicular channels filled with different mobility electrolyte solutions, to separate RNA from DNA in a collection channel.^{330–334} Shintaku et al. lysed single cells and quantified relative concentrations of DNA and RNA based on the fluorescence intensity of their respective bands (Figure 17D).³³⁰ Kuriyama et al. added a microfluidic T-junction with separate electrode connections for a timed, directional collection of faster-migrating RNA and bulkier gDNA for off-chip analysis.³³¹ Parimalam et al. found that fixing cells with a reversible cross-linker limited premature RNA degradation prior to sample collection.³³²

Abdelmoez et al. devised a single-cell integrated nuclear and cytosolic RNA sequencing (SINC-seq) workflow to better understand single-cell physiology.³³³ Surprisingly, gene expression profiles were different based on its origin of collection, indicating that the cell manipulates RNA expression during transport out of the nucleus.

Some metabolites are sensitive to intracellular enzymes in cell lysates that naturally break them down. For example, in microbial metabolomic analysis, mixing quenching solutions with cell lysates is necessary because intracellular metabolites rapidly degrade from enzymatic reactions.³³⁵ Rockenbach et al. found that electric pulses not only induced irreversible lysis of *E. coli* and *S. cerevisiae* but also inactivated the enzyme glucose-6-phosphate dehydrogenase so that glucose-6-phosphate could be collected without degradation.³³⁶ Additional microfluidic tools have been integrated to chemically lyse undesired enzymes. Filla et al.³³⁷ and Coulton and Edwards³³⁸ used flow-switching devices to switch seamlessly between different reagents for cell lysis and metabolite analysis. Rapid use of chemical lysing agents degraded intracellular enzymes that would otherwise decrease metabolite concentrations. The combination of electrical and chemical lysing techniques was 10× faster than chemical lysing alone. Collected samples were further analyzed off-chip with conventional methods such as MALDI, mass spectroscopy, and liquid chromatography.

4.3. On-Chip Assays

Microfluidics is an established field with an abundance of assays that can be performed on a device. Integration of microfluidic assays with microscale EP offers many benefits. Since EP and downstream analysis can be performed on the same chip, sample loss and processing time are reduced. Compared to off-chip analysis, the sensitivity of these assays is higher due to smaller working volume per sample. Microfluidic devices can also be used to compartmentalize cells into smaller pockets to study single-cell behavior in parallel. This functionality is more effective than bulk analysis of cell lysate to understand heterogeneous behavior of cells. The devices are also capable of electroporating slightly larger multicellular samples that are surrogates of larger biological systems. In all, this section covers how microscale EP pairs well with other microfluidic assays in studying cell activity.

4.3.1. Single-Cell Assays.—Static EP systems allow for single-cell monitoring by immobilizing and confining cells in small structures. Microscale EP devices can deliver a broad range of cargos to perform different assays. For example, EP devices can deliver robust biosensors made from different materials to optically detect specific intracellular gene expression. When targets do not have adequate deliverable biosensors, samples may be discretized to isolate single-cell lysates. Coupled with optical detection methods, microscale EP is suitable for performing assays to assess single-cell gene expression and response.

Delivery of biosensors into cells helps to assess intracellular changes such as gene expression following transfection or cell perturbation. For on-chip assays, fluorescent biosensors are widely used to study the location and quantity of intracellular molecules.^{339,340} Biosensors are designed to be highly specific to biomolecules and can track their movement and relative concentration within the cell. They are fabricated from a variety of materials, including semiconductors, nucleic acids, or metals, with drastically

different physical characteristics. Microscale EP is capable of delivering bulky cargos such as Förster resonance energy transfer (FRET)-based protein biosensors³⁴¹ and quantum dots (QDs)³⁴² in a dose-dependent fashion irrespective of cell type. Microscale EP enables nonendocytic delivery of QDs into cells for more rapid transport and concentration control because delivery is not cell-process-limited. Nonendocytic delivery is critical for 15–20 nm QDs with surface modifications to be effective in intracellular targeting.³⁴² QDs functionalized with antibodies specific to kinesin could track kinesin movement over time. The importance of nonendocytic delivery was also validated with the delivery of QDs and fluorescent oligonucleotides in ~64 nm lipoplex nanostructures.¹⁴⁵ Nanoparticles delivered with NEP rapidly lost fluorescent signal as the lipoplex broke down, and the FRET pairs separated in the cytosol. In comparison, structures delivered with bulk EP continued to accumulate and fluoresce in the endosome due to an inability to escape. Additionally, microscale devices can precisely introduce smaller cargos, such as molecular beacons (MBs), into cells. MBs are single-stranded, ~30 bp hairpin nucleic acid biosensors with bilabeled fluorescence in the presence of a target mRNA sequence.³⁴³ When a complementary target sequence binds to the MB, the quencher is separated from the fluorophore, enabling real-time, spatial identification of specific sequences within the cell. NEP devices have been used to deliver MBs targeting native proteins^{114,140,149,161,163,344} or validating the efficacy of RNAi gene silencing.^{141,142} Similar deliveries of domino nucleic acid probes have been applied to detect specific epidermal growth factor receptor (EGFR) mutations in primary cancer cells.¹³⁷ In one study, the nonendocytic delivery of larger cargos, such as multiwalled carbon nanotubes and QDs, into cells caused increased cellular stresses compared to endocytic delivery.¹⁴⁴ The finding suggested that the delivery of larger cargos *in vivo* should be accompanied by a method to quell nonendocytic transport, or cargos should have a biocompatible coating because the cell would otherwise recognize these biomolecules as foreign and react poorly.

Microscale EP has been effective in the isolation and detection of intracellular proteins in combination with various detection techniques. Sedgwick et al. captured intracellular β -actin from carcinoma cells with 10 μ m antibody-coated latex microspheres.¹⁹⁶ Single cells were trapped on and lysed by sawtooth-shaped electrodes before lysates flowed and accumulated on the downstream microparticles. This format was applicable to identify protein targets with known antibodies. For cancer therapy, it is also important to understand how nucleocytoplasmic transport and gene activation levels are affected by anticancer agent, both of which can be determined by studying protein translocation. Conventional determination methods include subcellular fractionation, Western blotting, or subcellular imaging, which are not suitable for large populations of cells in single-cell study. Microscale EP and on-chip flow cytometry have been paired to reveal single-cell protein translocation without imaging.^{219–221} Wang et al. developed an electroporative flow cytometer to observe the translocation of protein-tyrosine kinase Syk to the cell membrane after B cell activation²²⁰ and the kinetic behavior of transcription factor NF- κ B of CHO cells.²²¹ The protein of interest was labeled with a fluorescent probe prior to lysis, so the remnant fluorescence intensity is related to the fraction of cytosolic and membrane proteins.

Microscale EP devices have sufficiently small features for complete cell compartmentalization for effective delivery of biomolecules and analysis of cell lysates at

the single-cell level. Microwell arrays are simple to fabricate and enable large numbers of cells to be organized, electroporated, and monitored in parallel.^{345,346} Isolation of small numbers of cells and generated lysates allows for improved resolution when studying intracellular contents. Various microfluidic strategies, discussed in section 3.1.2, have been employed to load cells into isolated chambers. 3D micropore arrays that isolated each cell were used to show melanoma cell inhibition of a chemodrug, dacarbazine,¹¹⁴ and regulation of the GATA2 gene of leukemia cells.¹⁴⁶ Dong et al. demonstrated high-throughput gene mutation identification and drug resistance analysis by delivering sequence-specific domino probes.¹³⁷ This system could analyze >10 000 cells in 40 min, including incubation time. EGFR mutation ratios from 20 primary cancer cell samples, detected with single-cell resolution, correlated with expected drug resistance. This workflow would replace existing protocols for identification of specific mutations using single-cell sequencing which is powerful but low-throughput, expensive, and time-intensive.³⁴⁷ By fully sealing off individual cells prior to cell lysis, lysates may be individually isolated to perform on-chip assays with single-cell resolution. As a demonstration, caspase activity of individual RBCs was monitored over time. Kim et al. used DEP forces to guide bacteria or mammalian cells into individual micro-wells.^{197–199,348} The DEP forces fixed cells in place during solution exchange steps and microwell closing with a PDMS membrane to isolate each sample. After cell lysis, released intracellular contents remained within individual wells. This device displayed cellular heterogeneity in active β -galactosidase expression^{198,348} and pluripotency marker protein Nanog of mouse iPSCs.¹⁹⁹ Chatzimichail et al. designed microwells for cell capture, lysis, and protein detection using patterned antibody spots.²⁹² PDMS microwells were loaded with cells and sealed with a glass slide patterned with electrodes and anti-GFP antibodies. Following cell lysis, fluorescence intensity in each well due to accumulated GFP at the antibody spots roughly matched the number of cells. Li and Anand trapped single cells in individual wells using a wireless bipolar electrode array prior to lysis.³⁴⁹ Split electrodes were activated by an external electric field to nudge cells into the well with DEP forces and keep them trapped. A hydrophobic, conductive, low-viscosity ionic liquid sealed individual wells for minimal contamination prior to cell lysis. de Lange et al. electroporated single *E. coli* and encapsulated the cells in droplets for single-cell lysate analysis.³⁵⁰ A fluorescent catalysis reaction was used to quantify the fraction of lysed cells containing β -glucosidase, a cellulase used to convert biomass into biofuels.

Static EP systems enable continuous monitoring and repeated EP of the same cells over longer time spans. EP and targeted stimulation of neuronal axons were demonstrated by Chang and Sretavan using vertical sidewall electrodes.³⁵¹ Neurons were cultured such that randomly distributed cells adhered between the electrodes. After delivery of an impermeable calcium chelator, EGTA, a fluorescent calcium indicator in the axon was locally quenched, with the neural body and surrounding neurons unaffected. More recent techniques provided direct control of EP position on cell cultures. The NFP device uses a micromanipulator to select individual cells to permeabilize with precise control and supports long-term tracking of cellular response.^{161,163,165} The gentle cell transfection has applications in cell differentiation studies. Similarly, Janus particles held similar capabilities to gather, transport, and electroporate small numbers of bacteria¹⁷⁶ and mammalian cells¹⁷⁷ with high efficiency. Both techniques offer not only the ability to select which cells for EP but also

the opportunity to specify where on the cell to apply an electric field for delivery. This advantage provides opportunities to provide direct treatments toward specific regions on neurons and other elongated cells.

4.3.2. Cellular Response under an Electric Field.—Microscale EP provides the ability to study cell responses under electric fields. The technology exerts repeatable, consistent EP conditions onto cells at the single-cell level, so systematic screening of conditions can be performed. A better understanding of the cellular responses to applied electric fields may help adjust EP conditions to improve efficiency for translational applications and novel biological systems. Micro-scale EP allows for precise control over electrical and delivery conditions exerted on single cells and larger *in vitro* biological systems. For example, Gencturk et al. examined the response of *S. cerevisiae* cells to electric fields at different voltage magnitudes.³⁵² Cells treated at sub-EP voltages underwent prolonged mitosis and took 200–300 min to divide instead of the normal 80–90 min. This finding suggests that low voltages may be applied in combination with other therapies to slow tumor growth during *in vivo* treatment. Graybill et al. used nanofiber-based probes to study the cytoskeletal impacts of applied electric fields on single cells.³⁵³ Cells underwent three stages after EP: initial reduction of contractility, biphasic force response, and reversion to initial contractility (Figure 18). Electric fields applied parallel to the direction of cell elongation yielded higher cell viability, but perpendicular forces produced more uniform cargo delivery between the anodic and cathodic cell sides. Henslee et al. also found directional electric field effects on threshold EP conditions by manipulating cell pairs with optical tweezers.¹⁸⁴ Cell pairs perpendicularly aligned to the electric field direction were electroporated at weaker electric field compared to a single cell exposed to the same electric field direction. However, cells placed in parallel to the electric field shielded one another and required higher electric field strengths for EP while achieving lower efficiency. These findings may inform more efficient EP parameters for single-cell studies where cell position may be controlled. Changes in cytoplasm conductivity post-EP have been characterized and suggested as a label-free indicator of cell permeabilization.³⁵⁴

4.3.3. Electroporation of Multicellular Models.—Micro-scale EP devices are capable of processing both individual cells and larger samples that mimic tissues. For many cell types, 3D cell cultures better represent *in vivo* cell physiology than planar, 2D cultures.³⁵⁵ Zhu et al. devised a PDMS device designed to electroporate 50–150 μm 3D spheroids with ~ 10 cells.²⁶⁹ Intracellular delivery of 80% of all cells was demonstrated by orthogonally switching the polarity of the electric field. Artificial organ-on-a-chip technologies have been created to replicate elements of *in vivo* environmental conditions for inexpensive and physiologically relevant experimentation.³⁵⁶ For example, the blood–brain barrier (BBB) is notoriously difficult for biomolecules to traverse into the central nervous system. Biomolecules must travel either through endothelial cells (transcellular) or through intercell tight junctions (paracellular). Bonakdar et al. cultured mouse brain endothelial cells in a bilaterally converging device to determine optimal EP conditions for adequate delivery and high cell viability.²⁰⁵ Intracellular delivery achieved half of the goals of transcellular movement of brain disease therapeutics. Later, Bonakdar et al. designed a two-layer microfluidic device separated by a human cerebral microvascular endothelial cell monolayer

to mimic the BBB.³⁵⁷ This device enabled rapid testing of multiple experimental conditions using this model. High-frequency, low-electric-field-strength pulses, which were insufficient for cellular EP, were sufficient to transport molecules across the cell monolayer. This suggests that weaker, sub-EP electric fields may be preferable to permeabilize tight junctions for paracellular movement while improving the safety of treatment. Beating cardiomyocytes cultured within micro-scale EP devices allowed for sensitive testing of the effects of EP on the heart.^{157,167} The 3D hollow nanoelectrode system was employed to electroporate and take electrophysiological recordings of beating iPSC-derived cardiomyocytes.¹⁶⁷ Changes in depolarizing and repolarizing currents were noted when comparing electroporated cells compared to a normal state. These signal alterations are critical parameters for studying the intracellular effects of drugs on cardiac cells. Some exploratory work has led to the delivery of reporters into model organism embryos using microscale EP. Zebra fish embryos were electroporated with parallel plate electrodes to deliver dyes, QDs, and GFP plasmids.³⁵⁸ Embryos were loaded in a microwell array, so parallel *in vitro* transfection of embryos is achievable. Mazari et al. locally electroporated mouse embryos by positioning the organisms close to dielectric guide electrodes that limited electrolysis close to the organism.³⁵⁹ This tool was applied to fluorescently label distal cells and observe cell migration over time to better understand development. Beyond the scope of this Review, there also exist other works that focus on downstream electrotransfer for *in vivo* delivery of different therapeutics.^{360,361}

4.4. Cell Inactivation

One goal of microscale EP is the inactivation of target cells while preserving other analytes in the liquid sample. This goal is pertinent in applications like water disinfection or clearance of unwanted cells. In both instances, microscale EP is beneficial in generating reliable process conditions and reducing energy expenditure. Increasing the throughput of microscale EP to match bulk processing techniques for such applications is an added challenge.

Cell lysis is a viable approach in water disinfection or food sterilization to remove undesirable bacteria because electrical treatment can inactivate cells without degrading heat-sensitive ingredients.^{362,363} Existing cell inactivation methods, such as chlorination and UV radiation, are effective in cell inactivation but generate toxic byproducts and can consume excessive energy.^{364–366} Emerging microfluidic EP techniques mitigate these challenges by focusing on decreasing energy consumption and controlling precise lysis parameters while increasing throughput for practical device use. Low energy consumption is important for industrial use of bacterial lysis since it requires high electric field intensity (~ 10 kV/cm) and large processing volumes. Electric field enhancement strategies as presented in previous sections have been adopted for efficient cell inactivation in low voltage. *E. coli* were lysed with low-voltage pulses by reducing the electrode distance from millimeters to $100 \mu\text{m}$.²¹⁷ Huo et al. initially used CuO nanowires modified on a copper foam to achieve 7 log bacteria removal at 25 J/L.²⁴⁰ Huo et al. later opted for a carbon nanotube-decorated sponge for *E. coli* inactivation with a $<0.0001\%$ survival rate.²³⁸ This device required only 2 V for efficient lysis, which is lower than the voltage required for UV sterilization or membrane filtration, so samples could be purified with minimal energy consumption (20 J/L). Cell

lysis efficiency was increased by electrophoresis and DEP which transported cells close to the amplified electric field regions for more efficient lysis at lower voltages.²⁴² Huo et al. optimized the microfoam system using Cu₃P nanowires to filter the water using only 1.2 J/L.²³⁹ Liu et al. sought to inactivate microalgae in culture media to better replicate real-world conditions.²²⁹ Cell damage was attributed to the applied electric field and not the trace amounts of released copper ions, which have negative effects on human health. Yue et al. found that functionalizing CuO nanowires with silver beads improved antibacterial effects for high-throughput processing.²⁴³ At 2 L/min and an applied voltage of 10 V, silver NP-CuO nanostructures inactivated *E. coli* ~25% better than CuO nanostructures. These devices were effective in most water quality conditions, aside from the rare instance of high-molecular-weight or low-solubility organic matter at high concentrations.²⁴¹ Pudasaini et al. continuously electroporated bacteria with local electric field enhancement caused by micropillars²²⁸ or silica beads.²³⁰

Microscale EP technologies allow for fine-tuning electrical conditions to induce size-selective EP for cells of interest from heterogeneous cell populations. Selective cell inactivation has clinical relevance in lysing only circulating tumor cells (CTCs) from blood and preserving RBCs and white blood cells (WBCs).³⁶⁷ Bao et al. lysed cancer cells from blood²¹⁸ with a continuous, channel constriction EP device with a maximum flow rate of 1 mL/min for rapid processing.²¹⁰ Kinio et al. relied on the different magnitudes of DEP forces, based on cell size, to isolate surrogate CTCs from blood cells for lysis in a continuous device.³⁶⁸ Cancer and blood cells were subjected to identical electric field gradients, causing larger CTCs to deflect via DEP into a different streamline than blood cells because DEP force is dependent upon the cube of a cell radius.³⁶⁹ Cancer cells were positioned closer than blood cells to locally amplified electric fields, so only the cancer cells were lysed with 57% efficiency. Interestingly, Wimberger et al. found that the relationship between cell size and threshold EP voltage did not always correlate when lysing blood cells, possibly due to differences in cell shape.⁷⁷ Cancer cell lines whose diameters were >10 μm were lysed at 13 V, and nonspherical ~7.8 μm erythrocytes were lysed at ~17 V. 6–10 μm leukocytes required the harshest conditions of ~36 V for cell lysis. While this result was unexpected, cancer cells were still selectively lysed when mixed with leukocytes. Blood cells may also be the lysis target to preserve smaller bacteria, with potential applications in speeding up sepsis diagnosis. Wassermann et al. lysed blood cells with passivated electrodes while minimally affecting spiked bacteria viability.²⁶¹

4.5. Cell Fusion

Cell fusion is a process to merge the cytoplasm and/or nuclei of two or more cells together to generate hybrid cells. Fused cells have biological applications for antibody production,³⁷⁰ immunotherapy,³⁷¹ regenerative medicine,³⁷² production of cloned offspring,³⁷³ and nuclear reprogramming.³⁷⁴ Typical viral and polyethylene glycol (PEG)-assisted cell fusion methods are associated with increased toxicity and formation of larger cell aggregates. An alternative, electrofusion, uses an electric field to permeabilize and join the membranes of cells in close proximity.³⁷⁵ This method is attractive due to its lower toxicity and broader application to different cell types, but similar challenges remain in controllably forming only cell pairs, instead of multicell fusion, and evading toxic effects of Joule heating.³⁷⁶ Maintaining

cell contact and initiating reversible EP are imperative for successful electrofusion.³⁷⁷ As such, microscale EP is well-suited for electrofusion as devices can efficiently permeabilize cells. Moreover, there are numerous strategies to control cell placement and optimize the pairing of only two cells. Reducing cell movement during the pairing process is useful because fusion efficiency is higher when cells are paired prior to application of electric fields.³⁷⁸ An early microscale device achieved electrofusion in a continuous system using a channel constriction after chemically pairing cells together off-chip before electrofusion, but this technique required prior cell membrane functionalization.³⁷⁹ Instead, many existing electrofusion devices use structural or active components to facilitate cell assembly. In this section, we discuss cell assembly strategies that have been developed for electrofusion.

Passive cell pairing techniques with hydrodynamic forces use microstructures to pair cells together in a highly scalable manner. Voldman and colleagues devised an array of weir-based single- and double-cell hydrodynamic cell trap micro-structures for cell pairing before electrofusion (Figure 19A).^{182,380} Target cells were first individually confined in capture cups before being transferred into a larger trap by changing the flow direction¹⁸² or increasing the flow rate to squeeze cells through a constriction.³⁸⁰ Microstructure-assisted cell pairing works for homotypic and heterotypic cell pairing and is compatible with chemical and electrofusion. The passive technique enables scalable processing with microstructure arrays and on-chip observation of fusion events. Cells may also be confined in pairs using droplets. Schoeman et al. fabricated a continuous droplet generator to encapsulate suspended cells in droplets upstream of EP.³⁸¹ EP conditions were controlled by flow rate as droplets passed an interdigitated electrode array. Two-cell pairing efficiency was limited to 15% due to the natural Poisson distribution of cell encapsulation in droplets.

DEP forces are also widely used to actively align and guide cells to designated electrofusion regions with embedded electrodes. DEP has diverse uses in selecting cells for fusion, positioning cells close to enhanced electric fields, or transferring fused cells for collection. Cao et al. demonstrated how microscale features could improve cell fusion by aligning cells with DEP using serpentine channels fabricated with counter electrodes.³⁸² Hundreds of microelectrode pairs were fabricated in a single chip for fusion of ~450 cells per batch. The same group of researchers formed 2D³⁸³ and 3D³⁸⁴ electrodes to generate discrete electrode pairs and eliminate dead areas of cell pairing. Over 99% cells were aligned, and the averaged fusion efficiency reached 43%. Wu et al. deflected NIH 3T3 and mouse embryonic stem cells (mESCs) into microcavities with DEP forces for cell reprogramming into pluripotent stem cells (Figure 19B).³⁸⁵ Electrodes were patterned on the back wall of individual microcavities. Cells could be collected after electrofusion by turning off DEP forces, and the collected cells showed gene expression similar to mESCs. Zhang et al. fabricated the microwell electrodes on three channel walls to alter the TMP uniformity of captured cells.³⁸⁶ This design produced a more consistent cell membrane TMP distribution so that cells could be fused without undesirable irreversible EP. He et al. designed adjacent electrodes to attract two cells with pDEP forces.³⁸⁷ nDEP forces were then activated to push the two cells together for electrofusion. After fusion, cells could be collected in individual wells for culture and future analysis. Electrofusion was 4× faster and more efficient than PEG-assisted fusion (Figure 19C). DEP forces were also used for monitored selection and release of cell pairs from the continuous cell stream. Kirschbaum et al. developed a

cell manipulation device to select and fuse a pair of cells interested for cell fusion.³⁸⁸ Selected cells were deflected by DEP force to a field cage composed of eight electrodes for fusion under an AC pulse. Lu et al. devised a curved microfluidic device that combined hydrodynamic trapping with DEP forces for two-cell trapping and fusion.³⁸⁹ The first target cell was hydrodynamically trapped in a curved microchannel, and the second was brought close by using DEP forces. With this method, the maximum cell pairing and electrofusion efficiencies were 68% and 64%, respectively. Similarly, Pendharkar et al. trapped cells in separate hydrodynamic traps and flipped the device so cell pairs would settle in a microwell.³⁹⁰ By applying DEP forces, cells were joined together and electroporated for 73% electrofusion efficiency.

Subcellular channels may serve dual functions as a point for localized electric field enhancement and electrofusion. Masuda et al. first proposed a microfluidic electrofusion system with a subcellular channel in 1989.³⁹¹ Two kinds of cells were flowed from separate inlets and trapped at the pore in the middle of the channel by DEP for electrofusion. Arrays of subcellular channels for cell pairing allowed for parallelized observation of fused cells.³⁹² Sakamoto et al. flowed cell suspensions down microchannels connecting both ends of a subcellular channel (Figure 19D).³⁹³ High-frequency AC voltages generated DEP forces that caused single-cell pairing across the gap, and only the properly positioned cells were fused. The fused cells remained at the pores until they grew and divided. Okanojo et al. modified the experimental protocol to combine a somatic cell nucleus with iPSC intracellular cytoplasm to artificially program pluripotency with 60% efficiency.³⁹⁴ Somatic cells were initially paired with a sacrificial cell, and the flow rates were tuned to generate shear forces that squeeze the somatic cell cytoplasm into a sacrificial cell. Drag forces on the swollen sacrificial cell split the fused cells apart, and the somatic cell nucleus was then paired with a target iPSC. The flow rates were switched so that the iPSC cytoplasm combines with the somatic cell nucleus, and the reprogrammed cells could be collected.

5. CONCLUSION

In this Review, we outlined recent engineering advances and applications of microscale EP systems. Technological developments focus on improving both EP efficiency and processing throughputs using novel device design, application of external forces, or optimized electric field conditions. Operating on the microscale reduces the necessary voltages to achieve sufficiently high TMPs for cell EP, which improves cell viability and makes the overall system safer. Milder electrical conditions reduce the undesirable effects of electrolysis on cell viability. Cargo delivery is precisely controlled with micro-/nanofeatures, as cells experience more uniform electric field conditions. In addition, there is renewed focus on implementing microscale EP systems using fabrication and operational techniques that lower the overall costs.

We categorized microfluidic EP devices primarily as static or continuous systems based on cell movement during the application of electrical pulses. The distinction is useful to highlight specific engineering choices and advantages specific to a certain modality that help with improving cell EP performance. Cells processed by static EP devices are confined to a specific region by either natural cell adhesion or the application of passive or active

forces. Static EP is effective for localized enhancement of electric fields through subcellular channels or sharp features because cell placement is highly controllable. With these systems, there is potential for precise temporal and dose control because poration regions are well-defined. Static EP is useful for biomedical research applications impacted by the behavior of individual cells because each cell can be tracked and visualized in real time, instead of relying on bulk collection, where heterogeneous behaviors may be obfuscated. In comparison, continuous EP devices include systems where cells are constantly flowing past an EP region. Efforts are underway to focus electric fields within the microchannel and improve the uniformity of conditions applied to each cell. Different strategies have been applied to mitigate the negative effects of electrolysis. Continuous EP devices have inherently high throughput with potential applications in processing cells for clinical therapies. In addition to innovations in these microscale EP strategies, general advances have been made to passivate electrodes or improve permeabilization uniformity for improved EP performance, encapsulate cells in droplets, incorporate impedance measurements to extract additional information during cell processing, and reduce overall barriers to technology development and adoption.

Most microscale EP devices are developed by researchers who have micro-/nanofabrication experience to produce microfluidic channels and integrated micro-/nanoelectrodes. On-chip manipulation of cells also needs external systems for fluidic, electronic, or optical control. For biologists and clinicians who want to use microscale EP beyond proof-of-concept assays, user-friendly microscale EP devices are becoming commercially accessible. Existing systems include the neon transfection system (Thermo Fisher Scientific, Inc.) with microcapillaries and wire electrodes,²⁹⁰ the fully automated NFP-E system (iNfinitesimal, LLC) based on NFPs,^{161–165} and a continuous flow EP module (The Charles Stark Draper Laboratory, Inc.), which can process 500 million T cells at a rate of 20 million cells/min.²⁵³ An electrofusion device (Harvard Bioscience, Inc.) uses DEP force to align cells for fusion.³⁹⁵ These devices have enabled genetic modification of cells with potential therapeutic applications in cell therapy or tissue engineering. Additionally, applied EP studies helped determine the effect of external stimuli on cell behavior. Intracellular contents can be probed using targetable biosensors, via repeatable sampling, or by studying cell lysate following irreversible EP. Cell inactivation has general utility in water disinfection and clinical treatments. Finally, microscale EP enables controlled cell fusion to increase cell functionality. Microscale EP systems have already demonstrated significant potential as tools in clinical and research settings. Nevertheless, future works should be dedicated toward expanding the capabilities of these devices. For example, many devices are validated using known, immortal cancer cell lines that may be more resistant to external stimuli. Concerted efforts are needed to electroporate sensitive primary cells with such devices. In line with this goal, future studies should transition toward engineering cells with new functionalities with clinical relevance. Similarly, investigation of electroporating cells in nonidealized biological samples, such as blood, is warranted. Developing entire workflows from sample collection to EP may increase the utility and expansion of these devices. Alongside these goals, efforts should be made to better understand the mechanism of EP. More fundamental work is needed to determine optimal EP conditions irrespective of channel geometry, instead of the trial-and-error optimization currently practiced. Integration of EP with feedback systems

may help determine optimal experimental conditions more rapidly. With an improved understanding of the mechanisms of EP, more methods may be devised to improve cargo delivery to specific subcellular components, such as DNA to the nucleus, for more efficient transfection. Finally, efforts should be made to reduce the cost and complexity of device fabrication for broader technology adoption. These advances would help scale up microscale EP for applications for industry and clinical settings.

ACKNOWLEDGMENTS

The authors thank Professor Yun Chen for helpful suggestions and discussions. S.C.H. acknowledges financial support from Johnson and Johnson WiSTEM2D Scholar Program, the National Institute of Health grant 1R21CA229024, the Susan G. Komen Career Catalyst Award, and the Johns Hopkins Startup Fund.

Biographies

Sung-Eun Choi received his B.S. in Electrical Engineering and Chemical and Biological Engineering from Seoul National University in 2009. He received his M.S. in Electrical Engineering and Computer Science from Seoul National University in 2011. He obtained his Ph.D. in Physics from RWTH Aachen in 2016 under the supervision of Professor Andreas Offenhäusser. His Ph.D. research was about the supported lipid bilayer to construct the biomimetic neuron–chip interface. After his Ph.D. and postdoctoral research with Professor Andreas Offenhäusser in Forschungszentrum Jülich, he joined the laboratory of Professor Soojung Claire Hur. His current research includes microfluidic genetic modification of blood cells of patients for cell therapy and responsive hydrogel droplet development for single-cell proteomic study.

Harrison Khoo is currently pursuing a doctorate degree in Mechanical Engineering at Johns Hopkins University under the guidance of Professor Soojung Claire Hur. He previously received his B.S. in Bioengineering from UC Berkeley in 2019 and his M.S.E. in Mechanical Engineering from Johns Hopkins University in 2021. His current research interests lie in developing microfluidic tools for personalized cancer therapeutics and point-of-care diagnostics.

Soojung Claire Hur is the Clare Boothe Luce Assistant Professor in the Department of Mechanical Engineering at Johns Hopkins University, and she holds her secondary appointment in Department of Oncology at Johns Hopkins Medicine. She received her B.S., M.S., and Ph.D. in Mechanical Engineering from UCLA in 2005, 2007, and 2011, respectively. After her doctoral training, she joined the Rowland Institute at Harvard University as one of two Rowland Fellows in September 2011 with five years of research funding. Before joining the Johns Hopkins University, she managed the clinical studies funded by the Vortex Biosciences, Inc. as an assistant researcher at UCLA Department of Bioengineering. Her research group conducts various projects to develop microfluidic platforms facilitating simple and cost-effective biological assays, useful for oncology, immunology, gene therapy, and regenerative medicine.

ABBREVIATIONS

3DSTE	3D sharp-tipped electrode
AML	acute myeloid leukemia
AC	alternating current
bp	base pair
BBB	blood–brain barrier
CNP	cellular nanoporation
CPP	cell penetrating peptide
CAR	chimeric antigen receptor
CHO	Chinese hamster ovary
CTC	circulating tumor cell
CRISPR	clustered regularly interspaced short palindromic repeats
DEP	dielectrophoresis
DC	direct current
DOX	doxorubicin
EIS	electrical impedance spectroscopy
EP	electroporation
ELISA	enzyme-linked immunosorbent assay
EGFR	epidermal growth factor receptor
EpCAM	epithelial cell adhesion molecules
FRET	Förster resonance energy transfer
gDNA	genomic DNA
GFP	green fluorescent protein
ITO	indium tin oxide
iN	induced neuron
iPSC	induced pluripotent stem cell
ITP	isotachophoresis
LEPD	localized electroporation device
MN	magnetic nanoparticle

mRNA	messenger RNA
miRNA	microRNA
μPAR	micropost array railing
MB	molecular beacon
MD	molecular dynamics
mESC	mouse embryonic stem cell
NEP	nanochannel EP
NFP	nanofountain probe
NSP	nanospike
NES	nanostraw electroporation system
NEX	nanostraw extraction
NK	natural killer
PNA	peptide nucleic acid
PC	polycarbonate
PDMS	polydimethylsiloxane
PEG	polyethylene glycol
PET	poly(ethylene terephthalate)
PCR	polymerase chain reaction
PCB	printed circuit board
qRT-PCR	quantitative reverse transcription PCR
PI	propidium iodide
QD	quantum dot
RBC	red blood cell
RNP	ribonucleoprotein
RNAi	RNA interference
SAMDI	self-assembled monolayer for matrix-assisted laser desorption/ ionization
siRNA	small interfering RNA
SEB	surface-enhanced blocking

SERS	surface-enhanced Raman scattering
TMP	transmembrane potential
TENG	triboelectric nanogenerator
WBC	white blood cell

REFERENCES

- (1). Neumann E; Rosenheck K Permeability Changes Induced by Electric Impulses in Vesicular Membranes. *J. Membr. Biol.* 1972, 10, 279–290. [PubMed: 4667921]
- (2). Neumann E; Schaefer-Ridder M; Wang Y; Hofschneider P h. Gene Transfer into Mouse Lyoma Cells by Electroporation in High Electric Fields. *EMBO J.* 1982, 1, 841–845. [PubMed: 6329708]
- (3). Kotnik T; Frey W; Sack M; Haberl Megli S; Peterka M; Miklav i D Electroporation-Based Applications in Biotechnology. *Trends Biotechnol.* 2015, 33, 480–488. [PubMed: 26116227]
- (4). Zimmermann U Electric Field-Mediated Fusion and Related Electrical Phenomena. *Biochim. Biophys. Acta BBA - Rev. Biomembr.* 1982, 694, 227–277.
- (5). Ramos C; Bonato D; Winterhalter M; Stegmann T; Teissié J Spontaneous Lipid Vesicle Fusion with Electroporabilized Cells. *FEBS Lett.* 2002, 518, 135–138. [PubMed: 11997033]
- (6). Mir LM Nucleic Acids Electrotransfer-Based Gene Therapy (Electrogenotherapy): Past, Current, and Future. *Mol. Biotechnol.* 2009, 43, 167. [PubMed: 19562526]
- (7). Stewart MP; Sharei A; Ding X; Sahay G; Langer R; Jensen KF In Vitro and Ex Vivo Strategies for Intracellular Delivery. *Nature* 2016, 538, 183–192. [PubMed: 27734871]
- (8). Shi J; Ma Y; Zhu J; Chen Y; Sun Y; Yao Y; Yang Z; Xie J A Review on Electroporation-Based Intracellular Delivery. *Molecules* 2018, 23, 3044. [PubMed: 30469344]
- (9). Duckert B; Vinkx S; Braeken D; Fauvart M Single-Cell Transfection Technologies for Cell Therapies and Gene Editing. *J. Controlled Release* 2021, 330, 963–975.
- (10). Sack M; Sigler J; Frenzel S; Eing Chr.; Arnold J; Michelberger Th.; Frey W; Attmann F; Stukenbrock L; Müller G Research on Industrial-Scale Electroporation Devices Fostering the Extraction of Substances from Biological Tissue. *Food Eng. Rev.* 2010, 2, 147–156.
- (11). Mahni -Kalamiza S; Vorobiev E; Miklav i D Electroporation in Food Processing and Biorefinery. *J. Membr. Biol.* 2014, 247, 1279–1304. [PubMed: 25287023]
- (12). Golberg A; Sack M; Teissie J; Pataro G; Pliquett U; Saulis G; Stefan T; Miklavcic D; Vorobiev E; Frey W Energy-Efficient Biomass Processing with Pulsed Electric Fields for Bioeconomy and Sustainable Development. *Biotechnol. Biofuels* 2016, 9, 94. [PubMed: 27127539]
- (13). Chen Z; Lee WG Electroporation for Microalgal Biofuels: A Review. *Sustain. Energy Fuels* 2019, 3, 2954–2967.
- (14). Stewart MP; Langer R; Jensen KF Intracellular Delivery by Membrane Disruption: Mechanisms, Strategies, and Concepts. *Chem. Rev.* 2018, 118, 7409–7531. [PubMed: 30052023]
- (15). Rad DM; Rad MA; Bazaz SR; Kashaninejad N; Jin D; Warkiani ME A Comprehensive Review on Intracellular Delivery. *Adv. Mater.* 2021, 33, 2005363.
- (16). Zhang X; Godbey WT Viral Vectors for Gene Delivery in Tissue Engineering. *Adv. Drug Delivery Rev.* 2006, 58, 515–534.
- (17). Kesharwani P; Gajbhiye V; Jain NK A Review of Nanocarriers for the Delivery of Small Interfering RNA. *Biomaterials* 2012, 33, 7138–7150. [PubMed: 22796160]
- (18). Heerklotz H Interactions of Surfactants with Lipid Membranes. *Q. Rev. Biophys.* 2008, 41, 205–264. [PubMed: 19079805]
- (19). Klein TM; Wolf ED; Wu R; Sanford JC High-Velocity Microprojectiles for Delivering Nucleic Acids into Living Cells. *Nature* 1987, 327, 70–73.

- (20). Fechheimer M; Boylan JF; Parker S; Sisken JE; Patel GL; Zimmer SG Transfection of Mammalian Cells with Plasmid DNA by Scrape Loading and Sonication Loading. *Proc. Natl. Acad. Sci. U. S. A.* 1987, 84, 8463–8467. [PubMed: 2446324]
- (21). McNeil PL; Warder E Glass Beads Load Macromolecules into Living Cells. *J. Cell Sci.* 1987, 88, 669–678. [PubMed: 2459146]
- (22). Clarke MS; McNeil PL Syringe Loading Introduces Macromolecules into Living Mammalian Cell Cytosol. *J. Cell Sci.* 1992, 102, 533–541. [PubMed: 1506433]
- (23). Lentacker I; De Cock I; Deckers R; De Smedt SC; Moonen CTW Understanding Ultrasound Induced Sonoporation: Definitions and Underlying Mechanisms. *Adv. Drug Delivery Rev.* 2014, 72, 49–64.
- (24). Palumbo G; Caruso M; Crescenzi E; Tecce MF; Roberti G; Colasanti A Targeted Gene Transfer in Eucaryotic Cells by Dye-Assisted Laser Optoporation. *J. Photochem. Photobiol., B* 1996, 36, 41–46. [PubMed: 8988610]
- (25). Scherer F; Anton M; Schillinger U; Henke J; Bergemann C; Kruger A; Gänsbacher B; Plank C Magnetofection: Enhancing and Targeting Gene Delivery by Magnetic Force in Vitro and in Vivo. *Gene Ther.* 2002, 9, 102–109. [PubMed: 11857068]
- (26). Thomas CE; Ehrhardt A; Kay MA Progress and Problems with the Use of Viral Vectors for Gene Therapy. *Nat. Rev. Genet.* 2003, 4, 346–358. [PubMed: 12728277]
- (27). Liu J; Fraire JC; Smedt SCD; Xiong R; Braeckmans K Intracellular Labeling with Extrinsic Probes: Delivery Strategies and Applications. *Small* 2020, 16, 2000146.
- (28). Fajrial AK; He QQ; Wirusanti NI; Slansky JE; Ding X A Review of Emerging Physical Transfection Methods for CRISPR/Cas9-Mediated Gene Editing. *Theranostics* 2020, 10, 5532–5549. [PubMed: 32373229]
- (29). Brunner S; Fürtbauer E; Sauer T; Kursa M; Wagner E Overcoming the Nuclear Barrier: Cell Cycle Independent Nonviral Gene Transfer with Linear Polyethylenimine or Electroporation. *Mol. Ther.* 2002, 5, 80–86. [PubMed: 11786049]
- (30). Venslauskas MS; Šatkauskas S Mechanisms of Transfer of Bioactive Molecules through the Cell Membrane by Electroporation. *Eur. Biophys. J.* 2015, 44, 277–289. [PubMed: 25939984]
- (31). Potter H Electroporation in Biology: Methods, Applications, and Instrumentation. *Anal. Biochem.* 1988, 174, 361–373. [PubMed: 3071177]
- (32). Chang L; Li L; Shi J; Sheng Y; Lu W; Gallego-Perez D; Lee LJ Micro-/Nanoscale Electroporation. *Lab. Chip* 2016, 16, 4047–4062. [PubMed: 27713986]
- (33). Erickson D; Sinton D; Li D Joule Heating and Heat Transfer in Poly(Dimethylsiloxane) Microfluidic Systems. *Lab. Chip* 2003, 3, 141. [PubMed: 15100765]
- (34). Pataro G; Falcone M; Donsi G; Ferrari G Metal Release from Stainless Steel Electrodes of a PEF Treatment Chamber: Effects of Electrical Parameters and Food Composition. *Innov. Food Sci. Emerg. Technol.* 2014, 21, 58–65.
- (35). Chang L; Gallego-Perez D; Chiang C-L; Bertani P; Kuang T; Sheng Y; Chen F; Chen Z; Shi J; Yang H; et al. Controllable Large-Scale Transfection of Primary Mammalian Cardiomyocytes on a Nanochannel Array Platform. *Small* 2016, 12, 5971–5980. [PubMed: 27648733]
- (36). Shokouhi A-R; Aslanoglou S; Nisbet D; Voelcker NH; Elnathan R Vertically Configured Nanostructure-Mediated Electroporation: A Promising Route for Intracellular Regulations and Interrogations. *Mater. Horiz.* 2020, 7, 2810–2831.
- (37). Tay A The Benefits of Going Small: Nanostructures for Mammalian Cell Transfection. *ACS Nano* 2020, 14, 7714–7721. [PubMed: 32631053]
- (38). Huang Y; Rubinsky B Micro-Electroporation: Improving the Efficiency and Understanding of Electrical Permeabilization of Cells. *Biomed. Microdevices* 1999, 2, 145–150.
- (39). Kar S; Loganathan M; Dey K; Shinde P; Chang H-Y; Nagai M; Santra TS Single-Cell Electroporation: Current Trends, Applications and Future Prospects. *J. Micromechanics Microengineering* 2018, 28, 123002.
- (40). Fox MB; Esveld DC; Valero A; Luttge R; Mastwijk HC; Bartels PV; van den Berg A; Boom RM Electroporation of Cells in Microfluidic Devices: A Review. *Anal. Bioanal. Chem.* 2006, 385, 474. [PubMed: 16534574]

- (41). Lee WG; Demirci U; Khademhosseini A Microscale Electroporation: Challenges and Perspectives for Clinical Applications. *Integr. Biol.* 2009, 1, 242–251.
- (42). Movahed S; Li D Microfluidics Cell Electroporation. *Microfluid. Nanofluidics* 2011, 10, 703–734.
- (43). Geng T; Lu C Microfluidic Electroporation for Cellular Analysis and Delivery. *Lab. Chip* 2013, 13, 3803–3821. [PubMed: 23917998]
- (44). Wang S; Lee LJ Micro-/Nanofluidics Based Cell Electroporation. *Biomicrofluidics* 2013, 7, No. 011301. [PubMed: 23405056]
- (45). Brooks J; Minnick G; Mukherjee P; Jaber A; Chang L; Espinosa HD; Yang R High Throughput and Highly Controllable Methods for In Vitro Intracellular Delivery. *Small* 2020, 16, 2004917.
- (46). Nan L; Jiang Z; Wei X Emerging Microfluidic Devices for Cell Lysis: A Review. *Lab. Chip* 2014, 14, 1060–1073. [PubMed: 24480982]
- (47). Shehadul Islam M; Aryasomayajula A; Selvaganapathy PR A Review on Macroscale and Microscale Cell Lysis Methods. *Micromachines* 2017, 8, 83.
- (48). Jeon H; Kim S; Lim G Electrical Force-Based Continuous Cell Lysis and Sample Separation Techniques for Development of Integrated Microfluidic Cell Analysis System: A Review. *Microelectron. Eng.* 2018, 198, 55–72.
- (49). Grigorov E; Kirov B; Marinov MB; Galabov V Review of Microfluidic Methods for Cellular Lysis. *Micromachines* 2021, 12, 498. [PubMed: 33925101]
- (50). Kim J; Hwang I; Britain D; Chung TD; Sun Y; Kim D-H Microfluidic Approaches for Gene Delivery and Gene Therapy. *Lab. Chip* 2011, 11, 3941–3948. [PubMed: 22027752]
- (51). Yang Z; Chang L; Chiang C-L; Lee LJ Micro-/Nano-Electroporation for Active Gene Delivery. *Curr. Pharm. Des.* 2015, 21, 6081–6088. [PubMed: 26503150]
- (52). Le Gac S; van Uitert I Electroporation in Microfluidic Devices. In *Handbook of Electroporation*; Miklavcic D, Ed.; Springer International Publishing: Cham, 2016; pp 1–20. DOI: 10.1007/978-3-319-26779-1_136-1.
- (53). O'Connor CM; Adams JU *Essentials of Cell Biology*; NPG Education: Cambridge, MA, 2010.
- (54). Gautier A, Hinner MJ, Eds. *Site-Specific Protein Labeling: Methods and Protocols; Methods in Molecular Biology*; Springer New York: New York, 2015; Vol. 1266. DOI: 10.1007/978-1-4939-2272-7.
- (55). Glaser RW; Leikin SL; Chernomordik LV; Pastushenko VF; Sokirko AI Reversible Electrical Breakdown of Lipid Bilayers: Formation and Evolution of Pores. *Biochim. Biophys. Acta BBA - Biomembr.* 1988, 940, 275–287.
- (56). Teissié J; Rols MP An Experimental Evaluation of the Critical Potential Difference Inducing Cell Membrane Electro-permeabilization. *Biophys. J.* 1993, 65, 409–413. [PubMed: 8369446]
- (57). Weaver JC; Chizmadzhev Yu. A. *Theory of Electroporation: A Review.* *Bioelectrochem. Bioenerg.* 1996, 41, 135–160.
- (58). Kotnik T; Rems L; Tarek M; Miklavcic D Membrane Electroporation and Electropermeabilization: Mechanisms and Models. *Annu. Rev. Biophys.* 2019, 48, 63–91. [PubMed: 30786231]
- (59). Kotnik T; Bobanovic F; Miklavcic D. Sensitivity of Transmembrane Voltage Induced by Applied Electric Fields—A Theoretical Analysis. *Bioelectrochem. Bioenerg.* 1997, 43, 285–291.
- (60). Kotnik T; Miklavcic D. Analytical Description of Transmembrane Voltage Induced by Electric Fields on Spheroidal Cells. *Biophys. J.* 2000, 79, 670–679. [PubMed: 10920001]
- (61). Escoffier J-M; Portet T; Wasungu L; Teissié J; Dean D; Rols M-P What Is (Still Not) Known of the Mechanism by Which Electroporation Mediates Gene Transfer and Expression in Cells and Tissues. *Mol. Biotechnol.* 2009, 41, 286–295. [PubMed: 19016008]
- (62). Teissié J; Golzio M; Rols MP Mechanisms of Cell Membrane Electropermeabilization: A Minireview of Our Present (Lack of ?) Knowledge. *Biochim. Biophys. Acta BBA - Gen. Subj.* 2005, 1724, 270–280.
- (63). Hölzel R; Lamprecht I Dielectric Properties of Yeast Cells as Determined by Electrorotation. *Biochim. Biophys. Acta BBA - Biomembr.* 1992, 1104, 195–200.

- (64). Simeonova M; Wachner D; Gimsa J Cellular Absorption of Electric Field Energy: Influence of Molecular Properties of the Cytoplasm. *Bioelectrochemistry* 2002, 56, 215–218. [PubMed: 12009478]
- (65). Zheng Y; Shojaei-Baghini E; Wang C; Sun Y Microfluidic Characterization of Specific Membrane Capacitance and Cytoplasm Conductivity of Singlecells. *Biosens. Bioelectron.* 2013, 42, 496–502. [PubMed: 23246657]
- (66). Marszalek P; Liu DS; Tsong TY Schwan Equation and Transmembrane Potential Induced by Alternating Electric Field. *Biophys. J.* 1990, 58, 1053–1058. [PubMed: 2248989]
- (67). Mernier G; Piacentini N; Braschler T; Demierre N; Renaud P Continuous-Flow Electrical Lysis Device with Integrated Control by Dielectrophoretic Cell Sorting. *Lab. Chip* 2010, 10, 2077–2082. [PubMed: 20556306]
- (68). Faurie C; Phez E; Golzio M; Vossen C; Lesbordes J-C; Delteil C; Teissié J; Rols M-P Effect of Electric Field Vectoriality on Electrically Mediated Gene Delivery in Mammalian Cells. *Biochim. Biophys. Acta BBA - Biomembr.* 2004, 1665, 92–100.
- (69). Alberts B; Johnson A; Lewis J; Raff M; Roberts K; Walter P *Mol. Biol. Cell*, 4th ed.; Garland Science, 2002.
- (70). Krassowska W; Filev PD Modeling Electroporation in a Single Cell. *Biophys. J.* 2007, 92, 404–417. [PubMed: 17056739]
- (71). Kotnik T; Pucihar G; Miklavic D Induced Transmembrane Voltage and Its Correlation with Electroporation-Mediated Molecular Transport. *J. Membr. Biol.* 2010, 236, 3–13. [PubMed: 20617432]
- (72). Gehl J Electroporation: Theory and Methods, Perspectives for Drug Delivery, Gene Therapy and Research. *Acta Physiol. Scand.* 2003, 177, 437–447. [PubMed: 12648161]
- (73). Hibino M; Itoh H; Kinoshita K Time Courses of Cell Electroporation as Revealed by Submicrosecond Imaging of Transmembrane Potential. *Biophys. J.* 1993, 64, 1789–1800. [PubMed: 8369408]
- (74). Prausnitz MR; Corbett JD; Gimm JA; Golan DE; Langer R; Weaver JC Millisecond Measurement of Transport during and after an Electroporation Pulse. *Biophys. J.* 1995, 68, 1864–1870. [PubMed: 7612828]
- (75). Levine ZA; Vernier PT Life Cycle of an Electropore: Field-Dependent and Field-Independent Steps in Pore Creation and Annihilation. *J. Membr. Biol.* 2010, 236, 27–36. [PubMed: 20623350]
- (76). Levine ZA; Vernier PT Calcium and Phosphatidylserine Inhibit Lipid Electropore Formation and Reduce Pore Lifetime. *J. Membr. Biol.* 2012, 245, 599–610. [PubMed: 22815071]
- (77). Wimberger T; Köhler VK; Ehmoser EK; Wassermann KJ Capacitive Coupling Increases the Accuracy of Cell-Specific Tumour Disruption by Electric Fields. *Bioelectrochemistry* 2020, 134, No. 107495. [PubMed: 32182566]
- (78). Goffinet C; Keppler OT Efficient Nonviral Gene Delivery into Primary Lymphocytes from Rats and Mice. *FASEB J.* 2006, 20, 500–502. [PubMed: 16401643]
- (79). Van Meirvenne S; Straetman L; Heirman C; Dullaers M; De Greef C; Van Tendeloo V; Thielemans K Efficient Genetic Modification of Murine Dendritic Cells by Electroporation with mRNA. *Cancer Gene Ther.* 2002, 9, 787–797. [PubMed: 12189529]
- (80). Van Tendeloo VFI; Ponsaerts P; Lardon F; Nijs G; Lenjou M; Van Broeckhoven C; Van Bockstaele DR; Berneman ZN Highly Efficient Gene Delivery by mRNA Electroporation in Human Hematopoietic Cells: Superiority to Lipofection and Passive Pulsing of mRNA and to Electroporation of Plasmid CDNA for Tumor Antigen Loading of Dendritic Cells. *Blood* 2001, 98, 49–56. [PubMed: 11418462]
- (81). Chen C; Smye SW; Robinson MP; Evans JA Membrane Electroporation Theories: A Review. *Med. Biol. Eng. Comput.* 2006, 44, 5–14. [PubMed: 16929916]
- (82). Golzio M; Teissié J; Rols M-P Direct Visualization at the Single-Cell Level of Electrically Mediated Gene Delivery. *Proc. Natl. Acad. Sci. U. S. A.* 2002, 99, 1292–1297. [PubMed: 11818537]
- (83). Neumann E; Toensing K; Kakorin S; Budde P; Frey J Mechanism of Electroporative Dye Uptake by Mouse B Cells. *Biophys. J.* 1998, 74, 98–108. [PubMed: 9449314]

- (84). Pucihar G; Kotnik T; Miklav i D; Teissié J Kinetics of Transmembrane Transport of Small Molecules into Electroporabilized Cells. *Biophys. J.* 2008, 95, 2837–2848. [PubMed: 18539632]
- (85). Paganin-Gioanni A; Bellard E; Escoffre JM; Rols MP; Teissié J; Golzio M Direct Visualization at the Single-Cell Level of SiRNA Electrotransfer into Cancer Cells. *Proc. Natl. Acad. Sci. U. S. A.* 2011, 108, 10443–10447. [PubMed: 21670256]
- (86). Phez E; Faurie C; Golzio M; Teissié J; Rols M-P New Insights in the Visualization of Membrane Permeabilization and DNA/Membrane Interaction of Cells Submitted to Electric Pulses. *Biochim. Biophys. Acta BBA - Gen. Subj.* 2005, 1724, 248–254.
- (87). Rosazza C; Deschout H; Buntz A; Braeckmans K; Rols M-P; Zumbusch A Endocytosis and Endosomal Trafficking of DNA After Gene Electrotransfer In Vitro. *Mol. Ther. - Nucleic Acids* 2016, 5, e286. [PubMed: 26859199]
- (88). Egloff S; Runser A; Klymchenko A; Reisch A Size-Dependent Electroporation of Dye-Loaded Polymer Nanoparticles for Efficient and Safe Intracellular Delivery. *Small Methods* 2021, 5, 2000947.
- (89). Potter H; Heller R Transfection by Electroporation. *Curr. Protoc. Mol. Biol.* 2018, 121, 9.3.1–9.3.13.
- (90). Sherba JJ; Hogquist S; Lin H; Shan JW; Shreiber DI; Zahn JD The Effects of Electroporation Buffer Composition on Cell Viability and Electro-Transfection Efficiency. *Sci. Rep.* 2020, 10, 3053. [PubMed: 32080269]
- (91). Golzio M; Mora M-P; Raynaud C; Delteil C; Teissié J; Rols M-P Control by Osmotic Pressure of Voltage-Induced Permeabilization and Gene Transfer in Mammalian Cells. *Biophys. J.* 1998, 74, 3015–3022. [PubMed: 9635756]
- (92). Pucihar G; Kotnik T; Kandušer M; Miklav i , D. The Influence of Medium Conductivity on Electroporabilization and Survival of Cells in Vitro. *Bioelectrochemistry* 2001, 54, 107–115. [PubMed: 11694390]
- (93). Li Y; Wu M; Zhao D; Wei Z; Zhong W; Wang X; Liang Z; Li Z Electroporation on Microchips: The Harmful Effects of PH Changes and Scaling Down. *Sci. Rep.* 2016, 5, 17817.
- (94). Silve A; Leray I; Poignard C; Mir LM Impact of External Medium Conductivity on Cell Membrane Electroporabilization by Microsecond and Nanosecond Electric Pulses. *Sci. Rep.* 2016, 6, 19957. [PubMed: 26829153]
- (95). Zand E; Schottroff F; Steinacker E; Mae-Gano J; Schoenher C; Wimberger T; Wassermann KJ; Jaeger H Advantages and Limitations of Various Treatment Chamber Designs for Reversible and Irreversible Electroporation in Life Sciences. *Bioelectrochemistry* 2021, 141, No. 107841. [PubMed: 34098460]
- (96). Heiser WC Optimizing Electroporation Conditions for the Transformation of Mammalian Cells. In *Transcription Factor Protocols*; Tymms MJ, Ed.; Methods in Molecular Biology; Humana Press: Totowa, NJ, 2000; pp 117–134. DOI: 10.1385/1-59259-686-X:117.
- (97). Jordan ET; Collins M; Terefe J; Ugozzoli L; Rubio T Optimizing Electroporation Conditions in Primary and Other Difficult-to-Transfect Cells. *J. Biomol. Technol. JBT* 2008, 19, 328–334.
- (98). Stroh T; Erben U; Kühl AA; Zeitz M; Siegmund B Combined Pulse Electroporation – A Novel Strategy for Highly Efficient Transfection of Human and Mouse Cells. *PLoS One* 2010, 5, e9488. [PubMed: 20209146]
- (99). Sadik MM; Yu M; Zheng M; Zahn JD; Shan JW; Shreiber DI; Lin H Scaling Relationship and Optimization of Double-Pulse Electroporation. *Biophys. J.* 2014, 106, 801–812. [PubMed: 24559983]
- (100). Ziv R; Steinhardt Y; Pelled G; Gazit D; Rubinsky B Micro-Electroporation of Mesenchymal Stem Cells with Alternating Electrical Current Pulses. *Biomed. Microdevices* 2009, 11, 95. [PubMed: 18815886]
- (101). Tekle E; Astumian RD; Chock PB Electroporation by Using Bipolar Oscillating Electric Field: An Improved Method for DNA Transfection of NIH 3T3 Cells. *Proc. Natl. Acad. Sci. U. S. A.* 1991, 88, 4230–4234. [PubMed: 2034667]

- (102). Kotnik T; Miklavic D. Theoretical Evaluation of Voltage Inducement on Internal Membranes of Biological Cells Exposed to Electric Fields. *Biophys. J.* 2006, 90, 480–491. [PubMed: 16239325]
- (103). Chopinet L; Rols M-P Nanosecond Electric Pulses: A Mini-Review of the Present State of the Art. *Bioelectrochemistry* 2015, 103, 2–6. [PubMed: 25190180]
- (104). Ruzgys P; Novickij V; Novickij J; Šatkauskas S Nanosecond Range Electric Pulse Application as a Non-Viral Gene Delivery Method: Proof of Concept. *Sci. Rep.* 2018, 8, 15502. [PubMed: 30341389]
- (105). Weaver JC; Smith KC; Esser AT; Son RS; Gowrishankar TR A Brief Overview of Electroporation Pulse Strength–Duration Space: A Region Where Additional Intracellular Effects Are Expected. *Bioelectrochemistry* 2012, 87, 236–243. [PubMed: 22475953]
- (106). Schoenbach KH; Beebe SJ; Buescher ES Intracellular Effect of Ultrashort Electrical Pulses. *Bioelectromagnetics* 2001, 22, 440–448. [PubMed: 11536285]
- (107). Chen N; Schoenbach KH; Kolb JF; James Swanson R; Garner AL; Yang J; Joshi RP; Beebe SJ Leukemic Cell Intracellular Responses to Nanosecond Electric Fields. *Biochem. Biophys. Res. Commun.* 2004, 317, 421–427. [PubMed: 15063775]
- (108). Luo D; Saltzman WM Synthetic DNA Delivery Systems. *Nat. Biotechnol.* 2000, 18, 33–37. [PubMed: 10625387]
- (109). Huang Y; Rubinsky B Microfabricated Electroporation Chip for Single Cell Membrane Permeabilization. *Sens. Actuators Phys.* 2001, 89, 242–249.
- (110). Shin YS; Cho K; Kim JK; Lim SH; Park CH; Lee KB; Park Y; Chung C; Han D-C; Chang JK Electrotransfection of Mammalian Cells Using Microchannel-Type Electroporation Chip. *Anal. Chem.* 2004, 76, 7045–7052. [PubMed: 15571358]
- (111). Khine M; Lau A; Ionescu-Zanetti C; Seo J; Lee LP A Single Cell Electroporation Chip. *Lab. Chip* 2005, 5, 38–43. [PubMed: 15616738]
- (112). Valero A; Merino F; Wolbers F; Lutge R; Vermes I; Andersson H; Berg A van den. Apoptotic Cell Death Dynamics of HL60 Cells Studied Using a Microfluidic Cell Trap Device. *Lab. Chip* 2005, 5, 49–55. [PubMed: 15616740]
- (113). Cao Y; Chen H; Qiu R; Hanna M; Ma E; Hjort M; Zhang A; Lewis RS; Wu JC; Melosh NA Universal Intracellular Biomolecule Delivery with Precise Dosage Control. *Sci. Adv.* 2018, 4, eaat8131. [PubMed: 30402539]
- (114). Dong Z; Jiao Y; Xie B; Hao Y; Wang P; Liu Y; Shi J; Chitrakar C; Black S; Wang Y-C; et al. On-Chip Multiplexed Single-Cell Patterning and Controllable Intracellular Delivery. *Microsyst. Nanoeng.* 2020, 6, 1–11. [PubMed: 34567616]
- (115). Tay A; Melosh N Transfection with Nanostructure Electro-Injection Is Minimally Perturbative. *Adv. Ther.* 2019, 2, 1900133.
- (116). Chen S-C; Santra TS; Chang C-J; Chen T-J; Wang P-C; Tseng F-G Delivery of Molecules into Cells Using Localized Single Cell Electroporation on ITO Micro-Electrode Based Transparent Chip. *Biomed. Microdevices* 2012, 14, 811–817. [PubMed: 22674171]
- (117). Santra TS; Wang P-C; Chang H-Y; Tseng F-G Tuning Nano Electric Field to Affect Restrictive Membrane Area on Localized Single Cell Nano-Electroporation. *Appl. Phys. Lett.* 2013, 103, 233701.
- (118). Santra TS; Chang H-Y; Wang P-C; Tseng F-G Impact of Pulse Duration on Localized Single-Cell Nano-Electroporation. *Analyst* 2014, 139, 6249–6258. [PubMed: 25320952]
- (119). Santra TS; Chen C-W; Chang H-Y; Tseng F-G Dielectric Passivation Layer as a Substratum on Localized Single-Cell Electroporation. *RSC Adv.* 2016, 6, 10979–10986.
- (120). Santra TS; Kar S; Chang H-Y; Tseng F-G Nano-Localized Single-Cell Nano-Electroporation. *Lab. Chip* 2020, 20, 4194–4204. [PubMed: 33047768]
- (121). Huang Y; Rubinsky B Flow-through Micro-Electroporation Chip for High Efficiency Single-Cell Genetic Manipulation. *Sens. Actuators Phys.* 2003, 104, 205–212.
- (122). Díaz-Rivera RE; Rubinsky B Electrical and Thermal Characterization of Nanochannels between a Cell and a Silicon Based Micro-Pore. *Biomed. Microdevices* 2006, 8, 25–34. [PubMed: 16491328]

- (123). Kurosawa O; Oana H; Matsuoka S; Noma A; Kotera H; Washizu M Electroporation through a Micro-Fabricated Orifice and Its Application to the Measurement of Cell Response to External Stimuli. *Meas. Sci. Technol.* 2006, 17, 3127–3133.
- (124). Khine M; Ionescu-Zanetti C; Blatz A; Wang L-P; Lee LP Single-Cell Electroporation Arrays with Real-Time Monitoring and Feedback Control. *Lab. Chip* 2007, 7, 457–462. [PubMed: 17389961]
- (125). Valero A; Post JN; van Nieuwkastele JW; ter Braak PM; Kruijjer W; van den Berg A. van den. Gene Transfer and Protein Dynamics in Stem Cells Using Single Cell Electroporation in a Microfluidic Device. *Lab. Chip* 2008, 8, 62–67. [PubMed: 18094762]
- (126). Ionescu-Zanetti C; Blatz A; Khine M Electrophoresis-Assisted Single-Cell Electroporation for Efficient Intracellular Delivery. *Biomed. Microdevices* 2008, 10, 113–116. [PubMed: 17828458]
- (127). Bao N; Lu C A Microfluidic Device for Physical Trapping and Electrical Lysis of Bacterial Cells. *Appl. Phys. Lett.* 2008, 92, 214103.
- (128). Ma S; Bryson BD; Sun C; Fortune SM; Lu C RNA Extraction from a Mycobacterium under Ultrahigh Electric Field Intensity in a Microfluidic Device. *Anal. Chem.* 2016, 88, 5053–5057. [PubMed: 27081872]
- (129). Fei Z; Wang S; Xie Y; Henslee BE; Koh CG; Lee LJ Gene Transfection of Mammalian Cells Using Membrane Sandwich Electroporation. *Anal. Chem.* 2007, 79, 5719–5722. [PubMed: 17600386]
- (130). Fei Z; Hu X; Choi H; Wang S; Farson D; Lee LJ Micronozzle Array Enhanced Sandwich Electroporation of Embryonic Stem Cells. *Anal. Chem.* 2010, 82, 353–358. [PubMed: 19961232]
- (131). Fei Z; Wu Y; Sharma S; Gallego-Perez D; Higueta-Castro N; Hansford D; Lannutti JJ; Lee LJ Gene Delivery to Cultured Embryonic Stem Cells Using Nanofiber-Based Sandwich Electroporation. *Anal. Chem.* 2013, 85, 1401–1407. [PubMed: 23237665]
- (132). Ishibashi T; Takoh K; Kaji H; Abe T; Nishizawa M A Porous Membrane-Based Culture Substrate for Localized in Situ Electroporation of Adherent Mammalian Cells. *Sens. Actuators B Chem.* 2007, 128, 5–11.
- (133). Kang W; Giraldo-Vela JP; Nathamgari SSP; McGuire T; McNaughton RL; Kessler JA; Espinosa HD Microfluidic Device for Stem Cell Differentiation and Localized Electroporation of Postmitotic Neurons. *Lab. Chip* 2014, 14, 4486–4495. [PubMed: 25205561]
- (134). Mukherjee P; Nathamgari SSP; Kessler JA; Espinosa HD Combined Numerical and Experimental Investigation of Localized Electroporation-Based Cell Transfection and Sampling. *ACS Nano* 2018, 12, 12118–12128. [PubMed: 30452236]
- (135). Cao Y; Ma E; Cestellos-Blanco S; Zhang B; Qiu R; Su Y; Doudna JA; Yang P Nontoxic Nanopore Electroporation for Effective Intracellular Delivery of Biological Macromolecules. *Proc. Natl. Acad. Sci. U. S. A.* 2019, 116, 7899–7904. [PubMed: 30923112]
- (136). Islam MS; Shahid A; Kuryllo K; Li Y; Deen MJ; Selvaganapathy PR Electrophoretic Concentration and Electrical Lysis of Bacteria in a Microfluidic Device Using a Nanoporous Membrane. *Micromachines* 2017, 8, 45.
- (137). Dong Z; Yan S; Liu B; Hao Y; Lin L; Chang T; Sun H; Wang Y; Li H; Wu H; et al. Single Living Cell Analysis Nanoplatform for High-Throughput Interrogation of Gene Mutation and Cellular Behavior. *Nano Lett.* 2021, 21, 4878–4886. [PubMed: 33830766]
- (138). Mukherjee P; Berns EJ; Patino CA; Moully EH; Chang L; Nathamgari SSP; Kessler JA; Mrksich M; Espinosa HD Temporal Sampling of Enzymes from Live Cells by Localized Electroporation and Quantification of Activity by SAMDI Mass Spectrometry. *Small* 2020, 16, 2000584.
- (139). Gallego-Perez D; Otero JJ; Czeisler C; Ma J; Ortiz C; Gygli P; Catacutan FP; Gokozan HN; Cowgill A; Sherwood T; et al. Deterministic Transfection Drives Efficient Nonviral Reprogramming and Uncovers Reprogramming Barriers. *Nanomedicine Nanotechnol. Biol. Med.* 2016, 12, 399–409.
- (140). Boukany PE; Morss A; Liao W; Henslee B; Jung H; Zhang X; Yu B; Wang X; Wu Y; Li L; et al. Nanochannel Electroporation Delivers Precise Amounts of Biomolecules into Living Cells. *Nat. Nanotechnol.* 2011, 6, 747–754. [PubMed: 22002097]

- (141). Zhao X; Huang X; Wang X; Wu Y; Einfeld A-K; Schwind S; Gallego-Perez D; Boukany PE; Marcucci GI; Lee LJ Nanochannel Electroporation as a Platform for Living Cell Interrogation in Acute Myeloid Leukemia. *Adv. Sci.* 2015, 2, 1500111.
- (142). Gao K; Huang X; Chiang C-L; Wang X; Chang L; Boukany P; Marcucci G; Lee R; Lee LJ Induced Apoptosis Investigation in Wild-Type and FLT3-ITD Acute Myeloid Leukemia Cells by Nanochannel Electroporation and Single-Cell QRT-PCR. *Mol. Ther.* 2016, 24, 956–964. [PubMed: 26782640]
- (143). Gao K; Li L; He L; Hinkle K; Wu Y; Ma J; Chang L; Zhao X; Perez DG; Eckardt S; et al. Design of a Microchannel-Nanochannel-Microchannel Array Based Nanoelectroporation System for Precise Gene Transfection. *Small* 2014, 10, 1015–1023. [PubMed: 24173879]
- (144). Zhao X; Wu Y; Gallego-Perez D; Kwak KJ; Gupta C; Ouyang X; Lee LJ Effect of Nonendocytic Uptake of Nanoparticles on Human Bronchial Epithelial Cells. *Anal. Chem.* 2015, 87, 3208–3215. [PubMed: 25671340]
- (145). Boukany PE; Wu Y; Zhao X; Kwak KJ; Glazer PJ; Leong K; Lee LJ Nonendocytic Delivery of Lipoplex Nanoparticles into Living Cells Using Nanochannel Electroporation. *Adv. Healthc. Mater.* 2014, 3, 682–689. [PubMed: 23996973]
- (146). Chang L; Howdysheill M; Liao W-C; Chiang C-L; Gallego-Perez D; Yang Z; Lu W; Byrd JC; Muthusamy N; Lee LJ; et al. Magnetic Tweezers-Based 3D Microchannel Electroporation for High-Throughput Gene Transfection in Living Cells. *Small* 2015, 11, 1818–1828. [PubMed: 25469659]
- (147). Chang L; Gallego-Perez D; Zhao X; Bertani P; Yang Z; Chiang C-L; Malkoc V; Shi J; Sen CK; Odonnell L; et al. Dielectrophoresis-Assisted 3D Nanoelectroporation for Non-Viral Cell Transfection in Adoptive Immunotherapy. *Lab. Chip* 2015, 15, 3147–3153. [PubMed: 26105628]
- (148). Chang L; Bertani P; Gallego-Perez D; Yang Z; Chen F; Chiang C; Malkoc V; Kuang T; Gao K; Lee LJ; et al. 3D Nanochannel Electroporation for High-Throughput Cell Transfection with High Uniformity and Dosage Control. *Nanoscale* 2016, 8, 243–252. [PubMed: 26309218]
- (149). Bertani P; Lu W; Chang L; Gallego-Perez D; James Lee L; Chiang C; Muthusamy N Bosch Etching for the Creation of a 3D Nanoelectroporation System for High Throughput Gene Delivery. *J. Vac. Sci. Technol. B* 2015, 33, No. 06F903.
- (150). Gallego-Perez D; Pal D; Ghatak S; Malkoc V; Higueta-Castro N; Gnyawali S; Chang L; Liao W-C; Shi J; Sinha M; et al. Topical Tissue Nano-Transfection Mediates Non-Viral Stroma Reprogramming and Rescue. *Nat. Nanotechnol.* 2017, 12, 974–979. [PubMed: 28785092]
- (151). Yang Z; Shi J; Xie J; Wang Y; Sun J; Liu T; Zhao Y; Zhao X; Wang X; Ma Y; et al. Large-Scale Generation of Functional mRNA-Encapsulating Exosomes via Cellular Nanoporation. *Nat. Biomed. Eng.* 2020, 4, 69–83. [PubMed: 31844155]
- (152). Xie X; Xu AM; Leal-Ortiz S; Cao Y; Garner CC; Melosh NA Nanostraw–Electroporation System for Highly Efficient Intracellular Delivery and Transfection. *ACS Nano* 2013, 7, 4351–4358. [PubMed: 23597131]
- (153). Fang J; Xu J; Xiang Y; Li H; Xu D; Xie X; Hu N Accurate and Efficient Intracellular Delivery Biosensing System by Nanostrawed Electroporation Array. *Biosens. Bioelectron.* 2021, 194, No. 113583. [PubMed: 34464876]
- (154). He G; Feng J; Zhang A; Zhou L; Wen R; Wu J; Yang C; Yang J; Li C; Chen D; et al. Multifunctional Branched Nanostraw-Electroporation Platform for Intracellular Regulation and Monitoring of Circulating Tumor Cells. *Nano Lett.* 2019, 19, 7201–7209. [PubMed: 31557044]
- (155). Feng J; Mo J; Zhang A; Liu D; Zhou L; Hang T; Yang C; Wu Q; Xia D; Wen R; et al. Antibody-Free Isolation and Regulation of Adherent Cancer Cells via Hybrid Branched Microtube-Sandwiched Hydrodynamic System. *Nanoscale* 2020, 12, 5103–5113. [PubMed: 32068774]
- (156). Zhou L; Zhang A; Mo J; Xiu S; Hang T; Feng J; Wen R; Liu D; Yang C; Feng Y; et al. Degradable Porous Nanoflower Substrate-Embedded Microfluidic Device for Capture, Release and in Situ Manipulation of Cancer Cells. *Appl. Mater. Today* 2020, 19, No. 100617.
- (157). Cao Y; Hjort M; Chen H; Birey F; Leal-Ortiz SA; Han CM; Santiago JG; Pa ca, S. P.; Wu, J. C.; Melosh, N. A. Nondestructive Nanostraw Intracellular Sampling for Longitudinal Cell Monitoring. *Proc. Natl. Acad. Sci. U. S. A.* 2017, 114, E1866–E1874. [PubMed: 28223521]

- (158). He G; Yang C; Hang T; Liu D; Chen H-J; Zhang A; Lin D; Wu J; Yang B; Xie X Hollow Nanoneedle-Electroporation System To Extract Intracellular Protein Repetitively and Non-destructively. *ACS Sens.* 2018, 3, 1675–1682. [PubMed: 30148355]
- (159). Wen R; Zhang A; Liu D; Feng J; Yang J; Xia D; Wang J; Li C; Zhang T; Hu N; et al. Intracellular Delivery and Sensing System Based on Electroplated Conductive Nanostraw Arrays. *ACS Appl. Mater. Interfaces* 2019, 11, 43936–43948. [PubMed: 31696695]
- (160). Pop MA; Almquist BD Controlled Delivery of MicroRNAs into Primary Cells Using Nanostraw Technology. *Adv. NanoBiomed Res.* 2021, 1, 2000061. [PubMed: 34164629]
- (161). Kang W; Yavari F; Minary-Jolandan M; Giraldo-Vela JP; Safi A; McNaughton RL; Parpoil V; Espinosa HD Nanofountain Probe Electroporation (NFP-E) of Single Cells. *Nano Lett.* 2013, 13, 2448–2457. [PubMed: 23650871]
- (162). Kang W; McNaughton RL; Yavari F; Minary-Jolandan M; Safi A; Espinosa HD Microfluidic Parallel Patterning and Cellular Delivery of Molecules with a Nanofountain Probe. *J. Lab. Autom.* 2014, 19, 100–109. [PubMed: 23897012]
- (163). Giraldo-Vela JP; Kang W; McNaughton RL; Zhang X; Wile BM; Tsourkas A; Bao G; Espinosa HD Single-Cell Detection of mRNA Expression Using Nanofountain-Probe Electroporated Molecular Beacons. *Small* 2015, 11, 2386–2391. [PubMed: 25641752]
- (164). Yang R; Lemaître V; Huang C; Haddadi A; McNaughton R; Espinosa HD Monoclonal Cell Line Generation and CRISPR/Cas9 Manipulation via Single-Cell Electroporation. *Small* 2018, 14, 1702495.
- (165). Patino CA; Mukherjee P; Lemaitre V; Pathak N; Espinosa HD Deep Learning and Computer Vision Strategies for Automated Gene Editing with a Single-Cell Electroporation Platform. *SLAS Technol. Transl. Life Sci. Innov.* 2021, 26, 26–36.
- (166). Caprettini V; Cerea A; Melle G; Lovato L; Capozza R; Huang J-A; Tantussi F; Dipalo M; Angelis FD Soft Electroporation for Delivering Molecules into Tightly Adherent Mammalian Cells through 3D Hollow Nanoelectrodes. *Sci. Rep.* 2017, 7, 1–8. [PubMed: 28127051]
- (167). Cerea A; Caprettini V; Bruno G; Lovato L; Melle G; Tantussi F; Capozza R; Moia F; Dipalo M; Angelis FD Selective Intracellular Delivery and Intracellular Recordings Combined in MEA Biosensors. *Lab. Chip* 2018, 18, 3492–3500. [PubMed: 30306172]
- (168). Caprettini V; Huang J-A; Moia F; Jacassi A; Gonano CA; Maccaferri N; Capozza R; Dipalo M; Angelis FD Enhanced Raman Investigation of Cell Membrane and Intracellular Compounds by 3D Plasmonic Nanoelectrode Arrays. *Adv. Sci.* 2018, 5, 1800560.
- (169). Huang J-A; Caprettini V; Zhao Y; Melle G; Maccaferri N; Deleye L; Zambrana-Puyalto X; Ardini M; Tantussi F; Dipalo M; et al. On-Demand Intracellular Delivery of Single Particles in Single Cells by 3D Hollow Nanoelectrodes. *Nano Lett.* 2019, 19, 722–731. [PubMed: 30673248]
- (170). Riaz K; Leung S-F; Fan Z; Lee Y-K Electric Field Enhanced 3D Scalable Low-Voltage Nano-Spike Electroporation System. *Sens. Actuators Phys.* 2017, 255, 10–20.
- (171). Liu Z; Nie J; Miao B; Li J; Cui Y; Wang S; Zhang X; Zhao G; Deng Y; Wu Y; et al. Self-Powered Intracellular Drug Delivery by a Biomechanical Energy-Driven Triboelectric Nanogenerator. *Adv. Mater.* 2019, 31, 1807795.
- (172). Madiyar FR; Haller SL; Farooq O; Rothenburg S; Culbertson C; Li J AC Dielectrophoretic Manipulation and Electroporation of Vaccinia Virus Using Carbon Nanoelectrode Arrays. *ELECTROPHORESIS* 2017, 38, 1515–1525. [PubMed: 28211116]
- (173). Liu X; Chang A-Y; Ma Y; Hua L; Yang Z; Wang S Robust Three-Dimensional Nanotube-in-Micropillar Array Electrodes to Facilitate Size Independent Electroporation in Blood Cell Therapy. *Lab. Chip* 2021, 21, 4196–4207. [PubMed: 34546271]
- (174). Zu Y; Huang S; Lu Y; Liu X; Wang S Size Specific Transfection to Mammalian Cells by Micropillar Array Electroporation. *Sci. Rep.* 2016, 6, 1–10. [PubMed: 28442746]
- (175). Zu Y; Liu X; Chang A-Y; Wang S Flow Micropillar Array Electroporation to Enhance Size Specific Transfection to a Large Population of Cells. *Bioelectrochemistry* 2020, 132, No. 107417. [PubMed: 31830670]
- (176). Wu Y; Fu A; Yossifon G Active Particles as Mobile Microelectrodes for Selective Bacteria Electroporation and Transport. *Sci. Adv.* 2020, 6, eaay4412. [PubMed: 32064350]

- (177). Wu Y; Fu A; Yossifon G Micromotor-Based Localized Electroporation and Gene Transfection of Mammalian Cells. *Proc. Natl. Acad. Sci. U. S. A.* 2021, 118, No. e2106353118. [PubMed: 34531322]
- (178). Yun H; Hur SC Sequential Multi-Molecule Delivery Using Vortex-Assisted Electroporation. *Lab. Chip* 2013, 13, 2764. [PubMed: 23727978]
- (179). Vickers DAL; Ouyang M; Choi CH; Hur SC Direct Drug Cocktail Analyses Using Microscale Vortex-Assisted Electroporation. *Anal. Chem.* 2014, 86, 10099–10105. [PubMed: 25291206]
- (180). Ouyang M; Hill W; Lee JH; Hur SC Microscale Symmetrical Electroporator Array as a Versatile Molecular Delivery System. *Sci. Rep.* 2017, 7, 1–11. [PubMed: 28127051]
- (181). Sung HW; Choi S-E; Chu CH; Ouyang M; Kalyan S; Scott N; Hur SC Sensitizing Drug-Resistant Cancer Cells from Blood Using Microfluidic Electroporator. *PLoS One* 2022, 17, No. e0264907. [PubMed: 35259174]
- (182). Skelley AM; Kirak O; Suh H; Jaenisch R; Voldman J Microfluidic Control of Cell Pairing and Fusion. *Nat. Methods* 2009, 6, 147–152. [PubMed: 19122668]
- (183). Munce NR; Li J; Herman PR; Lilge L Microfabricated System for Parallel Single-Cell Capillary Electrophoresis. *Anal. Chem.* 2004, 76, 4983–4989. [PubMed: 15373432]
- (184). Henslee BE; Morss A; Hu X; Lafyatis GP; James Lee L Cell-Cell Proximity Effects in Multi-Cell Electroporation. *Biomicrofluidics* 2014, 8, 052002. [PubMed: 25332726]
- (185). Ashkin A Optical Trapping and Manipulation of Neutral Particles Using Lasers. *Proc. Natl. Acad. Sci. U. S. A.* 1997, 94, 4853–4860. [PubMed: 9144154]
- (186). Lee S-W; Tai Y-C A Micro Cell Lysis Device. *Sens. Actuators Phys.* 1999, 73, 74–79.
- (187). Park S; Bassat DB; Yossifon G Individually Addressable Multi-Chamber Electroporation Platform with Dielectrophoresis and Alternating-Current-Electro-Osmosis Assisted Cell Positioning. *Biomicrofluidics* 2014, 8, 024117. [PubMed: 24803966]
- (188). Guo X; Zhu R Controllable In-Situ Cell Electroporation with Cell Positioning and Impedance Monitoring Using Micro Electrode Array. *Sci. Rep.* 2016, 6, 1–8. [PubMed: 28442746]
- (189). Punjiya M; Nejad HR; Mathews J; Levin M; Sonkusale S A Flow through Device for Simultaneous Dielectrophoretic Cell Trapping and AC Electroporation. *Sci. Rep.* 2019, 9, 11988. [PubMed: 31427614]
- (190). Wang C-H; Lee Y-H; Kuo H-T; Liang W-F; Li W-J; Lee G-B Dielectrophoretically-Assisted Electroporation Using Light-Activated Virtual Microelectrodes for Multiple DNA Transfection. *Lab Chip* 2014, 14, 592–601. [PubMed: 24322338]
- (191). Huang S-H; Hung L-Y; Lee G-B Continuous Nucleus Extraction by Optically-Induced Cell Lysis on a Batch-Type Microfluidic Platform. *Lab. Chip* 2016, 16, 1447–1456. [PubMed: 26987542]
- (192). Liu L; Zhao L; Yang J; Wan X; Hu N; Yeh L-H; Joo SW; Qian S Low-Voltage Pulsed Electric Field Sterilization on a Microfluidic Chip. *Electroanalysis* 2013, 25, 1301–1309.
- (193). Jayasooriya V; Ringwelski B; Dorsam G; Nawarathna D MRNA-Based CAR T-Cells Manufactured by Miniaturized Two-Step Electroporation Produce Selective Cytotoxicity toward Target Cancer Cells. *Lab. Chip* 2021, 21, 3748. [PubMed: 34585697]
- (194). Çetin B; Li D Dielectrophoresis in Microfluidics Technology. *ELECTROPHORESIS* 2011, 32, 2410–2427. [PubMed: 21922491]
- (195). Zhang H; Chang H; Neuzil P DEP-on-a-Chip: Dielectrophoresis Applied to Microfluidic Platforms. *Micromachines* 2019, 10, 423. [PubMed: 31238556]
- (196). Sedgwick H; Caron F; Monaghan PB; Kolch W; Cooper JM Lab-on-a-Chip Technologies for Proteomic Analysis from Isolated Cells. *J. R. Soc. Interface* 2008, 5, S123–S130. [PubMed: 18534931]
- (197). Kim SH; Yamamoto T; Fourmy D; Fujii T An Electroactive Microwell Array for Trapping and Lysing Single-Bacterial Cells. *Biomicrofluidics* 2011, 5, No. 024114. [PubMed: 21772937]
- (198). Kim SH; Yamamoto T; Fourmy D; Fujii T Electroactive Microwell Arrays for Highly Efficient Single-Cell Trapping and Analysis. *Small* 2011, 7, 3239–3247. [PubMed: 21932278]

- (199). Kim SH; He X; Kaneda S; Kawada J; Fourmy D; Noji H; Fujii T Quantifying Genetically Inserted Fluorescent Protein in Single IPS Cells to Monitor Nanog Expression Using Electroactive Microchamber Arrays. *Lab. Chip* 2014, 14, 730–736. [PubMed: 24322270]
- (200). Zhang Z; Zheng T; Zhu R Single-Cell Individualized Electroporation with Real-Time Impedance Monitoring Using a Microelectrode Array Chip. *Microsyst. Nanoeng.* 2020, 6, 1–10. [PubMed: 34567616]
- (201). Jayasooriya V; Ringwelski B; Dorsam G; Nawarathna D mRNA-Based CAR T-Cells Manufactured by Miniaturized Two-Step Electroporation Produce Selective Cytotoxicity toward Target Cancer Cells. *Lab. Chip* 2021, 21, 3748–3761. [PubMed: 34585697]
- (202). Chung Y-C; Chen Y-S; Lin S-H Enhancement for Gene Transfection of Low-Descent-Velocity Bacteria Using Magnetic Attraction in Electroporation Chip. *Sens. Actuators B Chem.* 2015, 213, 261–267.
- (203). Kim JA; Cho K; Shin YS; Jung N; Chung C; Chang JK A Multi-Channel Electroporation Microchip for Gene Transfection in Mammalian Cells. *Biosens. Bioelectron.* 2007, 22, 3273–3277. [PubMed: 17395450]
- (204). Garcia PA; Ge Z; Moran JL; Buie CR Microfluidic Screening of Electric Fields for Electroporation. *Sci. Rep.* 2016, 6, 1–11. [PubMed: 28442746]
- (205). Bonakdar M; Wasson EM; Lee YW; Davalos RV Electroporation of Brain Endothelial Cells on Chip toward Permeabilizing the Blood-Brain Barrier. *Biophys. J.* 2016, 110, 503–513. [PubMed: 26789772]
- (206). Wang T; Chen H; Yu C; Xie X Rapid Determination of the Electroporation Threshold for Bacteria Inactivation Using a Lab-on-a-Chip Platform. *Environ. Int.* 2019, 132, No. 105040. [PubMed: 31387020]
- (207). Bian S; Zhou Y; Hu Y; Cheng J; Chen X; Xu Y; Liu P High-Throughput in Situ Cell Electroporation Microsystem for Parallel Delivery of Single Guide RNAs into Mammalian Cells. *Sci. Rep.* 2017, 7, 42512. [PubMed: 28211892]
- (208). Zhang Y; Yan Z; Xia X; Lin Y A Novel Electroporation System for Living Cell Staining and Membrane Dynamics Interrogation. *Micromachines* 2020, 11, 767. [PubMed: 32796554]
- (209). Huang D; Zhao D; Li J; Wu Y; Zhou W; Wang W; Liang Z; Li Z High Cell Viability Microfluidic Electroporation in a Curved Channel. *Sens. Actuators B Chem.* 2017, 250, 703–711.
- (210). Wang H-Y; Lu C Electroporation of Mammalian Cells in a Microfluidic Channel with Geometric Variation. *Anal. Chem.* 2006, 78, 5158–5164. [PubMed: 16841942]
- (211). Wang H-Y; Lu C Microfluidic Electroporation for Delivery of Small Molecules and Genes into Cells Using a Common DC Power Supply. *Biotechnol. Bioeng.* 2008, 100, 579–586. [PubMed: 18183631]
- (212). Zhan Y; Cao Z; Bao N; Li J; Wang J; Geng T; Lin H; Lu C Low-Frequency Ac Electroporation Shows Strong Frequency Dependence and Yields Comparable Transfection Results to Dc Electroporation. *J. Controlled Release* 2012, 160, 570–576.
- (213). Wang H-Y; Bhunia AK; Lu C A Microfluidic Flow-through Device for High Throughput Electrical Lysis of Bacterial Cells Based on Continuous Dc Voltage. *Biosens. Bioelectron.* 2006, 22, 582–588. [PubMed: 16530400]
- (214). Wang H-Y; Lu C Microfluidic Chemical Cytometry Based on Modulation of Local Field Strength. *Chem. Commun.* 2006, 3528–3530.
- (215). Lee DW; Cho Y-H A Continuous Electrical Cell Lysis Device Using a Low Dc Voltage for a Cell Transport and Rupture. *Sens. Actuators B Chem.* 2007, 124, 84–89.
- (216). Fox MB; Esveld DC; Mastwijk H; Boom RM Inactivation of *L. Plantarum* in a PEF Microreactor: The Effect of Pulse Width and Temperature on the Inactivation. *Innov. Food Sci. Emerg. Technol.* 2008, 9, 101–108.
- (217). Uchida S; Houjo M; Tochikubo F Efficient Sterilization of Bacteria by Pulse Electric Field in Micro-Gap. *J. Electrostat.* 2008, 66, 427–431.
- (218). Bao N; Le TT; Cheng J-X; Lu C Microfluidic Electroporation of Tumor and Blood Cells: Observation of Nucleus Expansion and Implications on Selective Analysis and Purging of Circulating Tumor Cells. *Integr. Biol.* 2010, 2, 113–120.

- (219). Zhan Y; Martin VA; Geahlen RL; Lu C One-Step Extraction of Subcellular Proteins from Eukaryotic Cells. *Lab. Chip* 2010, 10, 2046–2048. [PubMed: 20548993]
- (220). Wang J; Bao N; Paris LL; Wang H-Y; Geahlen RL; Lu C Detection of Kinase Translocation Using Microfluidic Electroporative Flow Cytometry. *Anal. Chem.* 2008, 80, 1087–1093. [PubMed: 18154306]
- (221). Wang J; Fei B; Zhan Y; Geahlen RL; Lu C Kinetics of NF-KB Nucleocytoplasmic Transport Probed by Single-Cell Screening without Imaging. *Lab. Chip* 2010, 10, 2911–2916. [PubMed: 20835431]
- (222). Wang H-Y; Lu C High-Throughput and Real-Time Study of Single Cell Electroporation Using Microfluidics: Effects of Medium Osmolarity. *Biotechnol. Bioeng.* 2006, 95, 1116–1125. [PubMed: 16817188]
- (223). Ye Y; Luan X; Zhang L; Zhao W; Cheng J; Li M; Zhao Y; Huang C Single-Cell Electroporation with Real-Time Impedance Assessment Using a Constriction Microchannel. *Micromachines* 2020, 11, 856. [PubMed: 32948046]
- (224). Geng T; Zhan Y; Wang H-Y; Witting SR; Cornetta KG; Lu C Flow-through Electroporation Based on Constant Voltage for Large-Volume Transfection of Cells. *J. Controlled Release* 2010, 144, 91–100.
- (225). Geng T; Zhan Y; Wang J; Lu C Transfection of Cells Using Flow-through Electroporation Based on Constant Voltage. *Nat. Protoc.* 2011, 6, 1192–1208. [PubMed: 21799488]
- (226). Bhattacharjee N; Horowitz LF; Folch A Continuous-Flow Multi-Pulse Electroporation at Low DC Voltages by Microfluidic Flipping of the Voltage Space Topology. *Appl. Phys. Lett.* 2016, 109, 163702. [PubMed: 27821874]
- (227). Won E-J; Thai DA; Duong DD; Lee NY; Song Y-J Microfluidic Electrical Cell Lysis for High-Throughput and Continuous Production of Cell-Free Varicella-Zoster Virus. *J. Biotechnol.* 2021, 335, 19–26. [PubMed: 34090951]
- (228). Pudasaini S; Perera ATK; Das D; Ng SH; Yang C Continuous Flow Microfluidic Cell Inactivation with the Use of Insulating Micropillars for Multiple Electroporation Zones. *ELECTROPHORESIS* 2019, 40, 2522–2529.
- (229). Liu P; Zhou J; Wang T; Yu C; Hong Y; Xie X Efficient Microalgae Inactivation and Growth Control by Locally Enhanced Electric Field Treatment (LEEFT). *Environ. Sci. Nano* 2020, 7, 2021–2031.
- (230). Pudasaini S; Perera ATK; Ahmed SSU; Chong YB; Ng SH; Yang C An Electroporation Device with Microbead-Enhanced Electric Field for Bacterial Inactivation. *Inventions* 2020, 5, 2.
- (231). Garcia PA; Ge Z; Kelley LE; Holcomb SJ; Buie CR High Efficiency Hydrodynamic Bacterial Electrotransformation. *Lab. Chip* 2017, 17, 490–500. [PubMed: 28067371]
- (232). Goma F; Garcia PA; Delaney J; Girguis PR; Buie CR; Edgcomb VP Toward Establishing Model Organisms for Marine Protists: Successful Transfection Protocols for Parabodo Caudatus (Kinetoplastida: Excavata). *Environ. Microbiol.* 2017, 19, 3487–3499. [PubMed: 28631386]
- (233). Staben ME; Davis RH Particle Transport in Poiseuille Flow in Narrow Channels. *Int. J. Multiph. Flow* 2005, 31, 529–547.
- (234). Shahini M; Yeow JTW Carbon Nanotubes for Voltage Reduction and Throughput Enhancement of Electrical Cell Lysis on a Lab-on-a-Chip. *Nanotechnology* 2011, 22, No. 325705. [PubMed: 21775777]
- (235). Shahini M; Yeow JTW Cell Electroporation by CNT-Featured Microfluidic Chip. *Lab. Chip* 2013, 13, 2585–2590. [PubMed: 23511307]
- (236). Poudineh M; Mohamadi RM; Sage A; Mahmoudian L; Sargent EH; Kelley SO Three-Dimensional, Sharp-Tipped Electrodes Concentrate Applied Fields to Enable Direct Electrical Release of Intact Biomarkers from Cells. *Lab. Chip* 2014, 14, 1785–1790. [PubMed: 24695906]
- (237). Liu Z; Liang X; Liu H; Wang Z; Jiang T; Cheng Y; Wu M; Xiang D; Li Z; Wang ZL; et al. High-Throughput and Self-Powered Electroporation System for Drug Delivery Assisted by Microfoam Electrode. *ACS Nano* 2020, 14, 15458–15467. [PubMed: 32991146]
- (238). Huo Z-Y; Luo Y; Xie X; Feng C; Jiang K; Wang J; Hu H-Y Carbon-Nanotube Sponges Enabling Highly Efficient and Reliable Cell Inactivation by Low-Voltage Electroporation. *Environ. Sci. Nano* 2017, 4, 2010–2017.

- (239). Huo Z-Y; Zhou J-F; Wu Y; Wu Y-H; Liu H; Liu N; Hu H-Y; Xie X A Cu3P Nanowire Enabling High-Efficiency, Reliable, and Energy-Efficient Low-Voltage Electroporation-Inactivation of Pathogens in Water. *J. Mater. Chem. A* 2018, 6, 18813–18820.
- (240). Huo Z-Y; Xie X; Yu T; Lu Y; Feng C; Hu H-Y Nanowire-Modified Three-Dimensional Electrode Enabling Low-Voltage Electroporation for Water Disinfection. *Environ. Sci. Technol.* 2016, 50, 7641–7649. [PubMed: 27341009]
- (241). Huo Z-Y; Li G-Q; Yu T; Lu Y; Sun H; Wu Y-H; Yu C; Xie X; Hu H-Y Impact of Water Quality Parameters on Bacteria Inactivation by Low-Voltage Electroporation: Mechanism and Control. *Environ. Sci. Water Res. Technol.* 2018, 4, 872–881.
- (242). Huo Z-Y; Li G-Q; Yu T; Feng C; Lu Y; Wu Y-H; Yu C; Xie X; Hu H-Y Cell Transport Prompts the Performance of Low-Voltage Electroporation for Cell Inactivation. *Sci. Rep.* 2018, 8, 15832. [PubMed: 30361540]
- (243). Yue L; Chen S; Wang S; Wang C; Hao X; Cheng YF Water Disinfection Using Ag Nanoparticle–CuO Nanowire Co-Modified 3D Copper Foam Nanocomposites in High Flow under Low Voltages. *Environ. Sci. Nano* 2019, 6, 2801–2809.
- (244). Lu K-Y; Wo AM; Lo Y-J; Chen K-C; Lin C-M; Yang C-R Three Dimensional Electrode Array for Cell Lysis via Electroporation. *Biosens. Bioelectron.* 2006, 22, 568–574. [PubMed: 16997544]
- (245). Mernier G; Martinez-Duarte R; Lehal R; Radtke F; Renaud P Very High Throughput Electrical Cell Lysis and Extraction of Intracellular Compounds Using 3D Carbon Electrodes in Lab-on-a-Chip Devices. *Micromachines* 2012, 3, 574–581.
- (246). Experton J; Wilson AG; Martin CR Low-Voltage Flow-Through Electroporation in Gold-Microtube Membranes. *Anal. Chem.* 2016, 88, 12445–12452. [PubMed: 28193019]
- (247). Chen Z; Akenhead MA; Sun X; Sapper H; Shin HY; Hinds BJ Flow-Through Electroporation of HL-60 White Blood Cell Suspensions Using Nanoporous Membrane Electrodes. *Adv. Healthc. Mater.* 2016, 5, 2105–2112.
- (248). Lo Y-J; Lei U A Continuous Flow-through Microfluidic Device for Electrical Lysis of Cells. *Micromachines* 2019, 10, 247. [PubMed: 31013954]
- (249). Lin Y-C; Jen C-M; Huang M-Y; Wu C-Y; Lin X-Z Electroporation Microchips for Continuous Gene Transfection. *Sens. Actuators B Chem.* 2001, 79, 137–143.
- (250). del Rosal B; Sun C; Loufakis DN; Lu C; Jaque D Thermal Loading in Flow-through Electroporation Microfluidic Devices. *Lab. Chip* 2013, 13, 3119–3127. [PubMed: 23760021]
- (251). Kim SK; Kim JH; Kim KP; Chung TD Continuous Low-Voltage Dc Electroporation on a Microfluidic Chip with Polyelectrolytic Salt Bridges. *Anal. Chem.* 2007, 79, 7761–7766. [PubMed: 17874852]
- (252). Wei Z; Zhao D; Li X; Wu M; Wang W; Huang H; Wang X; Du Q; Liang Z; Li Z A Laminar Flow Electroporation System for Efficient DNA and siRNA Delivery. *Anal. Chem.* 2011, 83, 5881–5887. [PubMed: 21678996]
- (253). Lissandrello CA; Santos JA; Hsi P; Welch M; Mott VL; Kim ES; Chesin J; Haroutunian NJ; Stoddard AG; Czarnecki A; et al. High-Throughput Continuous-Flow Microfluidic Electroporation of mRNA into Primary Human T Cells for Applications in Cellular Therapy Manufacturing. *Sci. Rep.* 2020, 10, 18045. [PubMed: 33093518]
- (254). Kang S; Kim B; Yim S-J; Kim J-O; Kim D-P; Kim Y-C On-Chip Electroporation System of Polyimide Film with Sheath Flow Design for Efficient Delivery of Molecules into Microalgae. *J. Ind. Eng. Chem.* 2020, 88, 159–166.
- (255). Luo Y; Yobas L Flow-through Electroporation of Mammalian Cells in Decoupled Flow Streams Using Microcapillaries. *Biomicrofluidics* 2014, 8, 052101. [PubMed: 24926393]
- (256). Sukhorukov VL; Reuss R; Zimmermann D; Held C; Müller KJ; Kiesel M; Geßner P; Steinbach A; Schenk WA; Bamberg E; et al. Surviving High-Intensity Field Pulses: Strategies for Improving Robustness and Performance of Electrotransfection and Electrofusion. *J. Membr. Biol.* 2005, 206, 187–201. [PubMed: 16456714]
- (257). Rashid M; Coombs KM Serum-Reduced Media Impacts on Cell Viability and Protein Expression in Human Lung Epithelial Cells. *J. Cell. Physiol.* 2019, 234, 7718–7724. [PubMed: 30515823]

- (258). Hsi P; Christianson RJ; Dubay RA; Lissandrello CA; Fiering J; Balestrini JL; Tandon V Acoustophoretic Rapid Media Exchange and Continuous-Flow Electrotransfection of Primary Human T Cells for Applications in Automated Cellular Therapy Manufacturing. *Lab. Chip* 2019, 19, 2978–2992. [PubMed: 31410419]
- (259). Lee G-B; Chang C-J; Wang C-H; Lu M-Y; Luo Y-Y Continuous Medium Exchange and Optically Induced Electroporation of Cells in an Integrated Microfluidic System. *Microsyst. Nanoeng.* 2015, 1, 1–9.
- (260). Wei Z; Li X; Zhao D; Yan H; Hu Z; Liang Z; Li Z Flow-Through Cell Electroporation Microchip Integrating Dielectrophoretic Viable Cell Sorting. *Anal. Chem.* 2014, 86, 10215–10222. [PubMed: 25252150]
- (261). Wassermann KJ; Barth S; Keplinger F; Noehammer C; Peham JR High-k Dielectric Passivation: Novel Considerations Enabling Cell Specific Lysis Induced by Electric Fields. *ACS Appl. Mater. Interfaces* 2016, 8, 21228–21235. [PubMed: 27466697]
- (262). Wimberger T; Peham JR; Ehmoser E-K; Wassermann KJ Controllable Cell Manipulation in a Microfluidic Pipette-Tip Design Using Capacitive Coupling of Electric Fields. *Lab. Chip* 2019, 19, 3997–4006. [PubMed: 31667478]
- (263). Pandian K; Ajanth Praveen M; Hoque SZ; Sudeepthi A; Sen AK Continuous Electrical Lysis of Cancer Cells in a Microfluidic Device with Passivated Interdigitated Electrodes. *Biomicrofluidics* 2020, 14, No. 064101. [PubMed: 33163136]
- (264). Talebpour A; Maaskant R; Khine AA; Alavie T Use of Surface Enhanced Blocking (SEB) Electrodes for Microbial Cell Lysis in Flow-Through Devices. *PLoS One* 2014, 9, No. e102707. [PubMed: 25033080]
- (265). Zhou Y; Lu Y; Cheng J; Xu Y Highly Uniform In-Situ Cell Electrotransfection of Adherent Cultures Using Grouped Interdigitated Electrodes. *Bioelectrochemistry* 2020, 132, No. 107435. [PubMed: 31855831]
- (266). Wang J; Zhan Y; Ugaz VM; Lu C Vortex-Assisted DNA Delivery. *Lab. Chip* 2010, 10, 2057–2061. [PubMed: 20563345]
- (267). Zheng M; Shan JW; Lin H; Shreiber DI; Zahn JD Hydrodynamically Controlled Cell Rotation in an Electroporation Microchip to Circumferentially Deliver Molecules into Single Cells. *Microfluid. Nanofluidics* 2016, 20, 16.
- (268). Longsine-Parker W; Wang H; Koo C; Kim J; Kim B; Jayaraman A; Han A Microfluidic Electro-Sonoporation: A Multi-Modal Cell Poration Methodology through Simultaneous Application of Electric Field and Ultrasonic Wave. *Lab. Chip* 2013, 13, 2144–2152. [PubMed: 23615834]
- (269). Zhu Q; Hamilton M; Vasquez B; He M 3D-Printing Enabled Micro-Assembly of a Microfluidic Electroporation System for 3D Tissue Engineering. *Lab. Chip* 2019, 19, 2362–2372. [PubMed: 31214669]
- (270). Shang L; Cheng Y; Zhao Y Emerging Droplet Micro-fluidics. *Chem. Rev.* 2017, 117, 7964–8040. [PubMed: 28537383]
- (271). Teh S-Y; Lin R; Hung L-H; Lee AP Droplet Microfluidics. *Lab. Chip* 2008, 8, 198. [PubMed: 18231657]
- (272). Luo C; Yang X; Fu Q; Sun M; Ouyang Q; Chen Y; Ji H Picoliter-Volume Aqueous Droplets in Oil: Electrochemical Detection and Yeast Cell Electroporation. *ELECTROPHORESIS* 2006, 27, 1977–1983. [PubMed: 16596709]
- (273). Qu B; Eu Y-J; Jeong W-J; Kim D-P Droplet Electroporation in Microfluidics for Efficient Cell Transformation with or without Cell Wall Removal. *Lab. Chip* 2012, 12, 4483–4488. [PubMed: 22976563]
- (274). Zhan Y; Wang J; Bao N; Lu C Electroporation of Cells in Microfluidic Droplets. *Anal. Chem.* 2009, 81, 2027–2031. [PubMed: 19199389]
- (275). Bringer MR; Gerdtz CJ; Song H; Tice JD; Ismagilov RF Microfluidic Systems for Chemical Kinetics That Rely on Chaotic Mixing in Droplets. *Philos. Transact. A Math. Phys. Eng. Sci.* 2004, 362, 1087–1104.
- (276). Choi K; Ng AHC; Fobel R; Wheeler AR Digital Microfluidics. *Annu. Rev. Anal. Chem.* 2012, 5, 413–440.

- (277). Shih SCC; Goyal G; Kim PW; Koutsoubelis N; Keasling JD; Adams PD; Hillson NJ; Singh AK A Versatile Microfluidic Device for Automating Synthetic Biology. *ACS Synth. Biol.* 2015, 4, 1151–1164. [PubMed: 26075958]
- (278). Madison AC; Royal MW; Vigneault F; Chen L; Griffin PB; Horowitz M; Church GM; Fair RB Scalable Device for Automated Microbial Electroporation in a Digital Microfluidic Platform. *ACS Synth. Biol.* 2017, 6, 1701–1709. [PubMed: 28569062]
- (279). Moore JA; Nemat-Gorgani M; Madison AC; Sandahl MA; Punnamaraju S; Eckhardt AE; Pollack MG; Vigneault F; Church GM; Fair RB Automated Electrotransformation of *Escherichia Coli* on a Digital Microfluidic Platform Using Bioactivated Magnetic Beads. *Biomicrofluidics* 2017, 11, 014110. [PubMed: 28191268]
- (280). Batista Napotnik T; Miklavic D In Vitro Electroporation Detection Methods – An Overview. *Bioelectrochemistry* 2018, 120, 166–182. [PubMed: 29289825]
- (281). Sun T; Morgan H Single-Cell Microfluidic Impedance Cytometry: A Review. *Microfluid. Nanofluidics* 2010, 8, 423–443.
- (282). Honrado C; Bisegna P; Swami NS; Caselli F Single-Cell Microfluidic Impedance Cytometry: From Raw Signals to Cell Phenotypes Using Data Analytics. *Lab. Chip* 2021, 21, 22–54. [PubMed: 33331376]
- (283). Sukas S; Schreuder E; de Wagenaar B; Swennenhuis J; van den Berg A; Terstappen L; Le Gac S A Novel Side Electrode Configuration Integrated in Fused Silica Microsystems for Synchronous Optical and Electrical Spectroscopy. *Lab. Chip* 2014, 14, 1821–1825. [PubMed: 24756127]
- (284). Ghadami M; Mahjoob MJ; Shagoshtasbi H; Lee Y-K Model-Based Feedback Control of a Microfluidic Electroporation System. *J. Micromechanics Microengineering* 2013, 23, No. 125032.
- (285). Mernier G; Hasenkamp W; Piacentini N; Renaud P Multiple-Frequency Impedance Measurements in Continuous Flow for Automated Evaluation of Yeast Cell Lysis. *Sens. Actuators B Chem.* 2012, 170, 2–6.
- (286). Bürgel SC; Escobedo C; Haandbæk N; Hierlemann A On-Chip Electroporation and Impedance Spectroscopy of Single-Cells. *Sens. Actuators B Chem.* 2015, 210, 82–90.
- (287). Stolwijk JA; Wegener J Impedance Analysis of Adherent Cells after in Situ Electroporation-Mediated Delivery of Bioactive Proteins, DNA and Nanoparticles in ML-Volumes. *Sci. Rep.* 2020, 10, 21331. [PubMed: 33288771]
- (288). Bhattacharjee N; Urrios A; Kang S; Folch A The Upcoming 3D-Printing Revolution in Microfluidics. *Lab. Chip* 2016, 16, 1720–1742. [PubMed: 27101171]
- (289). Sochol RD; Sweet E; Glick CC; Wu S-Y; Yang C; Restaino M; Lin L 3D Printed Microfluidics and Microelectronics. *Microelectron. Eng.* 2018, 189, 52–68.
- (290). Kim JA; Cho K; Shin MS; Lee WG; Jung N; Chung C; Chang JK A Novel Electroporation Method Using a Capillary and Wire-Type Electrode. *Biosens. Bioelectron.* 2008, 23, 1353–1360. [PubMed: 18242073]
- (291). Pavesi A; Adriani G; Tay A; Warkiani ME; Yeap WH; Wong SC; Kamm RD Engineering a 3D Microfluidic Culture Platform for Tumor-Treating Field Application. *Sci. Rep.* 2016, 6, 26584. [PubMed: 27215466]
- (292). Chatzimichail S; Supramaniam P; Ces O; Salehi-Reyhani A Micropatterning of Planar Metal Electrodes by Vacuum Filling Microfluidic Channel Geometries. *Sci. Rep.* 2018, 8, 14380. [PubMed: 30258167]
- (293). Han C; He X; Wang J; Gao L; Yang G; Li D; Wang S; Chen X; Peng Z A Low-Cost Smartphone Controlled Portable System with Accurately Confined on-Chip 3D Electrodes for Flow-through Cell Electroporation. *Bioelectrochemistry* 2020, 134, No. 107486. [PubMed: 32179452]
- (294). Wang J; Stine MJ; Lu C Microfluidic Cell Electroporation Using a Mechanical Valve. *Anal. Chem.* 2007, 79, 9584–9587. [PubMed: 18004820]
- (295). Unger MA; Chou H-P; Thorsen T; Scherer A; Quake SR Monolithic Microfabricated Valves and Pumps by Multilayer Soft Lithography. *Science* 2000, 288, 113–116. [PubMed: 10753110]
- (296). Metzker ML Sequencing Technologies — the next Generation. *Nat. Rev. Genet.* 2010, 11, 31–46. [PubMed: 19997069]

- (297). Ozsolak F; Milos PM RNA Sequencing: Advances, Challenges and Opportunities. *Nat. Rev. Genet.* 2011, 12, 87–98. [PubMed: 21191423]
- (298). Fire A; Xu S; Montgomery MK; Kostas SA; Driver SE; Mello CC Potent and Specific Genetic Interference by Double-Stranded RNA in *Caenorhabditis elegans*. *Nature* 1998, 391 (6669), 806–811. [PubMed: 9486653]
- (299). Dominska M; Dykxhoorn DM Breaking down the Barriers: SiRNA Delivery and Endosome Escape. *J. Cell Sci.* 2010, 123, 1183–1189. [PubMed: 20356929]
- (300). Thomson DW; Bracken CP; Szubert JM; Goodall GJ On Measuring MiRNAs after Transient Transfection of Mimics or Antisense Inhibitors. *PLoS One* 2013, 8, No. e55214. [PubMed: 23358900]
- (301). Ma S; Schroeder B; Sun C; Loufakis DN; Cao Z; Sriranganathan N; Lu C Electroporation-Based Delivery of Cell-Penetrating Peptide Conjugates of Peptide Nucleic Acids for Antisense Inhibition of Intracellular Bacteria. *Integr Biol.* 2014, 6, 973–978.
- (302). Kim YH; Kwon SG; Bae SJ; Park SJ; Im DJ Optimization of the Droplet Electroporation Method for Wild Type *Chlamydomonas Reinhardtii* Transformation. *Bioelectrochemistry* 2019, 126, 29–37. [PubMed: 30472569]
- (303). Chang A-Y; Liu X; Tian H; Hua L; Yang Z; Wang S Microfluidic Electroporation Coupling Pulses of Nanoseconds and Milliseconds to Facilitate Rapid Uptake and Enhanced Expression of DNA in Cell Therapy. *Sci. Rep.* 2020, 10, 6061. [PubMed: 32269260]
- (304). Ding X; Stewart MP; Sharei A; Weaver JC; Langer RS; Jensen KF High-Throughput Nuclear Delivery and Rapid Expression of DNA via Mechanical and Electrical Cell-Membrane Disruption. *Nat. Biomed. Eng.* 2017, 1, 1–7.
- (305). Jinek M; Chylinski K; Fonfara I; Hauer M; Doudna JA; Charpentier E A Programmable Dual-RNA-Guided DNA Endonuclease in Adaptive Bacterial Immunity. *Science* 2012, 337, 816–821. [PubMed: 22745249]
- (306). Cong L; Ran FA; Cox D; Lin S; Barretto R; Habib N; Hsu PD; Wu X; Jiang W; Marraffini LA; et al. Multiplex Genome Engineering Using CRISPR/Cas Systems. *Science* 2013, 339, 819–823. [PubMed: 23287718]
- (307). Hsu PD; Lander ES; Zhang F Development and Applications of CRISPR-Cas9 for Genome Engineering. *Cell* 2014, 157, 1262–1278. [PubMed: 24906146]
- (308). Wang H; La Russa M; Qi LS CRISPR/Cas9 in Genome Editing and Beyond. *Annu. Rev. Biochem.* 2016, 85, 227–264. [PubMed: 27145843]
- (309). Hong M; Clubb JD; Chen YY Engineering CAR-T Cells for Next-Generation Cancer Therapy. *Cancer Cell* 2020, 38, 473–488. [PubMed: 32735779]
- (310). Yan Z; Hui TH; Fong HW; Shao X; Cho WC; Ngan KC; Yip TC; Lin Y An Electroporation Platform for Erlotinib Resistance Screening in Living Non-Small Cell Lung Cancer (NSCLC) Cells. *Biomed. Phys. Eng. Express* 2018, 4, No. 027001.
- (311). Tan S; Wu T; Zhang D; Zhang Z Cell or Cell Membrane-Based Drug Delivery Systems. *Theranostics* 2015, 5, 863–881. [PubMed: 26000058]
- (312). Zhao D; Huang D; Li Y; Wu M; Zhong W; Cheng Q; Wang X; Wu Y; Zhou X; Wei Z; et al. A Flow-Through Cell Electroporation Device for Rapidly and Efficiently Transfecting Massive Amounts of Cells in Vitro and Ex Vivo. *Sci. Rep.* 2016, 6, No. srep18469.
- (313). Rao L; Cai B; Bu L-L; Liao Q-Q; Guo S-S; Zhao X-Z; Dong W-F; Liu W Microfluidic Electroporation-Facilitated Synthesis of Erythrocyte Membrane-Coated Magnetic Nanoparticles for Enhanced Imaging-Guided Cancer Therapy. *ACS Nano* 2017, 11, 3496–3505. [PubMed: 28272874]
- (314). Lestrell E; Patolsky F; Voelcker NH; Elnathan R Engineered Nano-Bio Interfaces for Intracellular Delivery and Sampling: Applications, Agency and Artefacts. *Mater. Today* 2020, 33, 87–104.
- (315). Zhan Y; Sun C; Cao Z; Bao N; Xing J; Lu C Release of Intracellular Proteins by Electroporation with Preserved Cell Viability. *Anal. Chem.* 2012, 84, 8102–8105. [PubMed: 22974138]
- (316). Lee HJ; Kim J-H; Lim HK; Cho EC; Huh N; Ko C; Park JC; Choi J-W; Lee SS Electrochemical Cell Lysis Device for DNA Extraction. *Lab. Chip* 2010, 10, 626–633. [PubMed: 20162238]

- (317). Ameri SK; Singh PK; Sonkusale S Utilization of Graphene Electrode in Transparent Microwell Arrays for High Throughput Cell Trapping and Lysis. *Biosens. Bioelectron.* 2014, 61, 625–630. [PubMed: 24967752]
- (318). Lu H; Schmidt MA; Jensen KF A Microfluidic Electroporation Device for Cell Lysis. *Lab. Chip* 2005, 5, 23–29. [PubMed: 15616736]
- (319). Morshed BI; Shams M; Mussivand T Investigation of Low-Voltage Pulse Parameters on Electroporation and Electrical Lysis Using a Microfluidic Device With Interdigitated Electrodes. *IEEE Trans. Biomed. Eng.* 2014, 61, 871–882. [PubMed: 24557688]
- (320). Wei X; Li J; Wang L; Yang F Low-Voltage Electrical Cell Lysis Using a Microfluidic Device. *Biomed. Microdevices* 2019, 21, 22. [PubMed: 30790126]
- (321). Geng T; Bao N; Sriranganathanw N; Li L; Lu C Genomic DNA Extraction from Cells by Electroporation on an Integrated Microfluidic Platform. *Anal. Chem.* 2012, 84, 9632–9639. [PubMed: 23061629]
- (322). Kim M; Wu L; Kim B; Hung DT; Han J Continuous and High-Throughput Electromechanical Lysis of Bacterial Pathogens Using Ion Concentration Polarization. *Anal. Chem.* 2018, 90, 872–880. [PubMed: 29193960]
- (323). Silver B; Zhu H Varicella Zoster Virus Vaccines: Potential Complications and Possible Improvements. *Viol. Sin.* 2014, 29, 265–273. [PubMed: 25358998]
- (324). McClain MA; Culbertson CT; Jacobson SC; Allbritton NL; Sims CE; Ramsey JM Microfluidic Devices for the High-Throughput Chemical Analysis of Cells. *Anal. Chem.* 2003, 75, 5646–5655. [PubMed: 14588001]
- (325). Hargis AD; Alarie JP; Ramsey JM Characterization of Cell Lysis Events on a Microfluidic Device for High-Throughput Single Cell Analysis. *ELECTROPHORESIS* 2011, 32, 3172–3179. [PubMed: 22025127]
- (326). Gao J; Yin X-F; Fang Z-L Integration of Single Cell Injection, Cell Lysis, Separation and Detection of Intracellular Constituents on a Microfluidic Chip. *Lab. Chip* 2004, 4, 47–52. [PubMed: 15007440]
- (327). Mellors JS; Jorabchi K; Smith LM; Ramsey JM Integrated Microfluidic Device for Automated Single Cell Analysis Using Electrophoretic Separation and Electrospray Ionization Mass Spectrometry. *Anal. Chem.* 2010, 82, 967–973. [PubMed: 20058879]
- (328). Hügler M; Dame G; Behrmann O; Rietzel R; Karthe D; Hufert FT; Urban GA A Lab-on-a-Chip for Preconcentration of Bacteria and Nucleic Acid Extraction. *RSC Adv.* 2018, 8, 20124–20130. [PubMed: 35541671]
- (329). Vulto P; Dame G; Maier U; Makohliso S; Podszun S; Zahn P; Urban GA A Microfluidic Approach for High Efficiency Extraction of Low Molecular Weight RNA. *Lab. Chip* 2010, 10, 610–616. [PubMed: 20162236]
- (330). Shintaku H; Nishikii H; Marshall LA; Kotera H; Santiago JG On-Chip Separation and Analysis of RNA and DNA from Single Cells. *Anal. Chem.* 2014, 86, 1953–1957. [PubMed: 24499009]
- (331). Kuriyama K; Shintaku H; Santiago JG Isotachopheresis for Fractionation and Recovery of Cytoplasmic RNA and Nucleus from Single Cells. *ELECTROPHORESIS* 2015, 36, 1658–1662. [PubMed: 25820552]
- (332). Subramanian Parimalam S; Oguchi Y; Abdelmoez MN; Tsuchida A; Ozaki Y; Yokokawa R; Kotera H; Shintaku H Electrical Lysis and RNA Extraction from Single Cells Fixed by Dithiobis(Succinimidyl Propionate). *Anal. Chem.* 2018, 90, 12512–12518. [PubMed: 30350601]
- (333). Abdelmoez MN; Iida K; Oguchi Y; Nishikii H; Yokokawa R; Kotera H; Uemura S; Santiago JG; Shintaku H SINC-Seq: Correlation of Transient Gene Expressions between Nucleus and Cytoplasm Reflects Single-Cell Physiology. *Genome Biol.* 2018, 19, 66. [PubMed: 29871653]
- (334). Abdelmoez MN; Oguchi Y; Ozaki Y; Yokokawa R; Kotera H; Shintaku H Distinct Kinetics in Electrophoretic Extraction of Cytoplasmic RNA from Single Cells. *Anal. Chem.* 2020, 92, 1485–1492. [PubMed: 31805233]
- (335). Pinu FR; Villas-Boas SG; Aggio R Analysis of Intracellular Metabolites from Microorganisms: Quenching and Extraction Protocols. *Metabolites* 2017, 7, 53. [PubMed: 29065530]
- (336). Rockenbach A; Sudarsan S; Berens J; Kosubek M; Lazar J; Demling P; Hanke R; Mennicken P; Ebert BE; Blank LM; et al. Microfluidic Irreversible Electroporation—A Versatile Tool

- to Extract Intracellular Contents of Bacteria and Yeast. *Metabolites* 2019, 9, 211. [PubMed: 31574935]
- (337). Filla LA; Sanders KL; Filla RT; Edwards JL Automated Sample Preparation in a Microfluidic Culture Device for Cellular Metabolomics. *Analyst* 2016, 141, 3858–3865. [PubMed: 27118418]
- (338). Coulton JB; Edwards JL Capillary Flow-Based Sample Preparation System for Metabolomic Analysis of Mammalian Cells in Suspension. *Anal. Bioanal. Chem.* 2021, 413, 2493. [PubMed: 33665672]
- (339). Morris MC Fluorescent Biosensors of Intracellular Targets from Genetically Encoded Reporters to Modular Polypeptide Probes. *Cell Biochem. Biophys.* 2010, 56, 19–37. [PubMed: 19921468]
- (340). Pendin D; Greotti E; Lefkimmiatis K; Pozzan T Exploring Cells with Targeted Biosensors. *J. Gen. Physiol.* 2017, 149, 1–36. [PubMed: 28028123]
- (341). Sun C; Ouyang M; Cao Z; Ma S; Alqublan H; Sriranganathan N; Wang Y; Lu C Electroporation-Delivered Fluorescent Protein Biosensors for Probing Molecular Activities in Cells without Genetic Encoding. *Chem. Commun.* 2014, 50, 11536–11539.
- (342). Sun C; Cao Z; Wu M; Lu C Intracellular Tracking of Single Native Molecules with Electroporation-Delivered Quantum Dots. *Anal. Chem.* 2014, 86, 11403–11409. [PubMed: 25341054]
- (343). Tyagi S; Kramer FR Molecular Beacons: Probes That Fluoresce upon Hybridization. *Nat. Biotechnol.* 1996, 14, 303–308. [PubMed: 9630890]
- (344). Chang L; Howdysshell M; Liao W-C; Chiang C-L; Gallego-Perez D; Yang Z; Lu W; Byrd JC; Muthusamy N; Lee LJ; et al. Magnetic Tweezers-Based 3D Microchannel Electroporation for High-Throughput Gene Transfection in Living Cells. *Small* 2015, 11, 1818–1828. [PubMed: 25469659]
- (345). Lee WC; Rigante S; Pisano AP; Kuypers FA Large-Scale Arrays of Picolitre Chambers for Single-Cell Analysis of Large Cell Populations. *Lab. Chip* 2010, 10, 2952–2958. [PubMed: 20838671]
- (346). Punjiya M; Mocker A; Napier B; Zeeshan A; Gutsche M; Sonkusale S CMOS Microcavity Arrays for Single-Cell Electroporation and Lysis. *Biosens. Bioelectron.* 2020, 150, No. 111931. [PubMed: 31929080]
- (347). Gawad C; Koh W; Quake SR Single-Cell Genome Sequencing: Current State of the Science. *Nat. Rev. Genet.* 2016, 17, 175–188. [PubMed: 26806412]
- (348). Kim SH; Fujii T Efficient Analysis of a Small Number of Cancer Cells at the Single-Cell Level Using an Electroactive Double-Well Array. *Lab. Chip* 2016, 16, 2440–2449. [PubMed: 27189335]
- (349). Li M; Anand RK Integration of Marker-Free Selection of Single Cells at a Wireless Electrode Array with Parallel Fluidic Isolation and Electrical Lysis. *Chem. Sci.* 2019, 10, 1506–1513. [PubMed: 30809368]
- (350). de Lange N; Tran TM; Abate AR Electrical Lysis of Cells for Detergent-Free Droplet Assays. *Biomicrofluidics* 2016, 10, No. 024114. [PubMed: 27051471]
- (351). Chang WC; Sretavan DW Single Cell and Neural Process Experimentation Using Laterally Applied Electrical Fields between Pairs of Closely Apposed Microelectrodes with Vertical Sidewalls. *Biosens. Bioelectron.* 2009, 24, 3600–3607. [PubMed: 19535240]
- (352). Gencturk E; Ulgen KO; Mutlu S Thermoplastic Microfluidic Bioreactors with Integrated Electrodes to Study Tumor Treating Fields on Yeast Cells. *Biomicrofluidics* 2020, 14, No. 034104. [PubMed: 32477443]
- (353). Graybill PM; Jana A; Kapania RK; Nain AS; Davalos RV Single Cell Forces after Electroporation. *ACS Nano* 2021, 15, 2554–2568. [PubMed: 33236888]
- (354). Salimi E; Braasch K; Butler M; Thomson DJ; Bridges GE Dielectrophoresis Study of Temporal Change in Internal Conductivity of Single CHO Cells after Electroporation by Pulsed Electric Fields. *Biomicrofluidics* 2017, 11, 014111. [PubMed: 28289483]
- (355). Ravi M; Paramesh V; Kaviya SR; Anuradha E; Solomon FDP 3D Cell Culture Systems: Advantages and Applications. *J. Cell. Physiol.* 2015, 230, 16–26. [PubMed: 24912145]
- (356). Zhang B; Korolj A; Lai BFL; Radisic M Advances in Organ-on-a-Chip Engineering. *Nat. Rev. Mater.* 2018, 3, 257–278.

- (357). Bonakdar M; Graybill PM; Davalos RV A Microfluidic Model of the Blood–Brain Barrier to Study Permeabilization by Pulsed Electric Fields. *RSC Adv.* 2017, 7, 42811–42818. [PubMed: 29308191]
- (358). Huang K-S; Lin Y-C; Su K-C; Chen H-Y An Electroporation Microchip System for the Transfection of Zebrafish Embryos Using Quantum Dots and GFP Genes for Evaluation. *Biomed. Microdevices* 2007, 9, 761–768. [PubMed: 17541746]
- (359). Mazari E; Zhao X; Migeotte I; Collignon J; Gosse C; Perea-Gomez A A Microdevice to Locally Electroporate Embryos with High Efficiency and Reduced Cell Damage. *Development* 2014, 141, 2349–2359. [PubMed: 24821988]
- (360). André F; Mir LM DNA Electrotransfer: Its Principles and an Updated Review of Its Therapeutic Applications. *Gene Ther.* 2004, 11, S33–S42. [PubMed: 15454955]
- (361). Rosazza C; Habert Meglic S; Zumbusch A; Rols M-P; Miklavcic D Gene Electrotransfer: A Mechanistic Perspective. *Curr. Gene Ther.* 2016, 16, 98–129. [PubMed: 27029943]
- (362). Picart L; Dumay E; Cheftel JC Inactivation of *Listeria Innocua* in Dairy Fluids by Pulsed Electric Fields: Influence of Electric Parameters and Food Composition. *Innov. Food Sci. Emerg. Technol.* 2002, 3, 357–369.
- (363). Ulmer H. m.; Heinz V; Gänzle M. g.; Knorr D; Vogel R. f. Effects of Pulsed Electric Fields on Inactivation and Metabolic Activity of *Lactobacillus Plantarum* in Model Beer. *J. Appl. Microbiol.* 2002, 93, 326–335. [PubMed: 12147082]
- (364). Tang X; Wu QY; Du Y; Yang Y; Hu HY Anti-Estrogenic Activity Formation Potential Assessment and Precursor Analysis in Reclaimed Water during Chlorination. *Water Res.* 2014, 48, 490–497. [PubMed: 24210544]
- (365). Guo M; Huang J; Hu H; Liu W; Yang J UV Inactivation and Characteristics after Photoreactivation of *Escherichia Coli* with Plasmid: Health Safety Concern about UV Disinfection. *Water Res.* 2012, 46, 4031–4036. [PubMed: 22683407]
- (366). Guo M-T; Yuan Q-B; Yang J Distinguishing Effects of Ultraviolet Exposure and Chlorination on the Horizontal Transfer of Antibiotic Resistance Genes in Municipal Wastewater. *Environ. Sci. Technol.* 2015, 49, 5771–5778. [PubMed: 25853586]
- (367). Hao S-J; Wan Y; Xia Y-Q; Zou X; Zheng S-Y Size-Based Separation Methods of Circulating Tumor Cells. *Adv. Drug Delivery Rev.* 2018, 125, 3–20.
- (368). Kinio S; Mills JK Localized Electroporation With Dielectrophoretic Field Flow Fractionation: Toward Removal of Circulating Tumour Cells From Human Blood. *IEEE Trans. NanoBioscience* 2017, 16, 802–809. [PubMed: 29053456]
- (369). Pethig R Review Article—Dielectrophoresis: Status of the Theory, Technology, and Applications. *Biomicrofluidics* 2010, 4, No. 022811. [PubMed: 20697589]
- (370). Köhler G; Milstein C Continuous Cultures of Fused Cells Secreting Antibody of Predefined Specificity. *Nature* 1975, 256, 495–497. [PubMed: 1172191]
- (371). Koido S Dendritic-Tumor Fusion Cell-Based Cancer Vaccines. *Int. J. Mol. Sci.* 2016, 17, 828. [PubMed: 27240347]
- (372). Lluís F; Cosma MP Cell-Fusion-Mediated Somatic-Cell Reprogramming: A Mechanism for Tissue Regeneration. *J. Cell. Physiol.* 2010, 223, 6–13. [PubMed: 20049847]
- (373). Wilmut I; Schnieke AE; McWhir J; Kind AJ; Campbell KHS Viable Offspring Derived from Fetal and Adult Mammalian Cells. *Nature* 1997, 385, 810–813. [PubMed: 9039911]
- (374). Cowan CA Nuclear Reprogramming of Somatic Cells After Fusion with Human Embryonic Stem Cells. *Science* 2005, 309, 1369–1373. [PubMed: 16123299]
- (375). Sugar IP; Förster W; Neumann E Model of Cell Electrofusion: Membrane Electroporation, Pore Coalescence and Percolation. *Biophys. Chem.* 1987, 26, 321–335. [PubMed: 3607233]
- (376). Hu N; Yang J; Joo SW; Banerjee AN; Qian S Cell Electrofusion in Microfluidic Devices: A Review. *Sens. Actuators B Chem.* 2013, 178, 63–85.
- (377). Kandušer M; Ušaj M Cell Electrofusion: Past and Future Perspectives for Antibody Production and Cancer Cell Vaccines. *Expert Opin. Drug Delivery* 2014, 11, 1885–1898.
- (378). Usaj M; Flisar K; Miklavcic D; Kanduser M Electrofusion of B16-F1 and CHO Cells: The Comparison of the Pulse First and Contact First Protocols. *Bioelectrochemistry* 2013, 89, 34–41. [PubMed: 23032299]

- (379). Wang J; Lu C Microfluidic Cell Fusion under Continuous Direct Current Voltage. *Appl. Phys. Lett.* 2006, 89, 234102.
- (380). Dura B; Liu Y; Voldman J Deformability-Based Micro-fluidic Cell Pairing and Fusion. *Lab. Chip* 2014, 14, 2783–2790. [PubMed: 24898933]
- (381). Schoeman RM; Beld WTE; Kemna EWM; Wolbers F; Eijkel JCT; Berg A Electrofusion of Single Cells in Picoliter Droplets. *Sci. Rep.* 2018, 8, 3714. [PubMed: 29487332]
- (382). Cao Y; Yang J; Yin ZQ; Luo HY; Yang M; Hu N; Yang J; Huo DQ; Hou CJ; Jiang ZZ; et al. Study of High-Throughput Cell Electrofusion in a Microelectrode-Array Chip. *Microfluid. Nanofluidics* 2008, 5, 669–675.
- (383). Qu Y; Hu N; Xu H; Yang J; Xia B; Zheng X; Yin ZQ Somatic and Stem Cell Pairing and Fusion Using a Microfluidic Array Device. *Microfluid. Nanofluidics* 2011, 11, 633–641.
- (384). Hu N; Yang J; Qian S; Joo SW; Zheng X A Cell Electrofusion Microfluidic Device Integrated with 3D Thin-Film Microelectrode Arrays. *Biomicrofluidics* 2011, 5, 034121–034121–12.
- (385). Wu W; Qu Y; Hu N; Zeng Y; Yang J; Xu H; Yin ZQ A Cell Electrofusion Chip for Somatic Cells Reprogramming. *PLoS One* 2015, 10, No. e0131966. [PubMed: 26177036]
- (386). Zhang X; Hu N; Chen X; Fan T; Wang Z; Zheng X; Yang J; Qian S Controllable Cell Electroporation Using Microcavity Electrodes. *Sens. Actuators B Chem.* 2017, 240, 434–442.
- (387). He W; Huang L; Feng Y; Liang F; Ding W; Wang W Highly Integrated Microfluidic Device for Cell Pairing. Fusion and Culture. *Biomicrofluidics* 2019, 13, No. 054109. [PubMed: 31893009]
- (388). Kirschbaum M; Guernth-Marschner CR; Cherré S; Peña A. de P.; Jaeger MS; Kroczeck RA; Schnelle T; Mueller T; Duschl C Highly Controlled Electrofusion of Individually Selected Cells in Dielectrophoretic Field Cages. *Lab. Chip* 2012, 12, 443–450. [PubMed: 22124613]
- (389). Lu Y-T; Pendharkar GP; Lu C-H; Chang C-M; Liu C-H A Microfluidic Approach towards Hybridoma Generation for Cancer Immunotherapy. *Oncotarget* 2015, 6, 38764–38776. [PubMed: 26462149]
- (390). Pendharkar G; Lu Y-T; Chang C-M; Lu M-P; Lu C-H; Chen C-C; Liu C-H A Microfluidic Flip-Chip Combining Hydrodynamic Trapping and Gravitational Sedimentation for Cell Pairing and Fusion. *Cells* 2021, 10, 2855. [PubMed: 34831078]
- (391). Masuda S; Washizu M; Nanba T Novel Method of Cell Fusion in Field Constriction Area in Fluid Integration Circuit. *IEEE Trans. Ind. Appl.* 1989, 25, 732–737.
- (392). Gel M; Kimura Y; Kurosawa O; Oana H; Kotera H; Washizu M Dielectrophoretic Cell Trapping and Parallel One-to-One Fusion Based on Field Constriction Created by a Micro-Orifice Array. *Biomicrofluidics* 2010, 4, No. 022808. [PubMed: 20697592]
- (393). Sakamoto S; Okeyo KO; Yamazaki S; Kurosawa O; Oana H; Kotera H; Washizu M Adhesion Patterning by a Novel Air-Lock Technique Enables Localization and in-Situ Real-Time Imaging of Reprogramming Events in One-to-One Electrofused Hybrids. *Biomicrofluidics* 2016, 10, No. 054122. [PubMed: 27822330]
- (394). Okanojo M; Okeyo KO; Hanzawa H; Kurosawa O; Oana H; Takeda S; Washizu M Nuclear Transplantation between Allogeneic Cells through Topological Reconnection of Plasma Membrane in a Microfluidic System. *Biomicrofluidics* 2019, 13, No. 034115. [PubMed: 31312284]
- (395). Clow AL; Gaynor PT; Oback BJ A Novel Micropit Device Integrates Automated Cell Positioning by Dielectrophoresis and Nuclear Transfer by Electrofusion. *Biomed. Microdevices* 2010, 12, 777–786. [PubMed: 20499188]

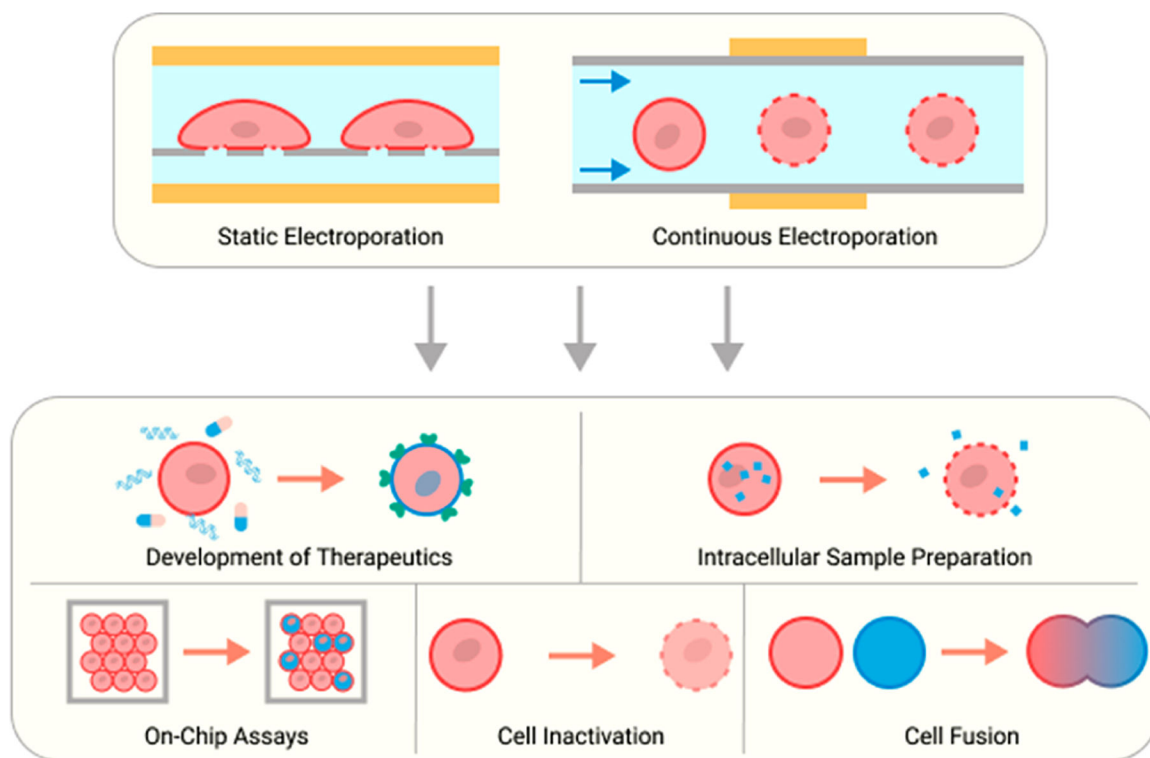


Figure 1. Overview of the microscale EP device types alongside clinical and research applications presented in this Review.

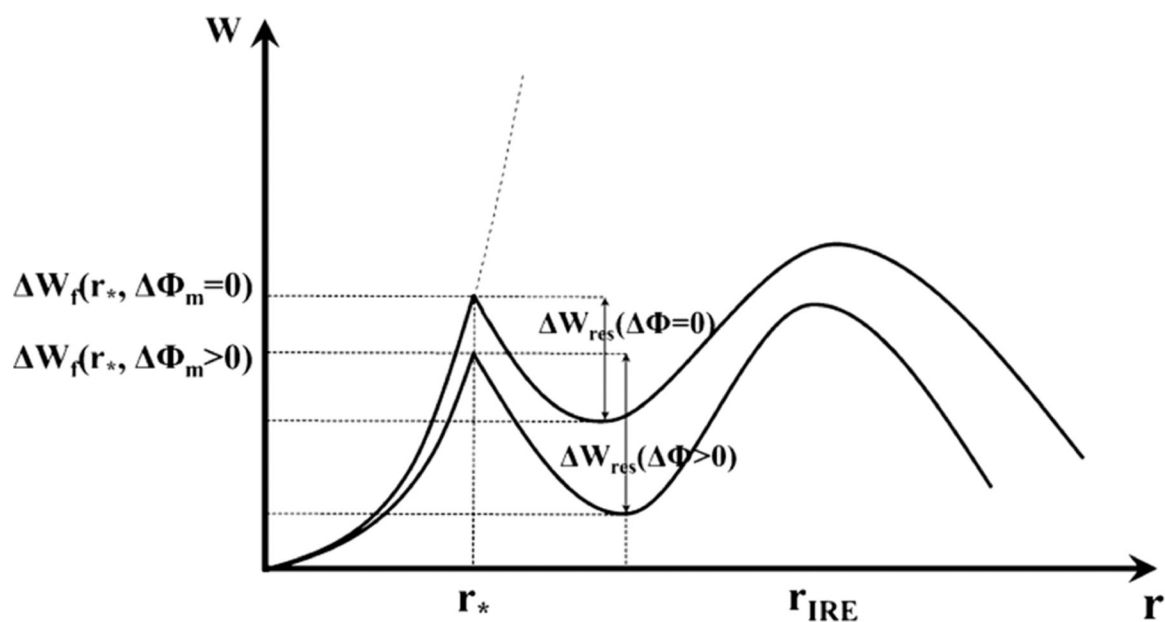


Figure 2. Relationship between the free energy change of a pore (ΔW) and pore radius (r) with ($\Delta \Phi_m > 0$) and without ($\Delta \Phi_m = 0$) an external change in TMP. The free energy change needed for pore formation (ΔW_f) decreases and pore resealing (ΔW_{res}) increases under an external field, which suggests that external electric fields favor stable pore formation. r^* is the critical radius for the hydrophobic to hydrophilic pore transition, and r_{IRE} is the pore radius triggering irreversible EP. Reproduced with permission from ref 30. Copyright 2015 Springer Nature.

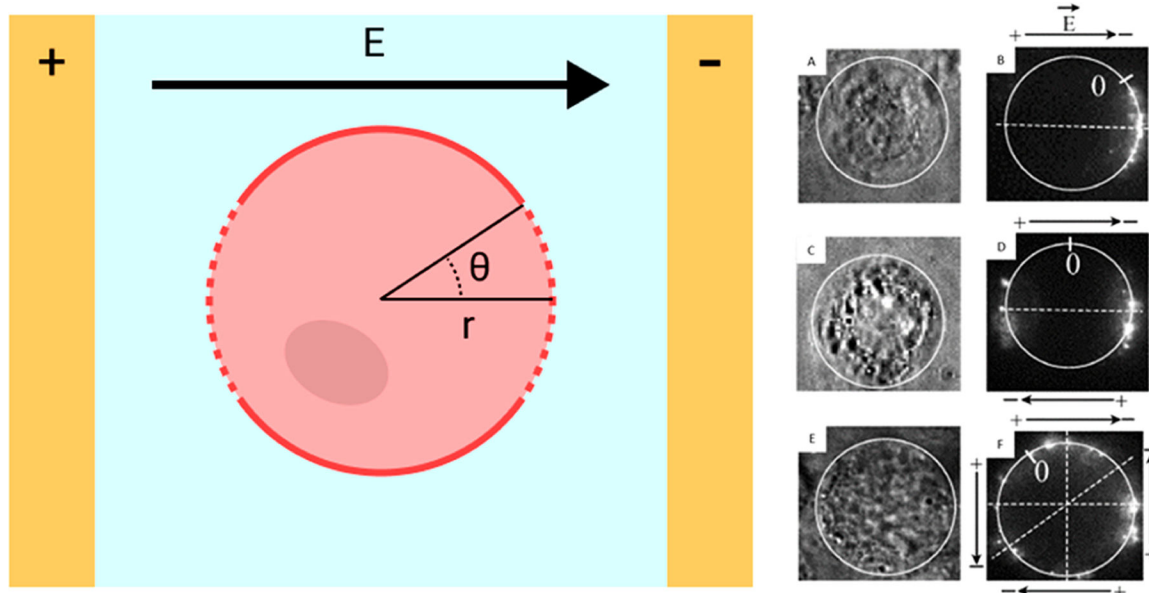


Figure 3. Schematic of a cell placed under uniform electric field E between two planar electrodes (left). $\theta(M)$ is a critical parameter for electric field strength. The TMP is the highest at the poles of the cell, and the permeabilized cell membrane appears as a dashed line. Chinese hamster ovary (CHO) cells were incubated with a fluorescently labeled, 4.7 kilobase pair (kbp) plasmid and electroporated with pulses in different polarities to demonstrate the directionality of nucleic acid delivery (right). Pulses were applied either in a single direction (A, B), in opposing directions (C, D), or in a cross pattern (E, F). Light contrast images before EP (A, C, E) and fluorescence images 30 s after EP (B, D, F) are shown. Black arrows indicate the electric field direction. Reproduced with permission from ref 68. Copyright 2004 Elsevier.

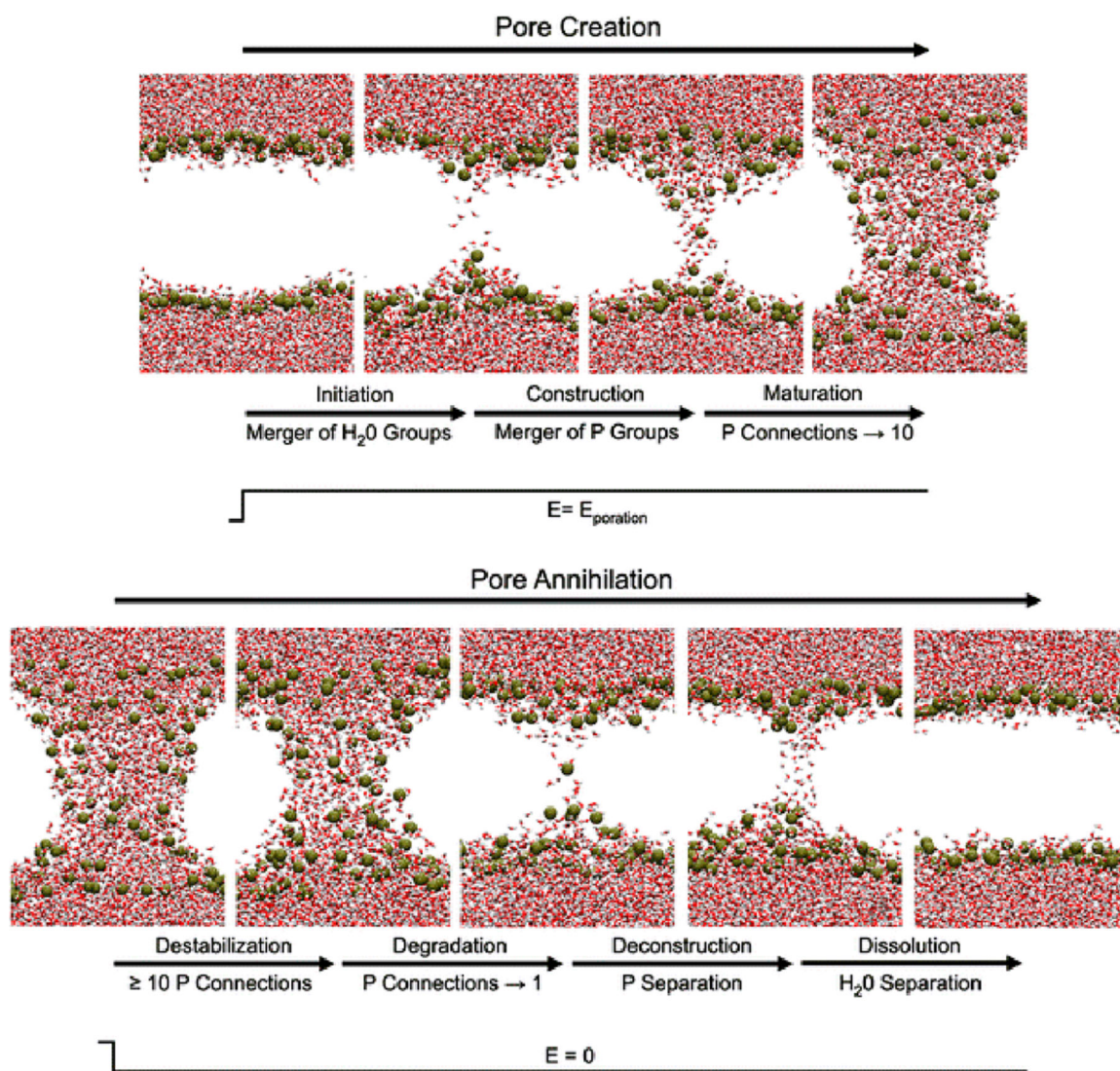


Figure 4. Pore creation and annihilation steps visualized with MD simulations. Only water molecules (red) and phosphorus atoms (gold) are shown for simplicity. When sufficient TMP is applied across the membrane, water molecules move through defects in the lipid bilayer, and lipid head groups are reorganized until mature pore formation (top). When the external electric field is removed, water molecules and lipid head groups migrate to the outside of the membrane, and pore size decreases (bottom). The lipid head groups revert to form a lipid bilayer as water molecules in the membrane escape. Reproduced with permission from ref 75. Copyright 2010 Springer Nature.

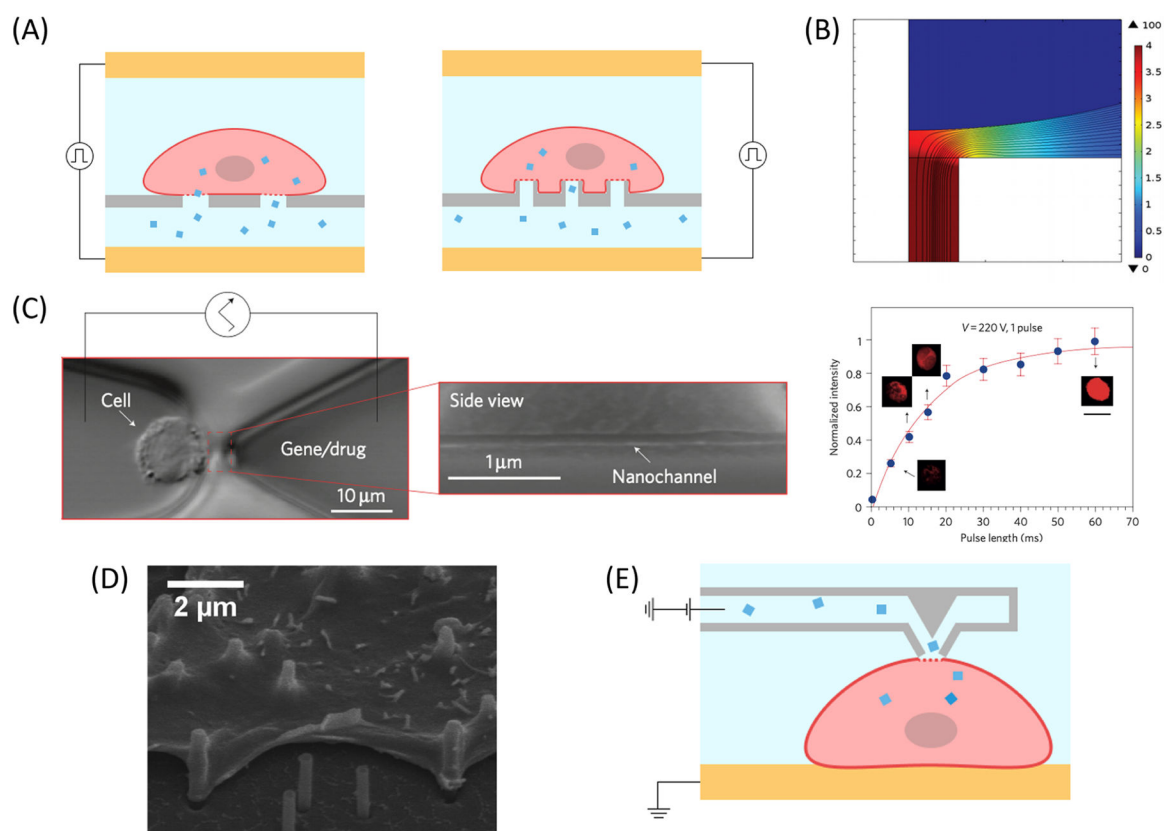


Figure 5.

Examples of subcellular channels implemented for static EP. (A) Schematic illustration of nanochannel (left) and nanostraw (right) EP systems with cells above the nanostructured membrane and biomolecular cargo below. Cells are plated on the nanochannel structures or nanostraws. Cargo is delivered through the nanostructure during EP. (B) Simulated 2D slice of electrical field lines and potential distribution at the cell–nanochannel interface with an applied voltage of 100 V. Reproduced with permission from ref 148. Copyright 2015 Royal Society of Chemistry. (C) Single-cell EP with NEP fabricated using the DNA combing technique.¹⁴⁰ A Jurkat cell is placed at the tip of a ~ 90 nm wide nanochannel using optical tweezers (left). Increasing the pulse length increases the fluorescence and quantity of fluorescently tagged oligonucleotides that are delivered into the cell (right). Reproduced with permission from ref 140. Copyright 2011 Springer Nature. (D) SEM image of CHO cells cultured on nanostraw covered surface for 24 h. Reproduced with permission from ref 152. Copyright 2013 American Chemical Society. (E) Schematic of NFP when the tip is in contact with the cell membrane. Contact is made by a micromanipulator, and an electric pulse is applied to deliver the cargo. Adapted with permission from ref 161. Copyright 2013 American Chemical Society.

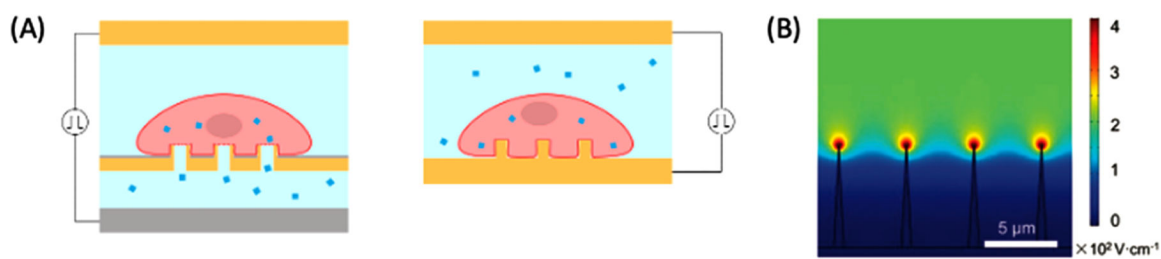


Figure 6.

Sharp nanoelectrodes for static EP. (A) Hollow (left) and solid (right) nanoelectrodes used for localized EP. Cells are placed on the nanoelectrodes protruding out from the passivation layer. Cargos are delivered through the hollow nanoelectrodes from the microfluidic channel underneath. (B) Simulation of electric field strength at the tips of nanoelectrodes with high aspect ratios. Up to 2.8 $\text{kV}\cdot\text{cm}^{-1}$ is reached at the tip when 20 V is applied. Reproduced with permission from ref 171. Copyright 2019 John Wiley and Sons.

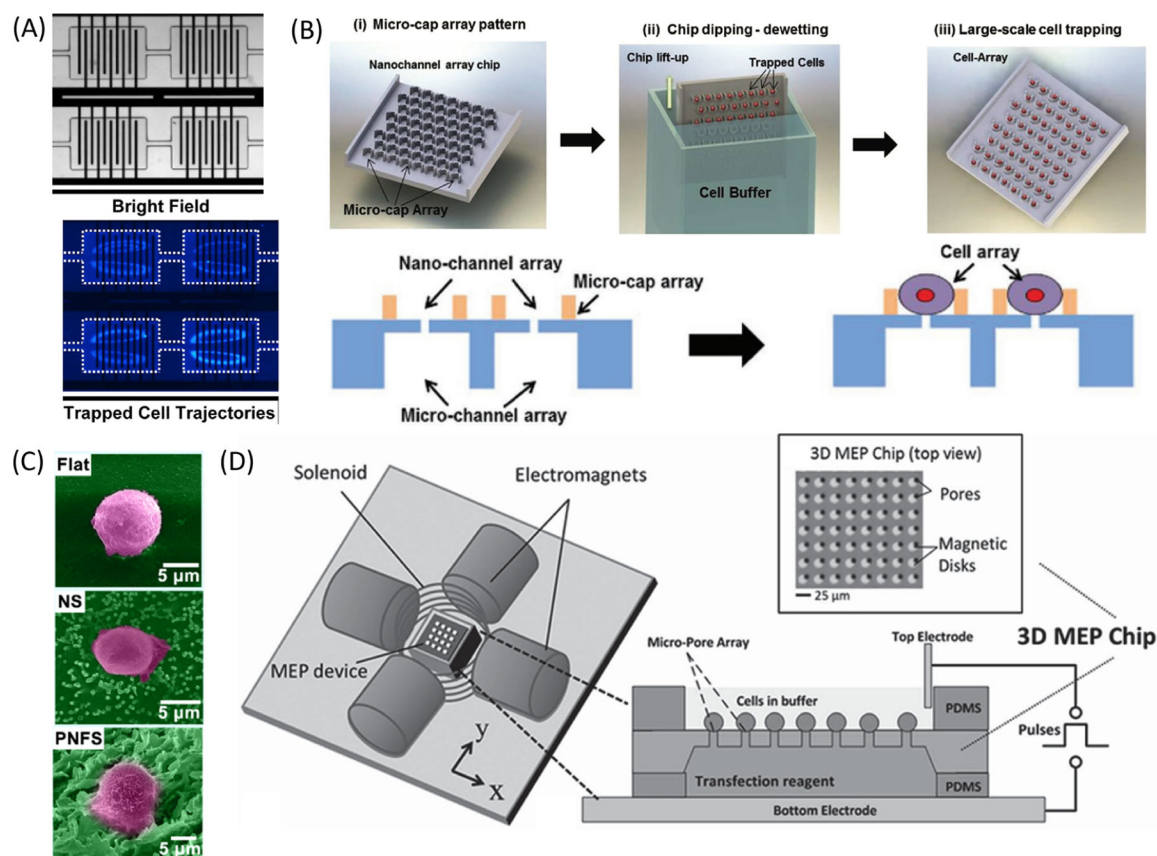


Figure 7. Different methods used for improved cell placement on static EP devices. (A) Bright field (top) and fluorescent (bottom) images of cells inertially trapped in microvortices within reservoirs patterned with interdigitated electrodes.¹⁸⁰ The nuclei of HEK293 cells are stained blue. Reproduced from ref 180. Copyright 2017 Springer Nature under Creative Commons CC BY license, <https://creativecommons.org/licenses/>. (B) Cells are trapped in U-shaped microcaps after dipping the array into cell suspension. Each cell is placed over a nanochannel for EP. Reproduced with permission from ref 35. Copyright 2016 John Wiley and Sons. (C) False color SEM images of a cell on a flat substrate (top), nanostraws (middle), or nanoflower (bottom). Reproduced with permission from ref 156. Copyright 2020 Elsevier. (D) Schematic of an electromagnetic setup for magnetic alignment of cells. Four orthogonal electromagnets and a solenoid create an external 3D magnetic field. Micropatterned permalloy disks are placed next to 5 μm pores to capture and electroporate cells labeled with magnetic beads.¹⁴⁶ Cells are attracted to the patterned magnetic disks that align with subcellular pores under an external magnetic field. Then, an enhanced electric field is applied through micropores to electroporate the cells. Reproduced with permission from ref 146. Copyright 2014 John Wiley and Sons.

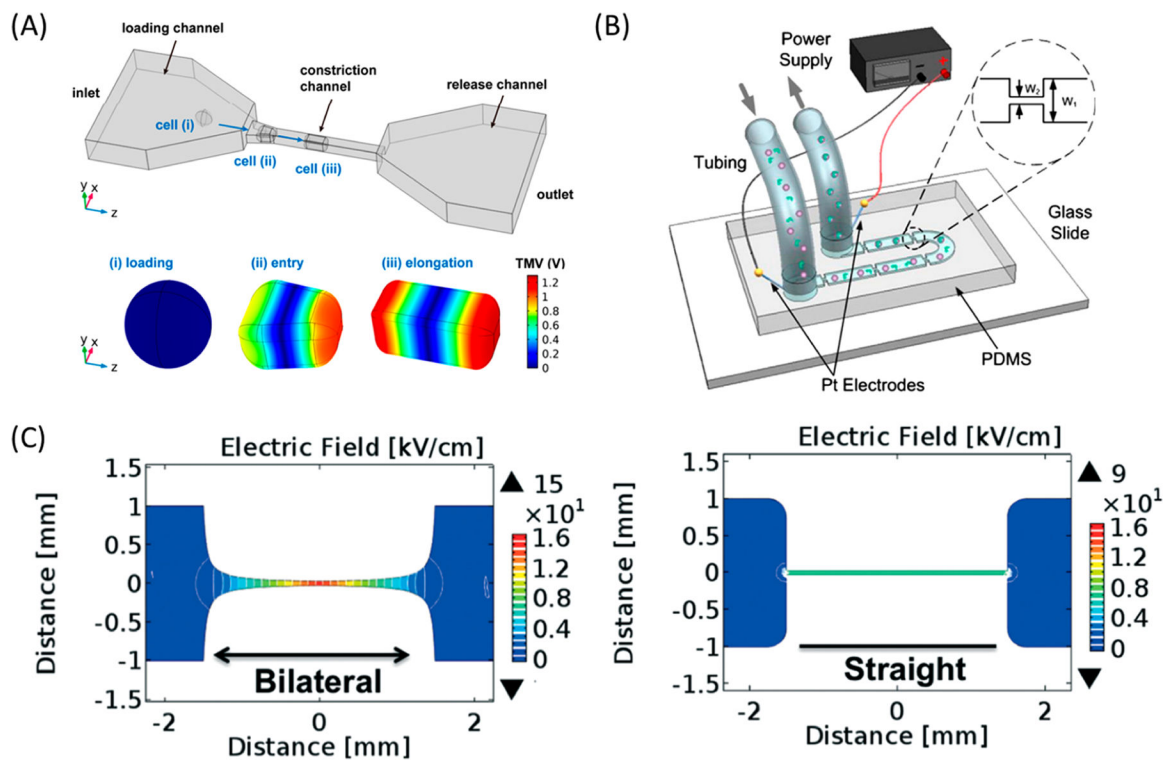


Figure 8. Examples of channel constrictions implemented for continuous EP. (A) Schematic of single-cell, continuous EP through a narrow uniform constriction (top).²²³ COMSOL Multiphysics simulations at three different points in the channel demonstrate sufficiently high TMP, but EP is achieved only when cells were elongated in the channel. Reproduced from ref 223. Copyright 2020 MDPI under Creative Commons CC BY 4.0 license, <https://creativecommons.org/licenses/by/4.0/>. (B) Illustration of a continuous device for enhanced electric field generation at each channel constriction in series.²²⁴ Reproduced with permission from ref 224. Copyright 2010 Elsevier. (C) Numerical simulations revealed the expected electric field intensity in a bilaterally converging constriction (left) and straight channel (right).²³¹ The maximum electric field intensity is around $2\times$ higher in a bilaterally converging channel compared to a straight channel. Reproduced with permission from ref 231. Copyright 2016 Royal Society of Chemistry.

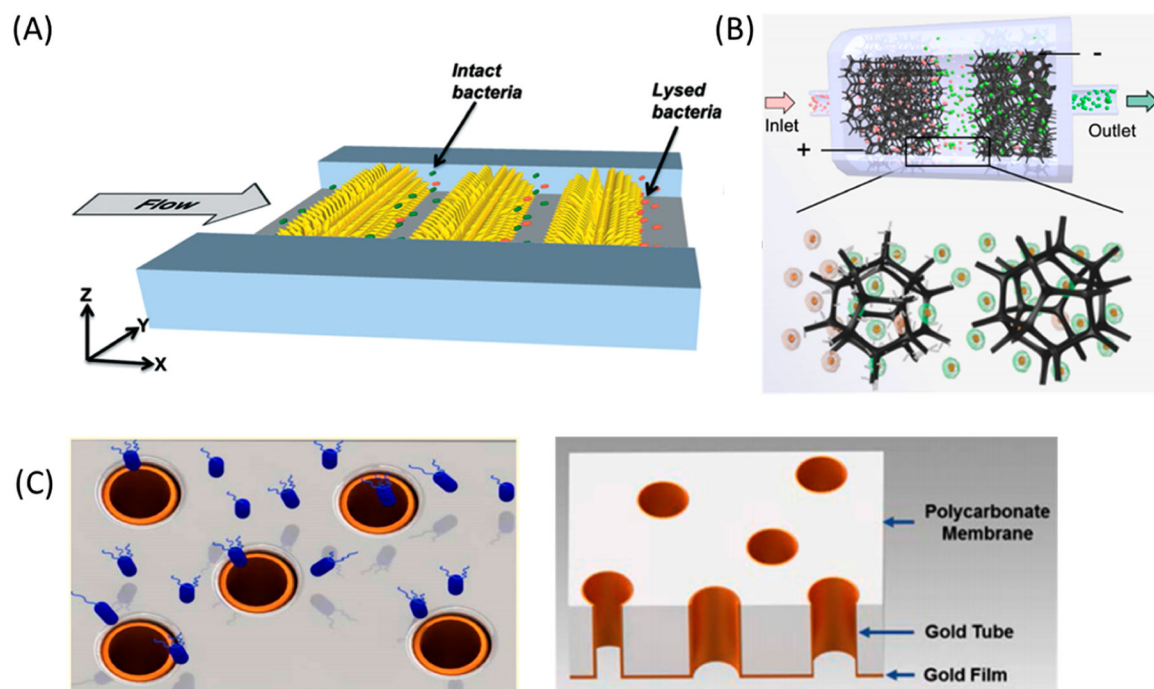


Figure 9. Examples of enhanced electric fields at electrode edges or tips. (A) Illustration of cell lysis by three-dimensional sharp-tipped electrode (3DSTE) arrays in the microfluidic channel.²³⁶ Bacteria are lysed when they flow between nanoelectrodes. Reproduced with permission from ref 236. Copyright 2014 Royal Society of Chemistry. (B) Overview of the TENG-powered, nanowire-modified microfoam for continuous EP. Cell suspensions flowed through microfoam electrodes placed in parallel within the flow channel. Polypyrrole microfoam was modified by silver nanowires at the anode to enhance the electric field at the tip of the nanowire. The cathode microfoam was left unmodified to increase cell viability. Reproduced with permission from ref 237. Copyright 2020 Royal Society of Chemistry. (C) Schematic of *E. coli* (blue) flowing through gold microtube electrodes (left).²⁴⁶ Illustration showing 3D structure of gold microtube on the PC membrane (right). Reproduced with permission from ref 246. Copyright 2016 Royal Society of Chemistry.

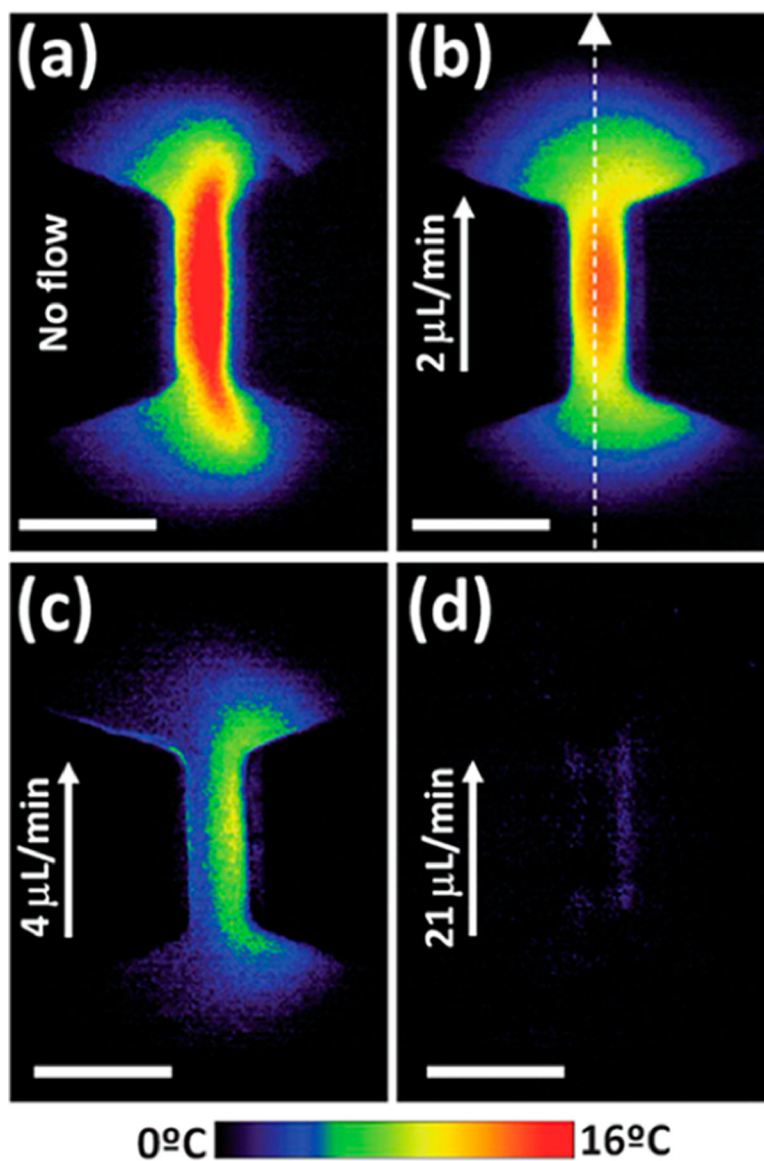


Figure 10. Effects of Joule heating on a channel constriction with flow rates at (a) 0 $\mu\text{L}/\text{min}$, (b) 2 $\mu\text{L}/\text{min}$, (c) 4 $\mu\text{L}/\text{min}$, and (d) 21 $\mu\text{L}/\text{min}$.²⁵⁰ Thermal images are obtained under an operational electric field of 500 V/cm and visualized by comparing images taken using temperature-sensitive and temperature-insensitive dyes. Reproduced with permission from ref 250. Copyright 2013 Royal Society of Chemistry.

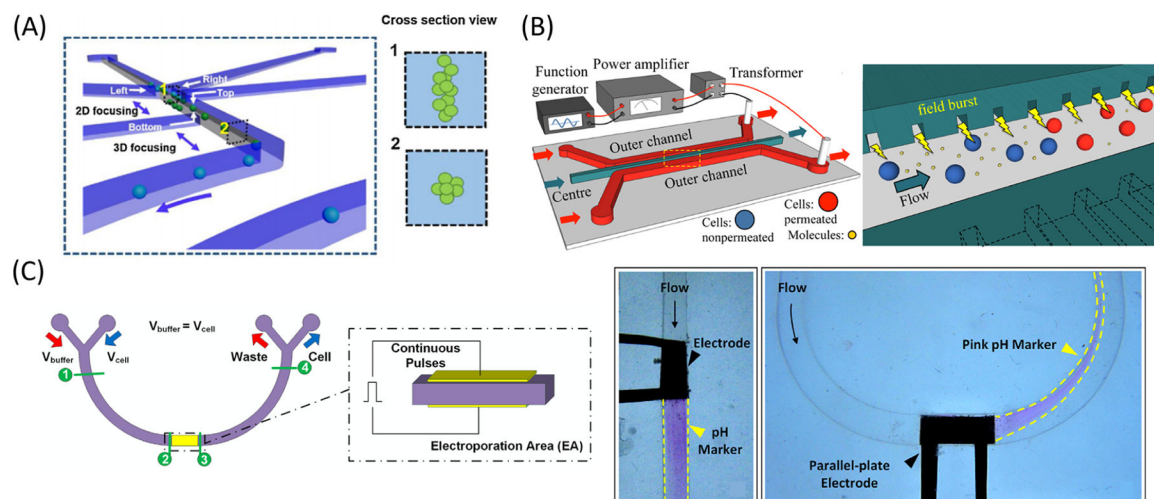


Figure 11.

Efforts to reduce the effects of electrolysis-generated toxins on cell viability. (A) 3D flow focusing channel to focus microalgae at the center of the channel.²⁵⁴ Cell suspension was introduced at the central inlet and two sheath flows, from the left and the right, to induce 2D focusing (see cross section view 1). Two additional sheath flows, from the top and the bottom, focused cells vertically to the center of the channel (cross section view 2). Reproduced with permission from ref 254. Copyright 2020 Elsevier. (B) Schematic of a continuous device that decoupled buffer channels from the main cell suspension channel using microcapillaries for electrical coupling. Reproduced with permission from ref 255. Copyright 2014 AIP Publishing. (C) Schematic of curved device that generated Dean flow with buffer and cell suspension in flow (left). Demonstration of pH changes from electrolysis in different channel geometries (right). Bubbles and hydroxyl ions (pink from a pH indicator) were not neutralized in a straight channel but were neutralized and flowed into a waste outlet in the curved channel. Reproduced with permission from ref 209. Copyright 2017 Elsevier.

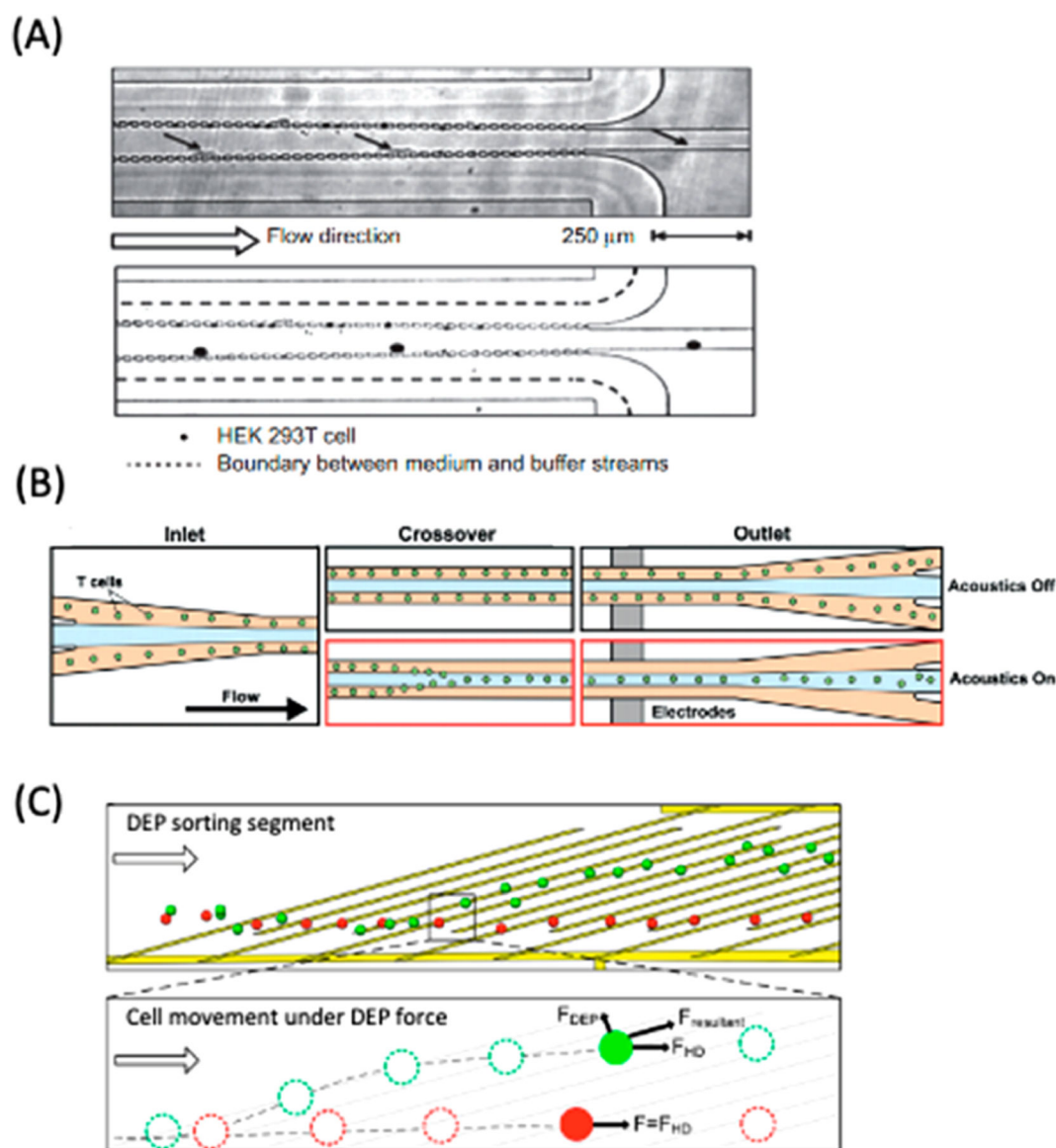


Figure 12.

Passive and active solution exchange techniques to improve cell viability. (A) Composite time-lapsed images of continuous medium exchange with μ PAR structures. HEK293 cells are transferred from cell culture medium to EP buffer. Time interval between images is 10 ms. Reproduced with permission from ref 259. Copyright 2015 Springer Nature. (B) Schematics of acoustophoresis-assisted solution exchange for high-throughput T cell EP. Cells were briefly transferred to EP buffer with low conductivity at the center of the channel by acoustic actuation followed by EP. Reproduced with permission from ref 258. Copyright 2019 Royal Society of Chemistry. (C) Schematic of DEP sorting segment downstream of cell EP to separate live and dead cells.²⁶⁰ After EP, live cells are deflected by DEP force and collected at a separate outlet from dead cells, which do not deflect. Reproduced with permission from ref 260. Copyright 2014 American Chemical Society.

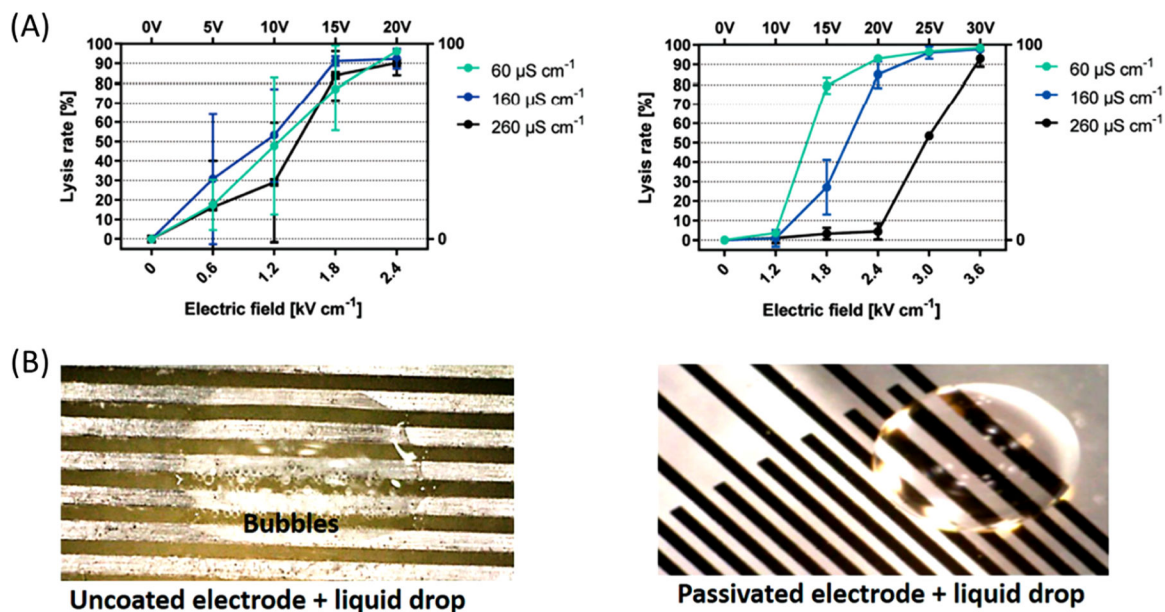
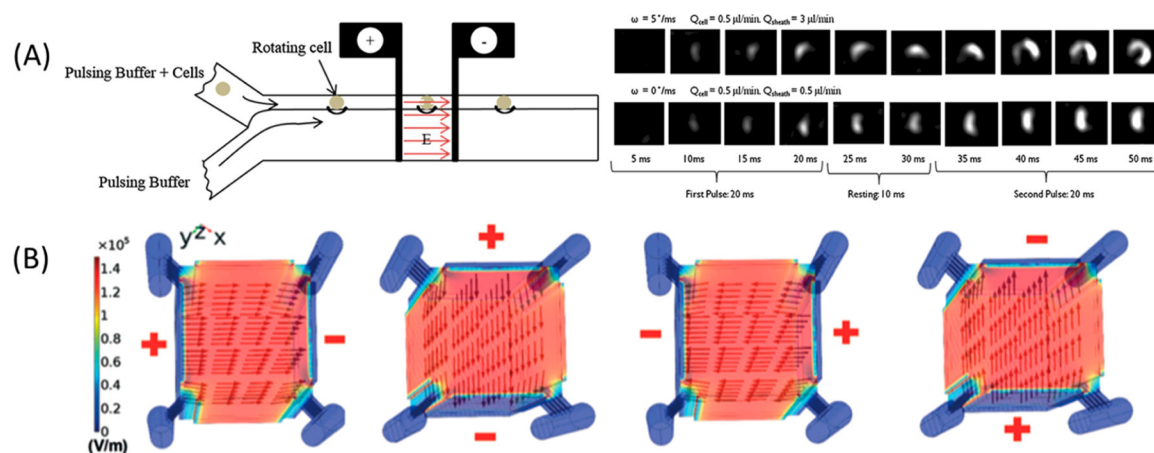


Figure 13.

Experimental validation of the electrolysis inhibition with passivated electrodes. (A) Lysis efficiency of HEK293 cells using nonpassivated (left) and passivated (right) electrodes in buffers with three different conductivities. Passivation decreases the variation in lysis efficiency across all buffer types. Reproduced with permission from ref 262. Copyright 2019 Royal Society of Chemistry. (B) Comparison of bubble formation and electrode erosion in bare (left) and PDMS-passivated (right) electrodes. Bubble formation was observed within 5 min at 10 V without passivation, but the 18 μm PDMS layer over electrodes inhibited electrolysis even after 2 h under 800 V. Reproduced with permission from ref 263. Copyright 2020 AIP Publishing.

**Figure 14.**

Different strategies to improve the homogeneity of applied electric fields and cell poration.

(A) Schematic illustrating induced cell rotation using pinched flow (left). Buffer infused from bottom inlet pinched and rotated cells.²⁶⁷ Dye delivery into cells rolling at $5^\circ/\text{ms}$ or $0^\circ/\text{ms}$ were visualized during two electric pulses (right). Reproduced with permission from ref 267. Copyright 2016 Springer Nature. (B) COMSOL Multiphysics simulation of a multidirectional electric field across a 3D culture chamber. Planar electrodes were placed on four sides of the main cell culture chamber, and medium perfusion channels were placed outside of the cell culture chamber. The arrows indicate the intensity and direction of the electric field. Reproduced with permission from ref 269. Copyright 2019 Royal Society of Chemistry.

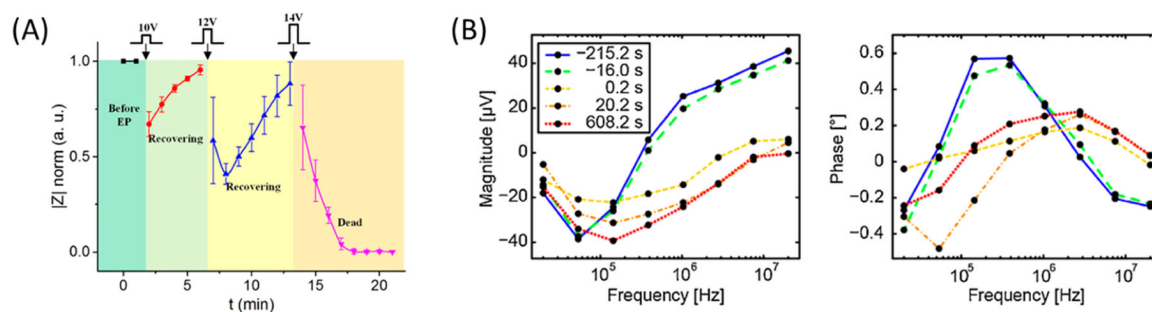


Figure 15.

Monitoring how cell EP affects impedance. (A) Normalized impedance change after reversible EP (10 V, 12 V) and irreversible EP (14 V).¹⁸⁸ Cell impedance eventually recovered after reversible EP but continued declining after irreversible EP. Reproduced from ref 188. Copyright 2016 Springer Nature under Creative Commons CC BY 4.0 license, <https://creativecommons.org/licenses/by/4.0/>. (B) Electrical impedance spectroscopy (EIS) spectra of a single cell before and after EP at five selected time points. Both magnitude (left) and phase spectrum (right) changed in 200 ms after EP, implying that the material exchange across plasma membrane begins within 200 ms. Reproduced with permission from ref 286. Copyright 2015 Elsevier.

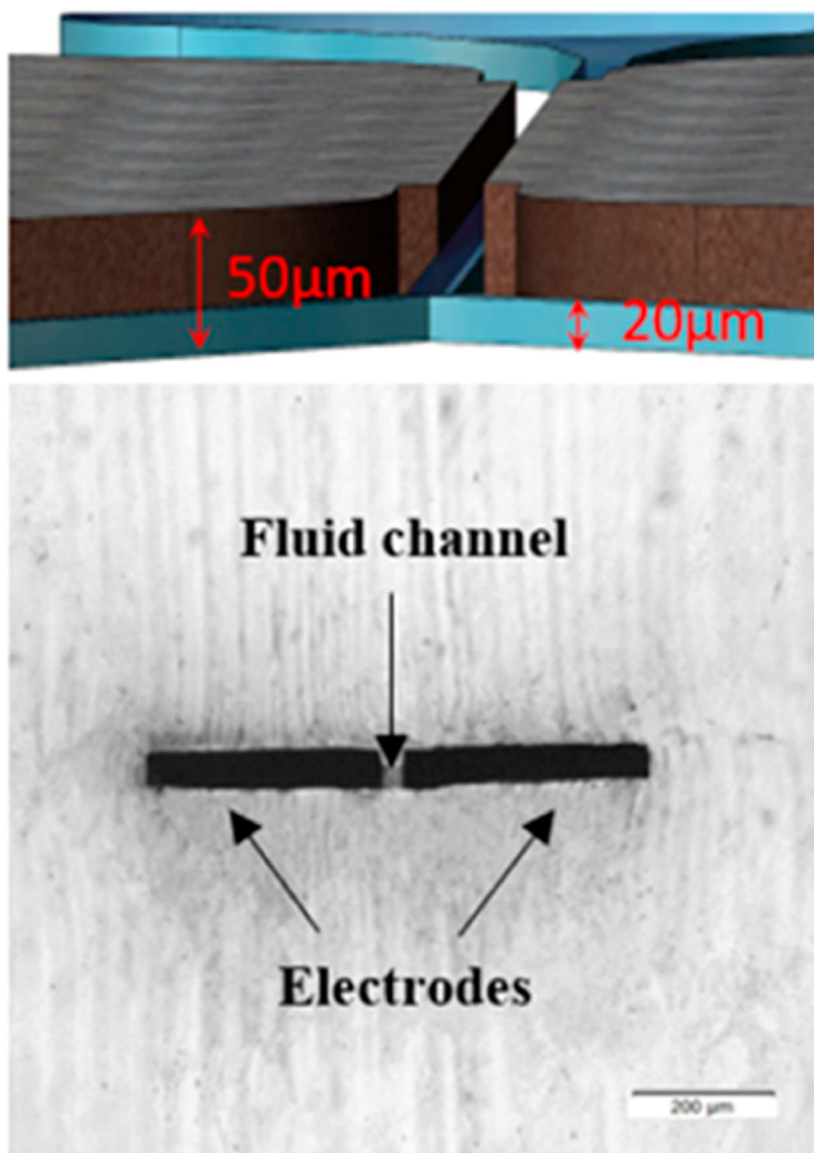


Figure 16. Integration of liquid electrodes for device fabrication at lower costs.²⁹³ The liquid alloy was injected in 50 μm tall side channels and stopped at the 20 μm tall channel restriction. Cell suspension flowed through the central channel, and a uniform electric field could be applied. Reproduced with permission from ref 293. Copyright 2020 Elsevier.

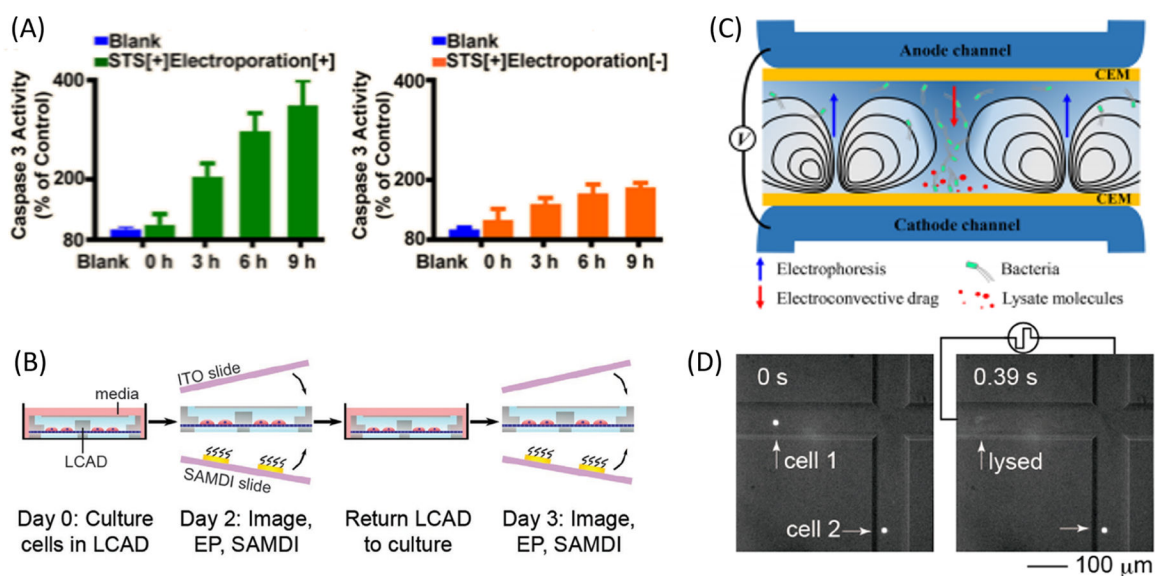


Figure 17.

Examples of studies designed to analyze intracellular contents. (A) Longitudinal analysis of intracellular caspase-3 enzyme at four sampling points.¹⁵⁹ Enzymes were extracted from HeLa cells in a staurosporine solution and analyzed using a caspase-3 colorimetric assay kit. (B) Repetitive enzyme sampling and mass spectrometry measurement of the same cells using a removable SAMDI slide. Reproduced with permission from ref 138. Copyright 2020 John Wiley and Sons. (C) Schematic of electromechanical bacteria lysis by electroconvective vortices.³²² Drag forces caused bacteria to migrate toward the cathode, where conditions were sufficiently harsh for irreversible EP. (D) Single-cell lysis and RNA extraction in a cross chamber using ITP.³³⁰ Due to the electrode positions, cell 1 (left channel) was lysed whereas cell 2 in the lower channel was not.

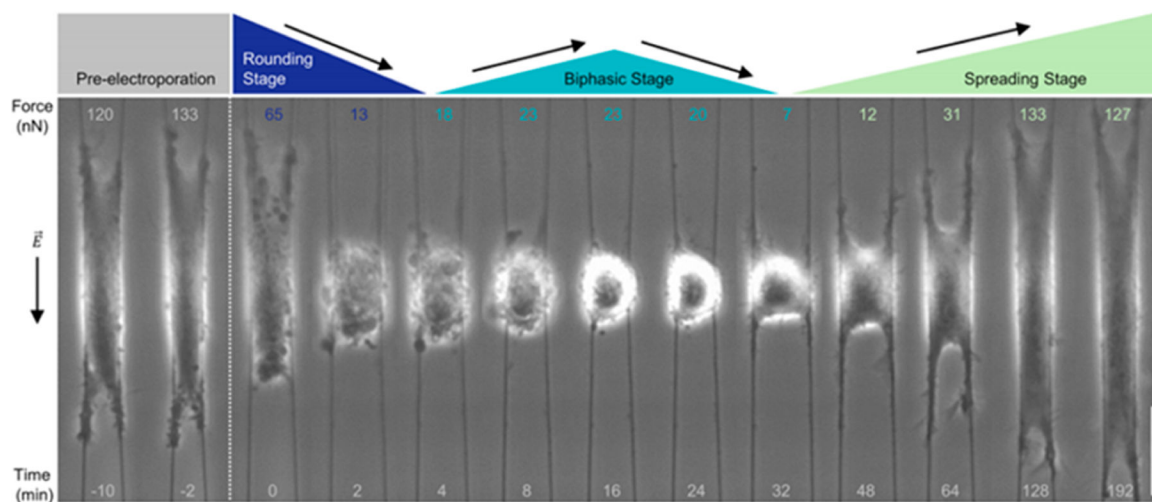


Figure 18. Biphasic force recovery of electroperated cells.³⁵³ A glioblastoma cell was placed on extracellular matrix-mimicking nanofibers to detect changes of cytoskeleton-driven forces by fiber deflection as it underwent multistage recovery after EP. Scale bar: 25 μm .

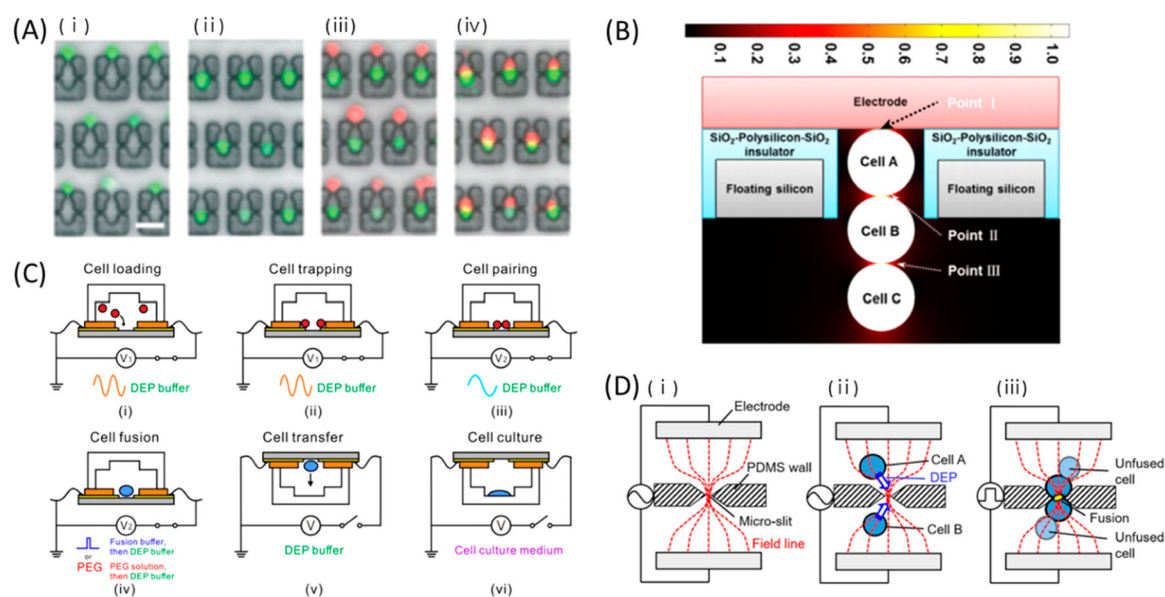


Figure 19.

Passive (A) and active (B–D) cell pairing strategies for cell fusion. (A) Sequential images of the cell loading and fusion process. eGFP expressing NIH 3T3 cells were (i) captured at the traps and (ii) transferred into two-cell traps by flow-induced deformation. (iii, iv) DsRed expressing NIH 3T3 cells were trapped with the same protocol followed by fusion. Scale bar: 50 μm . Reproduced with permission from ref 380. Copyright 2014 Royal Society of Chemistry. (B) Electrical simulation showing electric field and TMP distribution at the microcavity/discrete microelectrode structure.³⁸⁵ TMP at points I and II were similar and higher than that at point III which is beneficial to selectively fuse two cells. Reproduced from ref 385. Copyright 2015 PLOS under Creative Commons Attribution License, <https://creativecommons.org/licenses/by/4.0/>. (C) Procedure for cell pairing by DEP, electrofusion, and culture using adjacent electrodes. pDEP, nDEP, and fusing electric fields are achieved using the same electrodes by changing electrical conditions. Reproduced with permission from ref 387. Copyright 2019 AIP Publishing. (D) Schematic process of one-to-one cell pairing at microslits for fusion using a channel constriction. Reproduced with permission from ref 393. Copyright 2016 AIP publishing.